Phosphorus Cations and Bulky Cyclopentadienyl Ligands

By
Alex J. Veinot

A Thesis Submitted to
Saint Mary's University, Halifax, Nova Scotia
in Partial Fulfillment of the Requirements for
the Degree of Master of Science in Applied Science.

April 2017, Halifax, Nova Scotia

Approved:	Dr. Jason Masuda Supervisor Department of Chemistry
Approved:	Dr. Kai Ylijoki Supervisory Committee Member Department of Chemistry
Approved:	Dr. Samuel Veres Supervisory Committee Member Division of Engineering
Approved:	Dr. Gregory Welch External Examiner Department of Chemistry University of Calgary
Date:	April 27, 2017

Phosphorus Cations and Bulky Cyclopentadienyl Ligands

by Alex J. Veinot

Abstract

The synthesis and characterisation of some ethynylphosphonium salts are described starting from 1-bromo-2-phenylacetylene and tertiary phosphines. Structural information for these molecules has been obtained using X-ray crystallography, and deviant reactivity was observed at elevated temperatures when the electron-rich tris(2,4,6-trimethoxyphenyl)phosphine was employed. A new approach to the corresponding 1,4-bis(ethynylphosphonium) salts was also developed by a similar reaction, and the first bis(ethynylphosphonium) salts were characterised using X-ray crystallography.

Exploratory research into the synthesis of *m*-terphenyl substituted cyclopentadienyl ligands ($Ter^{Mes}Cp$ and $Ter^{Dipp}Cp$) is also described. A new synthetic route is presented and is accomplished through the reaction of aryl lithium reagents with cobaltocenium salts, followed by oxidation of the intermediate cobalt(I) species to afford the corresponding cyclopentadiene. The preparation, structural, and spectroscopic properties of the alkali metal salts (Li–Cs) is described, and some preliminary coordination chemistry is presented.

April 27, 2017

Acknowledgements

First and foremost I would like to thank my supervisor Dr. Jason Masuda for his time and effort in mentoring me as a scientist, for preparing me for my future endeavours in chemistry and allowing me the freedom (and encouraging me) to take this work in my own creative direction. I would also like to acknowledge the contributions of my previous supervisor Dr. Bobby Ellis in giving me both the skills and knowledge necessary to be successful during my time at Saint Mary's University. I would also like to thank Dr. Katherine Robertson for her assistance with all things crystallography related, and for teaching me some of the transferrable skills necessary to solve my own structures, and Alyssa Doué, Darlene Goucher, Patricia Granados, Elizabeth McLeod, and Mary Jane MacNeil for their assistance and technical support.

I would also like to thank Darcie Stack for her endless support, for helping me stay organised, remembering deadlines, as well as ordering the occasional item on Amazon for Christmas. I would also like to thank both the past and present Masuda group members Connor McLeod, Angela Todd, and Jennifer Wright for their hands in some of the synthesis. I would also like to thank Michael Land for the occasional drive home, and interesting discussions on all things chemistry related.

I would like to acknowledge NSERC, FGSR and the Dean of Science offices for financial support.

I would like to thank my committee members Dr. Kai Ylijoki and Dr. Samuel Veres for their time and effort over the duration of this process.

Most importantly, I would like to thank my wife Nicole for her constant support through both the good and bad times over the last two years, and for dealing with me no matter how insufferable I became while writing this thesis.

Table of Contents

Table of Figures

Table of Schemes

Table of Tables

List of Abbreviations

°	degrees
°C	degrees Celsius
Å	Angstrom
Ar	aryl
B3LYP	Becke, three-parameter, Lee-Yang-Parr
br	broad
Bu	butyl
ca.	approximately
cat.	catalytic amount
cm	centimeter
COSY	correlation spectroscopy
Cp	cyclopentadienyl
Cp*	pentamethylcyclopentadienyl
d	doublet
D	deuterium
DBU	1,8-diazabicyclo(5.4.0)undec-7-ene
dd	doublet of doublets
DEPTQ	distortionless enhancement by polarisation transfer quaternaries
dme	dimethoxyethane
DOSY	diffusion-ordered spectroscopy
eq.	equivalent
Et	ethyl
g	gram
h	hour
HSQC	heteronuclear single-quantum correlation spectroscopy
Hz	hertz
i-	*ipso*
in situ	in the reaction medium
in vacuo	under vacuum
iPr	isopropyl
IR	infrared
J	coupling
K	degrees Kelvin
kcal	kilocalorie
kJ	kilojoule
L	Litre
M	molarity
m	multiplet (NMR spectroscopy)
m	medium (IR spectroscopy)

m-	*meta*
m.p.	melting point
Me	methyl
Mes	mesityl
mg	milligram
MHz	MegaHertz
min	minute
mL	millilitre
mmol	millimole
NBS	*N*-bromosuccinimide
NMR	nuclear magnetic resonance
NOESY	nuclear Overhauser effect spectroscopy
Nu	nucleophile
o-	ortho
o-An	*ortho*-anisole
OTf	triflate
o-Tol	*ortho*-tolyl
p-	*para*
p-An	*para*-anisole
Ph	phenyl
pin	pinacol
pKa	acidity measurement
ppm	parts per million
PTFE	polytetrafluoroethylene
q	quartet
r.t.	room temperature
s	singlet (NMR spectroscopy)
s	second
s	strong (IR spectroscopy)
T	triplet
*t*Bu	*tert*-butyl
Ter^{Dipp}	2,6-bis(2,6-diisopropyllphenyl)phenyl
Ter^{Mes}	2,6-bis(2,4,6-trimethylphenyl)phenyl
Ter^{Ph}	2,6-di(phenyl)phenyl
THF	tetrahydrofuran
TMPP	tris(2,4,6-trimethoxyphenyl)phosphine
TMS	tetramethylsilane
UV-Vis	ultraviolet-visible
via	by way of
vs	very strong
w	week
w	weak (IR spectroscopy)

δ	chemical shift
Δ	heat
ε	molar absorptivity coefficeint
η	hapticity
λ	wavelength
ν	wavenumber

Compounds Prepared

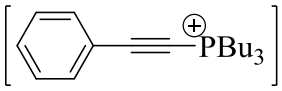

1

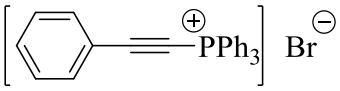

2

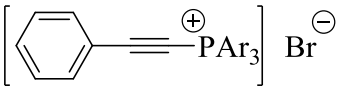

3

Ar = 2,4,6-$(MeO)_3C_6H_2$

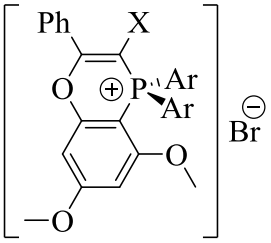

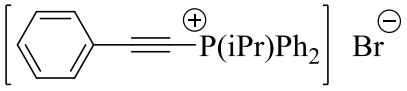

5

4; **(a)** X = H, **(b)** Me
Ar = 2,4,6-$(MeO)_3C_6H_2$

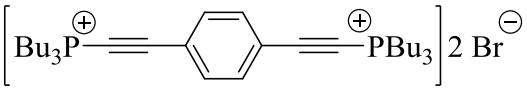

6

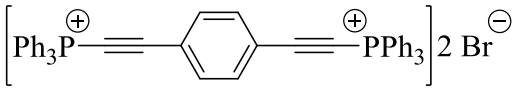

7

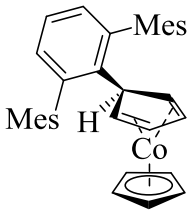

8

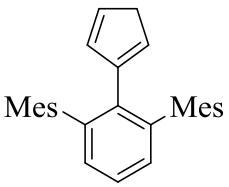

9a

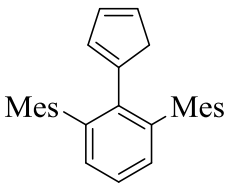

9b

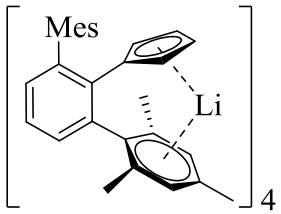

10

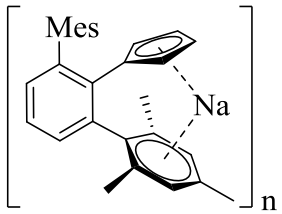

11

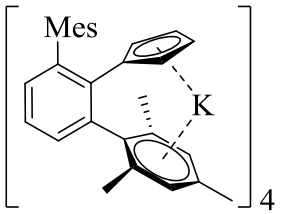

12

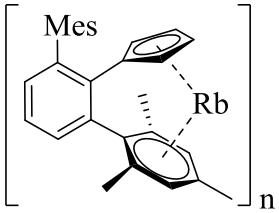

13

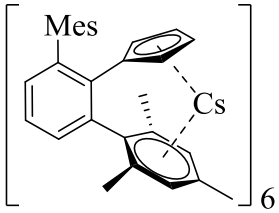

14

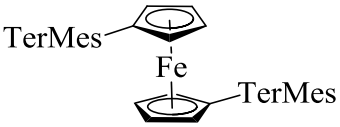

15

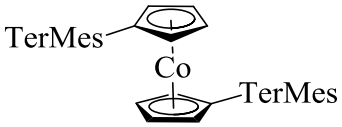

16

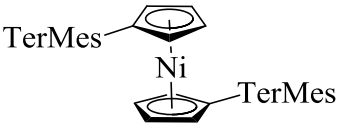

17

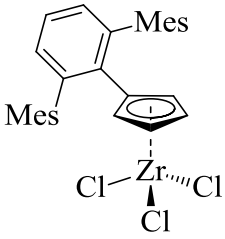

18a

or

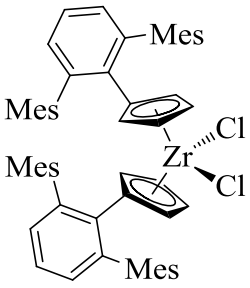

18b

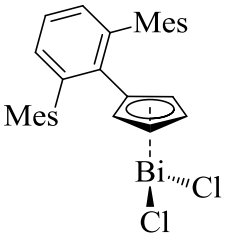

19

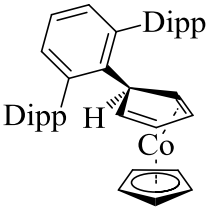

20

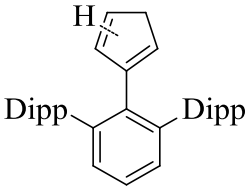

21

Preface

The following thesis is divided into two sections with references appearing at the end of each section, with each section representing a major research project that was undertaken during the Master of Science in Applied Science program. The first project investigated the structural and spectroscopic properties, in addition to the preparation and reactivity of some derivatives of ethynylphosphonium salts. The second project focused on the preparation of new sterically hindered cyclopentadienyl ligands and the exploration of some of the coordination chemistry that these new molecules are capable of participating in with both main group and transition metal elements. These projects are mutually independent and only fundamental academic interest relates them.

Fundamental academic research (or basic research) is an important first step in research and development; the other two being applied research and then development. Basic research promotes curiosity with little or no specific commercial goals, but fosters creative solutions to relevant problems and can evolve into applied research that serves to discover new knowledge related to a specific commercial objective. As applied research progresses, development quickly follows which often focuses on inventing or improving a specific process or product. This process is both cyclical and heavily intertwined, with basic and applied researchers producing the scientific capital that is required to bring new products or processes to market. The development stage often uncovers new problems that spur further curiosity by basic and applied researchers and once again provides further knowledge that may lead to commercial applications.

An example of this is the ethynylphosphonium salts studies during the first project. These molecules were first discovered in 1962, and have since remained as a subject of academic interest. Only just recently, however, it has been discovered that some of these molecules exhibit anticancer properties, and has shifted research interests towards applying these molecules in medicinal chemistry. These molecules have not reached the development stage as of yet, but do show promise and have the potential for future therapeutic use.

1 Ethynylphosphonium Salts

1.1 Overview

Phosphonium salts are polyatomic ionic species and can be generally described by the formula $[PR_4]X$ in which PR_4 is a quaternary phosphorus cation (R= any group) and X may be any anion to balance the net ionic charge. Replacement of one or more R groups with an alkynyl group gives rise to the more electrophilic ethynylphosphonium derivatives (Figure 1.1).

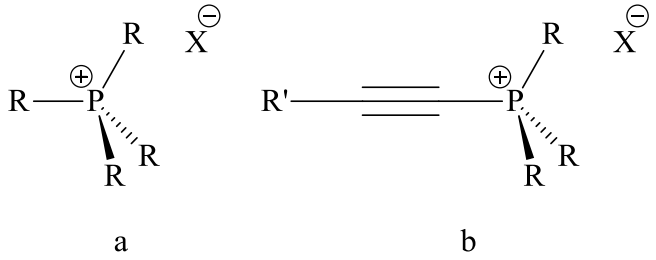

Figure 1.1. Generic phosphonium salt (a) and ethynylphosphonium salt (b).

Since their initial discovery, ethynylphosphonium salts continue to be popular and extremely valuable building blocks in organic synthesis. The reactivity of these molecules with various nucleophiles has been studied extensively,[1-11] however, more recently it has been discovered that mono-substituted (phenylethynyl)phosphonium salts have the potential to be used as therapeutic agents for cancer treatment.[12-14] Ethynylphosphonium salts of the type $[R_3PC{\equiv}CR'][X]$ are uncommon in the literature and are most commonly synthesised *via* quaternisation of tertiary phosphines with alkynyl halides.[1,2,15-18] Other routes have been reported[19,20], but have not seen extensive use. Modification of ethynylphosphonium salts typically takes place at the R' position[19,21] (Figure 1.1), while structural diversity within the ligands bound to phosphorus remains an underdeveloped

area. The lack of diversity in the ligands attached to phosphorus comes as quite a surprise given that traditional interest in ethynylphosphonium species lies primarily on their reactivity with nucleophiles,[3] which would likely be sensitive to the electronic properties of the phosphorus cation. Likely the lack of variety originates from the ease of synthesis of [$Ph_3PC{\equiv}CR'$]Br and the effectiveness of the phosphorus cation in activating the alkyne.[3,5] After examining the literature, it was found that despite their widespread use there is relatively little structural data available for even the simplest of ethynylphosphonium salts, and early spectroscopic data collected for phenylethynylphosphonium salts was determined to be incomplete (Figure 1.2, [$PhC{\equiv}CPBu_3$]Br, for a discussion of what has been previously reported see section 1.3.1),[2] or scattered throughout the literature (Figure 1.2, [$PhC{\equiv}CPPh_3$]Br).[2,18,22] To date, only [$PhC{\equiv}CPMe_3$]Br[17] and [$PhC{\equiv}CP(o\text{-}An)_2Ph][BF_4$][5] (*o*-An = 2-methoxyphenyl) have been structurally characterised using X-ray crystallography.

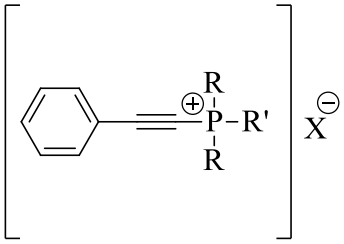

R = R' = Bu, X = Cl, Br
R = R' = Ph, X = Cl, Br, I
R = R' = Me, X = Br, $PhC{\equiv}CAuBr$, $(C_6F_5)C{\equiv}CAuBr$
R = Me, R' = Ph, X = Br
R = *o*-$(MeO)C_6H_4$, R' = Ph, X = Br, BF_4
R = R' = *p*-$(MeO)C_6H_4$, X = Br

Figure 1.2. Currently known phenylethynylphosphonium derivatives.

Structural properties related to these compounds are significant because it has been recently discovered that [PhC≡CPPh$_3$]Br is capable of inhibiting the mammalian protein HSP70 and its bacterial analogue DnaK by binding to C-terminal allosteric pockets within these proteins *via* its phenylacetylene fragment.[12] These proteins are important for mediating a wide variety of cellular functions, particularly during periods of increased cellular stress, and are essential for the survival of tumour cells.[12] Recent studies have demonstrated that the inhibition of these proteins with [PhC≡CPPh$_3$]Br is a promising strategy for the treatment of cancers that heavily rely on HSP70 or DnaK, such as multiple myeloma.[12-14] Evidence that the phenylacetylene fragment interacts significantly with DnaK was provided by protein crystallography**,** and it was shown that these interactions are primarily due to the complimentary shape of the phenylacetylene fragment with the allosteric pockets within these proteins.[12] The resolution limit for the structure of DnaK-[PhC≡CPPh$_3$]Br was 3.45 Å, which is suitable for protein crystallography but inadequate for elucidating any fine structural details of the inhibitor that could allow fine-tuning of structural features of the ethynylphosphonium species. Some closely related compounds involving the acetylenic fragment either σ- or π-bound to a metal,[23-25] or cationic phosphorus heterocycles have been structurally characterised,[26-28] but these examples are too specific to provide representative structural details that may be relevant for further applications. Limited information is also available for the electrochemical properties of these compounds; only one cyclic voltammetry study could be found which included [PhC≡CPPh$_3$]Br.[29]

The closely related bis(ethynylphosphonium) salts are much less common in the literature; all known bis(ethynylphosphonium) salts separated by an organic linker are

shown in Figure 1.3. Beyond demonstrating their syntheses, these compounds have received very little attention despite being likely to exhibit chemistry similar to their related mono-substituted analogues. The initially published synthesis required the carbodiphosphorane $Ph_3P{=}C{=}PPh_3$, limiting the scope of these compounds to phenyl substituents attached to phosphorus.[19] A more recent synthesis has also been reported,[20] but is also undesirable because it requires multiple steps to complete and produces multiple equivalents of toxic Bu_3SnCN as waste. For reaction schemes, see section 1.1.1.2.

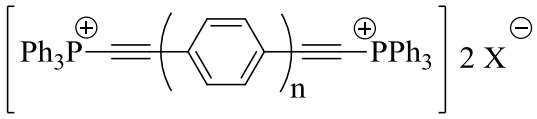

n = 1 X = Cl, OTf n = 2 X = OTf

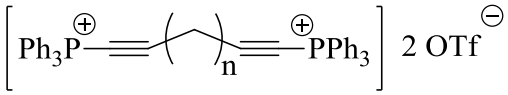

n = 2, 4, 5

Figure 1.3. Currently known bis(ethynylphosphonium) derivatives in which the ethynylphosphonium fragment is separated by an organic linker.

Considering recent developments in the medicinal properties of these compounds and their relevance in organic synthesis, it seemed prudent to reinvestigate several of these mono(ethynylphosphonium) salts to determine their structural features and to consolidate the characterisation data in the literature. Additionally, a simplified and more environmentally benign approach to the synthesis for bis(ethynylphosphonium) salts is reported herein to expand the applications of these compounds that are potentially useful for organic synthesis.

1.1.1 Synthesis of Ethynylphosphonium Salts

1.1.1.1 Mono(phenylethynyl)phosphonium Salts

The earliest synthetic routes towards phenylethynylphosphonium salts were discovered while studying nucleophilic substitution reactions at acetylenic carbons, specifically between triphenyl- or tributylphosphine and 1-bromo-2-phenylacetylene (Scheme 1.1).[15] Kinetic studies suggest that triphenylphosphine may follow both paths A and C, while tributylphosphine prefers to react according to path C (Scheme 1.1).[15] Pathway C is proposed based on products obtained after quenching the reaction with methanol (reaction E).[15] Kinetic data was also collected for both 1-chloro- and 1-bromo-2-phenylacetylene, and indicated that paths A and C are prevalent for 1-chloro-2-phenylacetylene, while 1-bromo-2-phenylacetylene follows path C.[15] Regeneration of the carbon-carbon triple bond in the intermediate **1** (reaction B), or nucleophilic addition by the acetylide to the phosphonium cation of **2** (reaction D) afford the desired ethynylphosphonium salts **3** (Scheme 1.1).[15]

Unfortunately 1-chloro- and 1-bromo-2-phenylacetylene are prohibitively expensive, so synthesising these starting materials is the first step. Early synthetic routes to 1-bromo-2-phenylacetylene often utilised aqueous alkaline mixtures of bromine (Br_2) with phenylacetylene,[2,30] however this reaction is rather inconvenient because it requires at least 60 hours to reach completion, 800 mL of water as the solvent, and the use of a large mechanical shaker. The benefit of this route is that it allows for a relatively large scale, with the above time and volume suitable for approximately 100 g of 1-bromo-2-phenylacetylene.[2,30] Alternatively 1-chloro-2-phenylacetylene can be prepared using a similar procedure and with some phosphines even displayed higher rates of substitution.[2]

Unfortunately chlorine (Cl_2) gas was required for these earlier procedures making this synthetic route even less convenient.[2,30] Early reports of the analogous reactions with 1-iodo-2-phenylacetylene could not be found.

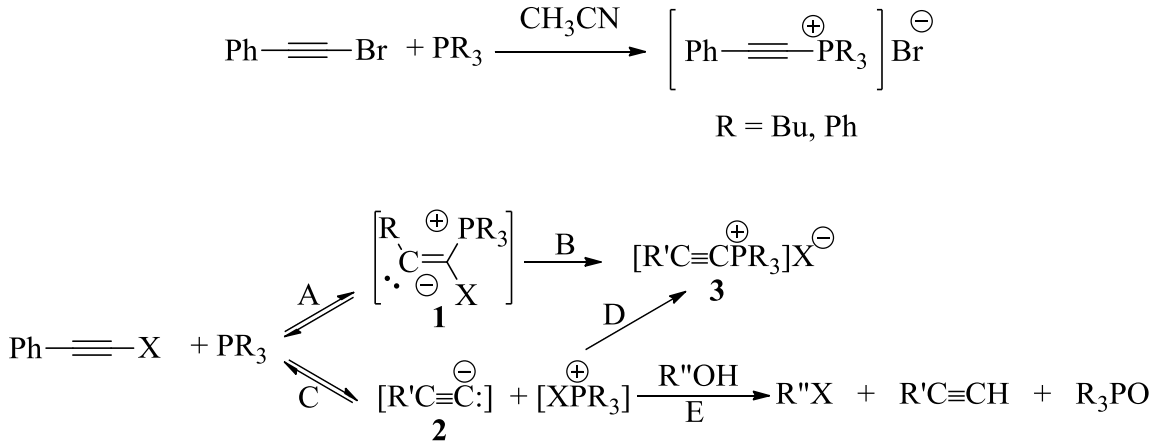

Scheme 1.1. Earliest synthetic route to ethynylphosphonium salts.

An alternative and efficient synthesis of 1-haloalkynes has since been reported,[31] which uses DBU (DBU = 1,8-diazabicyclo(5.4.0)undec-7-ene), *N*-haloimides and terminal alkynes. When this new synthetic route is used, multi-gram quantities of 1-bromo-2-phenylacetylene can be prepared within several minutes, followed by purification *via* flash chromatography and also allows for the synthesis of dibromoethynylacetylenes (Scheme 1.2).

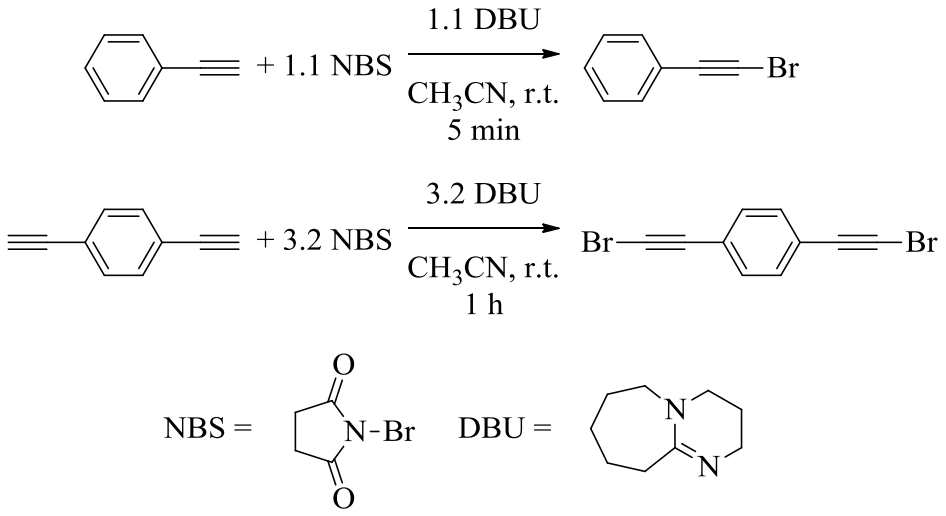

Scheme 1.2. Synthetic route to 1-bromoalkynes used during this project. Equivalents of NBS and DBU were based on optimised syntheses.[31]

Aside from nucleophilic substitution reactions, the only other synthetic route to mono(ethynylphosphonium) salts incorporates aromatic acid chlorides and hexaphenylcarbodiphosphorane as starting materials (Scheme 1.3). The authors of the paper claim to generate a diphosphorus species which eliminates triphenylphosphine oxide upon heating to generate the corresponding mono(ethynylphosphonium) salts.[19] Unfortunately ^{1}H and $^{13}C\{^{1}H\}$ NMR spectroscopic data were not reported; compounds were characterised by melting point, elemental analysis (no values provide, only statements they were correct), IR (only C≡C stretches provided), and ^{31}P NMR spectroscopies. Details regarding the preparation of samples for analysis are also not provided; such as method of preparation of IR samples (i.e. KBr pellet or NaCl/Nujol mull), and the solvent used for NMR spectroscopic analysis.

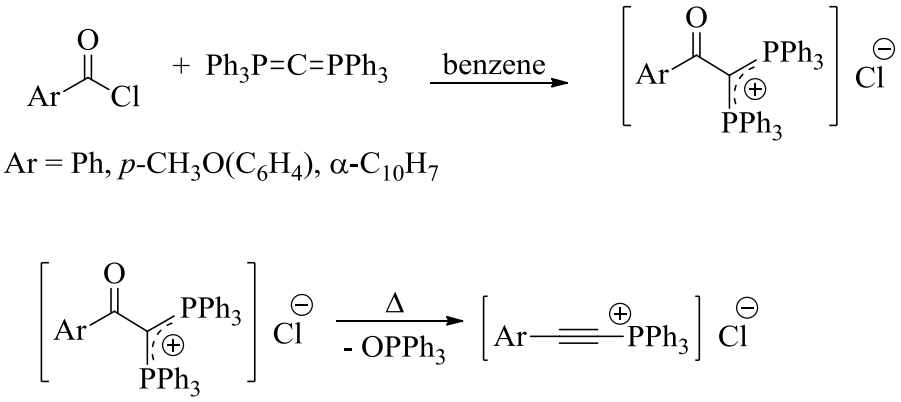

Scheme 1.3. Synthetic route to mono(ethynylphosphonium) salts *via* phosphine oxide elimination (α-$C_{10}H_7$ = 1-naphthyl).

1.1.1.2 Bis(ethynylphosphonium) Salts

The first reported preparation of a bis(ethynylphosphonium) salt occurred in 1977 using the phosphine oxide elimination route.[19] Reaction of terephthaloyl dichloride and hexaphenylcarbodiphosphorane furnishes the bis(ethynylphosphonium) salt $[Ph_3PC{\equiv}C(C_6H_4)C{\equiv}CPPh_3]Cl_2$ after heating (Scheme 1.4). Unfortunately, like the monoethynylphosphonium salts prepared using the same route, this compound was characterised by only melting point, IR (only C≡C stretches provided), and ^{31}P NMR spectroscopies with only vague details for sample preparation provided.

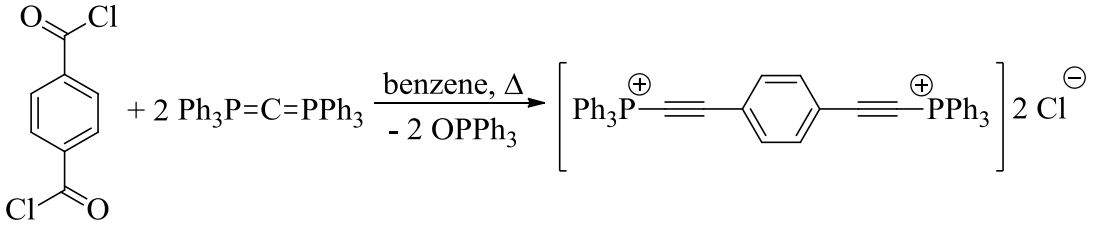

Scheme 1.4. Earliest reported synthesis of a bis(ethynylphosphonium) salt.

Only one alternative synthesis has been reported since 1977, and is essentially a modification of the nucleophilic substitution reactions reported earlier for monoethynyl species (Scheme 1.5).[20] The key difference to this route in comparison to the haloacetylene

routes is that the leaving group is much better; 1-iodobenzene is a much weaker base (and therefore a superior leaving group) than any halogen consequently making the nucleophilic substitution reaction much more favourable.

Reaction between a bis(tributyl)tin diacetylene and Stang's reagent, [PhICN][OTf], yields the corresponding bis(phenyliodonium) diyne triflate salts, which can then be combined with triphenylphosphine to afford the bis(ethynylphosphonium) triflate salts (Scheme 1.5).[20] The bis(ethynylphosphonium) triflate salts were verified on the basis of strong C≡C stretches ranging from 2205–2171 cm^{-1} in the IR spectra, consistent with known mono(ethynylphosphonium) salts and the bis(ethynylphosphonium) salt $[Ph_3PC{\equiv}C(C_6H_4)C{\equiv}CPPh_3]Cl_2$,[20] in addition to multinuclear (^1H, ^{13}C, ^{19}F, and ^{31}P) NMR spectroscopies and fast atom bombardment high resolution mass spectrometry (FAB HRMS).[20]

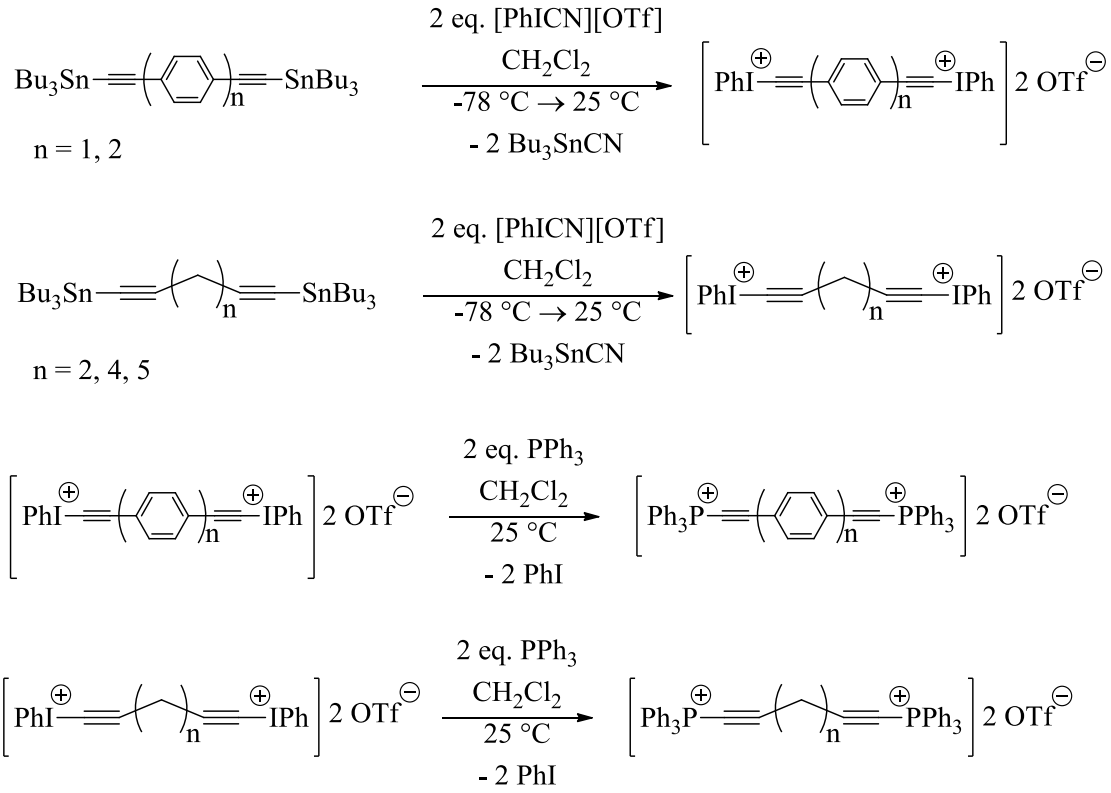

Scheme 1.5. Synthesis of bis(ethynylphosphonium) salt using phenyliodonium salts.

Interestingly, the ethynylphosphonium triflate salts exhibited singlets in their ^{31}P NMR spectra between δ 6–8 ppm in CD_3CN, which the authors claim is characteristic of an acetylenic phosphonium species.[20] This appears to be contrary to the earlier reports given with the synthesis of $[Ph_3PC{\equiv}C(C_6H_4)C{\equiv}CPPh_3]Cl_2$ (δ = -6.5 ppm),[19] in which the authors suggest the low chemical shifts in the ^{31}P NMR spectra are a result of strong interactions between the π-electrons of the acetylenic fragment and the phosphorus cation.[19] This conclusion is debatable when the corresponding alkyl mono(ethynylphosphonium) salt $[MeC{\equiv}CPPh_3]Br$ is considered, which resonates at δ 5.3 ppm in $CDCl_3$, and should display similar interactions.[32] Interestingly, the possibility of triphenylphosphine (δ -6.0 ppm)[33] being present in the reaction mixture was not discussed. However, it is difficult to make comparisons between the chloride and triflate

ethynylphosphonium salts because the anions are significantly different; furthermore the solvent used for collecting the ^{31}P NMR spectrum for $[Ph_3PC{\equiv}C(C_6H_4)C{\equiv}CPPh_3]Cl_2$ was not reported.[19] Unfortunately no further studies have been carried out on these compounds; rather, the primary focus of the journal article was to discuss synthesis and reactivity of the bis(phenyliodonium) diyne triflate salts instead.[20]

1.1.2 Other Pnictogen Derivatives

A precursory survey of the literature revealed that analogues of ethynylphosphonium salts with the remaining pnictogens N,[34] As,[35,36] Sb,[37] and Bi,[38,39] are also known. The number of examples decline with an increase of the period: nitrogen and phosphorus analogues are the most studied, while arsenic, antimony, and bismuth analogues are the least. Early kinetic studies involving haloacetylenes and tertiary amines have indicated that the isolated products are quite dependent on the reaction conditions.[34,40] Ethynylarsonium derivatives can be prepared in a similar fashion to the phenyliodonium route outlined for ethynylphosphonium salts,[36] but are also accessible *via* quaternisation using methyliodide.[35] Ethynylstibonium analogues are also accessible using methyliodide and has even lead to the synthesis of the bis(ethynylstibonium) salt $[(iPr)_2MeSbC{\equiv}CSbMe(iPr)_2]I_2$.[37] Ethynylbismuthonium salts were first synthesised using triphenylbismuth difluoride, alkynylisopropoxyboranes and $BF_3{\cdot}OEt_2$, and the *tert*-butyl derivative $[t\text{BuC}{\equiv}\text{CBiPPh}_3][BF_4]$ has been structurally characterised by X-ray crystallography.[38]

1.2 Experimental

All manipulations were carried out under an inert atmosphere of dry nitrogen or argon gas using either standard Schlenk techniques or in an mBraun inert atmosphere glovebox unless otherwise stated. Calculations (B3LYP,[41-44] 6-31G(d)[45]) were completed using the Gaussian 09W suite of programs[46] and results were visualised using the program GaussView.[47] Glassware was dried for a minimum of four hours prior to use in a 150 °C oven. Alumina and 4 Å molecular sieves were pre-dried in an oven at 150 °C for one day prior to drying at 300 °C *in vacuo*. Celite and silica gel were dried by storing in a 150 °C oven for a minimum of three days prior to use. NMR solvents were purchased from Cambridge Isotope Laboratories, Inc. and stored over 4 Å molecular sieves for a minimum of one day prior to use. NMR spectra were recorded at 298 K on a 300 MHz spectrometer (Bruker) unless otherwise indicated and are reported in ppm. ^{1}H NMR spectra are collected in deuterated (^{2}H, defined as D) solvents and referenced[48] internally to either residual protio (^{1}H) solvents relative to tetramethylsilane, TMS (δ = 0 ppm), or using an internal TMS standard ($CDCl_3$ only). The $^{13}C\{^{1}H\}$ NMR spectra were referenced[48] internally to the respective deuterated solvents in which they were collected relative to TMS (δ = 0 ppm). ^{31}P NMR chemical shifts are referenced to an external standard of 85% phosphoric acid (δ = 0 ppm). Coupling constants are reported in Hz and are given as absolute values. IR spectra were collected as KBR pellets using an ALPHA FT-IR spectrometer (Bruker) unless otherwise indicated. Melting points were recorded on an Electrothermal MEL-Temp 3.0 using glass capillaries sealed under inert conditions. Elemental analysis was performed by the Centre for Environmental Analysis and Remediation (CEAR) facility at Saint Mary's University using a Perkin Elmer 2400 II series Elemental Analyser. Deionised

water was used in synthetic procedures unless otherwise indicated. Dichloromethane (Caledon Laboratory Chemicals), diethyl ether (ACP Chemicals Inc.), THF (Caledon Laboratory Chemicals), toluene (Caledon Laboratory Chemicals) and pentane (Fisher Scientific) were dried using an alumina-based solvent purification system from Vacuum Atmospheres. Diethyl ether, THF, toluene and pentane were further dried using KH followed by filtration through alumina and stored over 4 Å molecular sieves. Dichloromethane was stored over 4 Å molecular sieves for a minimum of three days prior to use. Acetonitrile (Fisher Scientific) was pre-dried using CaH_2 before drying with P_2O_5, and purified by distillation. All reagents were purchased from Sigma-Aldrich and used as received, unless otherwise noted. Isopropyldiphenylphosphine was purchased from Alfa Aesar and used without further purification.

1.2.1 X-ray crystallography

Under inert conditions, crystals were prepared for mounting by suspending them in paratone-N oil on a microscope slide. Crystals were attached to the tip of an appropriately sized MiTeGen loop with paratone-N oil and cooled to 125 K. Measurements were made on a Bruker APEX2 CCD equipped diffractometer (30 mA, 50 mV) using monochromated Mo Kα radiation (λ = 0.71073 Å) at 125 K. The initial orientation and unit cell were indexed[49] using a least-squares analysis of a random set of reflections collected from three series of 0.5° wide scans, 10 seconds per frame and 12 frames per series that were well distributed in reciprocal space. For data collection, four ω-scan frame series were collected with 0.5° wide scans and 366 frames per series at varying φ angles (φ = 0°, 90°, 180°, 270°). The frame length was adjusted between 10 s and 60 s to provide an expected resolution limit below 0.8 Å. The crystal to detector distance was set to 6 cm and a complete

sphere of data was collected. Cell refinement and data reduction were performed with the Bruker SAINT software,[50] which corrects for beam inhomogeneity, possible crystal decay, Lorentz and polarization effects. Data processing and a multi-scan absorption correction was applied using the APEX3 software package.[50] Structures were solved using direct[50] or intrinsic methods[51] and all non-hydrogen atoms were refined anisotropically using the ShelXLE[52] graphical user interface and SHELXL.[53] Hydrogen atoms were included at geometrically idealized positions and were fixed (Ar-H, C-H, CH_2) or in the case of methyl groups, the dihedral angle of the idealized tetrahedral CH_3 fragment was allowed to refine, and coupled with isotropic temperature factors. Figures were made using ORTEP-3 for Windows.[54]

During the refinement of **3**, one molecule was present along a three-fold axis. This caused disorder in the phenyl ring. This was modelled by fixing the site occupancies of C36, C37, and C38 to 0.3333, and 0.5000 for C39 and C40. The atoms P2, Br1, and Br3 were also part of this disorder and their occupancies were fixed at 0.3333, 0.1667, and 0.1667, respectively. Toluene had co-crystallised with **3** and also exhibited disorder along a three-fold axis. C51, C52, and C53 were part of this disorder and were modelled using the PART-1 command. The site occupancy for C53 was fixed to 0.3333. The thermal ellipsoids of C10, O1, and C15 were restrained to be approximately isotropic using the ISOR command.

During the refinement of **4a**+**b**, substitutional disorder was encountered in the atoms attached to C1 (either H1 or C35). This was modelled using the PART command and the site occupancies were allowed to freely refine. Disorder was also modelled for some of the

methoxy substituents using the PART command, with site occupancies freely refined. The anisotropic displacement paramters of C16a, C16b, C1, and C35 were constrained using the EADP command.

During the refinement of **6**, the butyl groups were disordered and different components of the disorder were separated using the PART command. Site occupancies were allowed to freely refine. Rigid bond restraints were applied using the RIGU command. The thermal ellipsoid of C7B was restrained to be approximately isotropic using the ISOR command. For the butyl groups, P-C bond lengths, 1,2-distances, and 1,3-distances were restrained appropriately using the DFIX command.

During the refinement of **7**, disorder was encountered in a molecule of co-crystallised dichloromethane. Different components of the disorder were separated using the PART command. Site occupancies were allowed to freely refine. Distances between C-Cl were restrained to be approximately equal using the SADI command, and restrained using the DFIX command.

1.2.2 Synthesis of PhC≡CBr

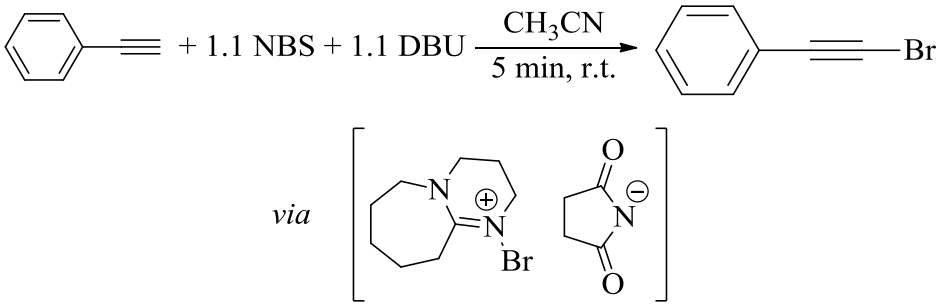

Following a procedure similar to what was reported in the literature,[31] in a 250 mL Erlenmeyer flask, 5.02 g (49.0 mmol, 1 eq.) of orange coloured phenylacetylene were dissolved in 100 mL of acetonitrile producing a pale yellow coloured solution. To this

solution, 9.88 g (55.4 mmol, 1.13 eq.) of colourless NBS were added, producing a brownish-orange coloured mixture. Subsequent addition of 8.30 g (54.5 mmol, 1.11 eq.) of pale yellow coloured DBU *via* syringe instantly produced a warm, bright orange coloured mixture with a copious amount of colourless precipitate, presumably caused by the transfer of Br from NBS to DBU.[31] Shortly after the mixture turned brown in colour and no further change was observed for the duration of the reaction. After one hour, 100 mL of water were added, producing a dark brown coloured mixture. After stirring for *ca*. 5 minutes, the reaction mixture was transferred into a 250 mL separatory funnel and extracted with CH_2Cl_2 (3 x 75 mL). The brown coloured organic layers were combined and washed with water (2 x 60 mL) before removing the solvent *via* rotary evaporation which produced a viscous yellow coloured liquid. This residue was extracted with *ca*. 200 mL pentane, and passed through a silica gel plug yielding a pale yellow coloured solution. Removal of the pentane by rotary evaporation yielded a pale yellow coloured liquid which darkened upon storage at ambient temperature.

Yield: 7.07 g (80 %)

^{1}H NMR ($CDCl_3$): δ 7.45–7.42 (m, 2H), 7.33–7.25 ppm (m, 3H).

1.2.3 Synthesis of 1,4-BrC≡C(C$_6$H$_4$)C≡CBr

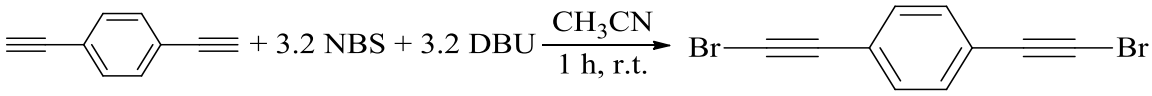

Following a procedure similar to what was reported in the literature,[31] in a 250 mL Erlenmeyer flask, 1.98 g (15.7 mmol, 1 eq.) of orange coloured 1,4-diethynylbenzene crystals were dissolved in 100 mL of acetonitrile producing a reddish-orange coloured

solution. To this solution, 8.99 g (50.5 mmol, 3.22 eq.) of colourless NBS were added, producing a brownish-orange coloured mixture. Subsequent addition of 7.75 mL (51.8 mmol, 3.31 eq.) of pale yellow coloured DBU *via* syringe instantly produced a warm, bright orange coloured mixture with a copious amount of colourless precipitate. Shortly after the mixture turned brown in colour and no further change was observed for the duration of the reaction. After one hour, 100 mL of water were added, producing a dark brown coloured mixture. After stirring for *ca*. 5 minutes, the reaction mixture was transferred into a 250 mL separatory funnel and extracted with CH_2Cl_2 (3 x 75 mL). The brown coloured organic layers were combined and washed with water (2 x 60 mL) before removing the solvent *via* rotary evaporation, which produced a brown coloured solid. This solid was extracted with *ca*. 100 mL pentane, and passed through a silica gel plug yielding a colourless solution. Removal of the pentane by rotary evaporation yielded a minimal amount of colourless powder which was identified as the desired product by comparing the ^{1}H chemical shifts with those reported in the literature. The brown coloured residue was dissolved in *ca.* 10 mL of CH_2Cl_2 and another 100 mL of pentane were added before transferring the brown coloured mixture to a silica gel plug and eluting with pentane (3 x 250 mL), yielding a bright yellow coloured solution each time. Removal of the pentane solvent yielded bright yellow coloured crystals which were impure by ^{1}H NMR spectroscopy. These were dissolved in pentane before repeating the work up once more which yielded extremely pale yellow coloured crystals that were pure by ^{1}H NMR spectroscopy.

Yield: 1.85 g (41 %)

^{1}H NMR ($CDCl_3$): δ 7.37 ppm (s, 4H).

1.2.4 Synthesis of [PhC≡CPBu$_3$]Br – 1

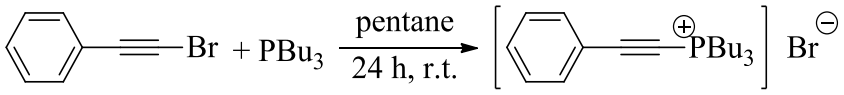

In a 20 mL scintillation vial, 2.00 g (11.0 mmol) of pale yellow coloured 1-bromo-2-phenylacetylene liquid were dissolved in 10 mL of pentane producing a pale yellow coloured solution. To this solution, 2.24 g (2.76 mL, 11.1 mmol, 1.01 eq.) of colourless tributylphosphine liquid were added dropwise, immediately producing a beige coloured precipitate. Further addition of tributyl phosphine produced a dark brown coloured viscous oil. This mixture was left to stir overnight. The following day the stirring was stopped and the pentane was decanted off, and contents of the flask were washed with a small amount of THF and dried *in vacuo*, producing a dark brown coloured oil which crystallised upon standing overnight. These crystals were not of suitable quality for X-ray diffraction, and so the brown mixture of oil/crystals was triterated multiple times with *ca*. 5 mL of pentane, and dried *in vacuo* to produce a brown coloured powder.

Yield: 3.55 g (84%)

EA: Calc. for $C_{20}H_{32}PBr$: C: 62.66 %, H: 8.41 %, N: 0.00 %. Found: C: 61.15 %, H: 8.21 %, N: 0.02 %.

m.p. (°C): 71.7–72.0.

^{31}P{^{1}H} NMR (CD_2Cl_2): δ 21.5 ppm (s).

^{1}H NMR (CD_2Cl_2): δ 7.68–7.63 (m, 2H), 7.60 (tt, $^{3}J_{HH}$ = 7.5 Hz, $^{4}J_{HH}$ = 2.3 Hz, 1H), 7.48 (t, $^{3}J_{HH}$ = 7.5 Hz, 2H), 2.87–2.78 (m, 6H), 1.69–1.66 (m, 6H), 1.57 (sextet, $^{3}J_{HH}$ = 7.4 Hz, 6H), 0.99 ppm (t, $^{3}J_{HH}$ = 7.3 Hz, 9H).

^{13}C{^{1}H} NMR (CD_2Cl_2): δ 133.2 (d, $^{4}J_{CP}$ = 2.2 Hz, *o*-(C_6H_5)), 132.7 (s, *m*-(C_6H_5)), 129.3 (s, *p*-(C_6H_5)), 118.1 (d, $^{3}J_{CP}$ = 4.4 Hz, P-C≡C-C), 114.2 (d, $^{2}J_{CP}$ = 23.2 Hz, P-C≡C), 69.5 (d, $^{1}J_{CP}$ = 149.5 Hz, P-C≡C), 24.7 (d, $^{2}J_{CP}$ = 5.5 Hz, CH_2), 24.0 (d, $^{3}J_{CP}$ = 16.6 Hz, CH_2), 22.6 (d, $^{1}J_{CP}$ = 53.3 Hz, CH_2), 13.6 ppm (s, CH_3).

IR (KBr pellet): ν 3054 (w), 3013 (m), 2960 (vs), 2932 (vs), 2903 (s), 2869 (vs), 2179 (vs, C≡C), 1623 (w), 1489 (s), 1462 (s), 1446 (s), 1402 (m), 1382 (m), 1314 (w), 1283 (m), 1231 (m), 1206 (w), 1185 (w), 1158 (w), 1099 (s), 1027 (w), 1003 (w), 967 (w), 911 (s), 866 (s), 819 (m), 767 (vs), 726 (m), 695 (s), 635 (w), 540 (m), 466 (w), 446 cm^{-1} (w).

Attempts at producing crystals suitable for X-ray diffraction from the brown coloured powder using standard methods (evaporation, vapour diffusion, solvent layering) were unsuccessful. To obtain crystals suitable for X-ray diffraction, the reaction was repeated under the following conditions: In a 20 mL test tube, 0.239 g (1.32 mmol) of pale yellow coloured 1-bromo-2-phenylacetylene liquid were added and cooled to -35 °C using a freezer. Once cooled, 5 mL of pentane were layered over the bromophenylacetylene, and the mixture was cooled once again to -35 °C. This process was repeated once more for a total of 10 mL of pentane layered over the neat 1-bromo-2-phenylacetylene. The two layers were cooled to -35 °C before layering a colourless solution of 0.265 g (1.31 mmol, 0.99 eq.) of tributyl phosphine in 10 mL of pentane. The test tube was sealed using a rubber septum pierced with a needle and left to sit overnight. The following day the pentane was

decanted, and an incredibly viscous, pale yellow coloured oil remained in the bottom of the test tube. The oil readily crystallised upon standing to form pale yellow coloured crystals suitable for X-ray diffraction. The yield of this reaction was not recorded.

1.2.5 Synthesis of [PhC≡CPPh$_3$]Br – 2

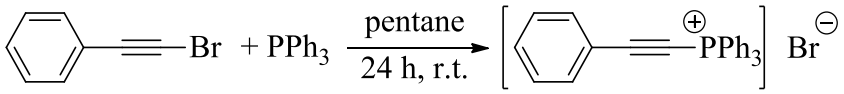

In a 100 mL round-bottomed flask, 4.00 g (22.1 mmol) of pale yellow coloured 1-bromo-2-phenylacetylene liquid were dissolved in 40 mL of pentane producing a pale yellow coloured solution. To this solution, 5.80 g (22.1 mmol, 1.0 eq.) of colourless triphenylphosphine granules were added, producing a pale yellow coloured mixture. This mixture was left to stir overnight. The following day the stirring was stopped and the contents of the flask were allowed to settle, producing a pale yellow coloured solution over a tan coloured precipitate. The pentane was decanted, and the residual solid was washed with pentane and dried *in vacuo* to afford a pale yellow coloured powder which was recrystallised from dichloromethane layered with pentane to afford pale yellow crystals.

Yield: 5.46 g (56 %)

EA: Calc. for $C_{26}H_{20}PBr$: C: 70.44 %, H: 4.55 %, N: 0.00 %. Found: C: 70.25 %, H: 4.43 %, N: 0.02 %.

m.p. (°C): 209.6–210.2.

$^{31}P\{^1H\}$ NMR ($CDCl_3$): δ 6.5 ppm (s).

^1H NMR ($CDCl_3$): δ 7.97–7.79 (m, 17H), 7.66 (tt, $^3J_{HH}$ = 7.5 Hz, $^4J_{HH}$ = 2.3 Hz, 1H), 7.55 ppm (t, $^3J_{HH}$ = 7.4 Hz, 2H).

$^{13}C\{^{1}H\}$ NMR ($CDCl_3$): δ 136.2 (d, $^{4}J_{CP}$ = 3.1 Hz, *p*-Ph_3) 133.7 (d, $^{4}J_{CP}$ = 2.2 Hz, *o*-(C_6H_5)), 133.5 (s, *m*-(C_6H_5)), 133.2 (d, $^{2}J_{CP}$ = 12.4 Hz, *o*-Ph_3), 131.1 (d, $^{3}J_{CP}$ = 14.2 Hz, *m*-Ph_3), 129.4 (s, *p*-(C_6H_5)), 118.7 (d, $^{2}J_{CP}$ = 31.4 Hz, P-C≡C), 118.0 (d, $^{1}J_{CP}$ = 100.3 Hz, *ipso*-Ph_3), 116.7 (d, $^{3}J_{CP}$ = 4.8 Hz, P-C≡C-C), 69.0 ppm (d, $^{1}J_{CP}$ = 188.0 Hz, P-C≡C).

IR (KBr pellet): ν 3046 (m), 3023 (m), 3014 (m), 2998 (m), 2985 (m), 2911 (w), 2584 (w), 2465 (w), 2167 (vs, C≡C), 2099 (m), 1810 (w), 1626 (w), 1584 (m), 1482 (m), 1317 (w), 1287 (w), 1261 (w), 1234 (w), 1185 (w), 1163 (w), 1113 (vs), 1025 (w), 997 (m), 930 (w), 871 (s), 840 (m), 803 (w, br), 770 (s), 759 (s) 750 (m), 727 (vs), 701 (s), 687 (vs), 655 (m), 621 (w), 543 (s), 523 (vs), 495 (s), 460 cm^{-1} (w).

1.2.6 Synthesis of [PhC≡CP(C_6H_2(OMe)$_3$)]Br – 3

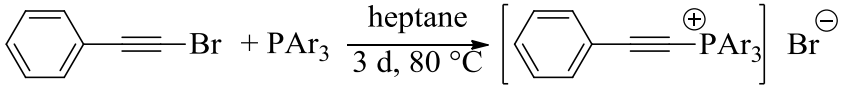

Ar = 2,4,6-$(MeO)_3C_6H_2$

In a 100 mL sealed reaction vessel, 0.882 g (1.66 mmol) of colourless tris(2,4,6-trimethoxyphenyl)phosphine were suspended in 25 mL of heptane producing a colourless suspension. To this suspension, 0.319 g (1.76 mmol, 1.06 eq.) of pale yellow coloured 1-bromo-2-phenylacetylene were added, producing a pale yellow coloured mixture. This mixture was warmed to 80 °C and left to stir for three days, monitoring by $^{31}P\{^{1}H\}$ NMR spectroscopy. The reaction did not reach completion after three days at 80 °C but a new signal appeared in the $^{31}P\{^{1}H\}$ NMR spectrum with an integration of 0.6:1 with respect to starting material. The stirring was stopped and the contents of the flask were allowed to settle, producing a pale yellow coloured mixture. The heptane was decanted off before suspending the contents of the flask in *ca.* 10 mL of pentane and transferring to a vial. The

pentane was decanted, and the residual solid was washed with 3 x 15 mL portions of toluene and dried *in vacuo* to afford a colourless powder. Large colourless block-shaped crystals suitable for X-ray analysis were obtained by dissolving the phosphonium salt in a 5:1 mixture of toluene and acetonitrile and allowing the mixture to slowly evaporate.

Yield: 0.10 g (8 %)

EA: Calc. for $C_{35}H_{38}O_9PBr$: C: 58.91 %, H: 5.37 %, N: 0.00 %. Found: C: 59.52 %, H: 5.70 %, N: 0.04 %.

m.p. (°C): 94.1–94.7.

$^{31}P\{^1H\}$ NMR (CD_3CN): δ -27.7 ppm (s).

^1H NMR (CD_3CN): δ 7.56–7.48 (m, 3H, *o*-C_6H_4, *p*-C_6H_4), 7.46-7.40 (m, $^3J_{HH}$ = 7.6 Hz, $^3J_{HH}$ = 6.8 Hz, 2H, *m*-C_6H_4), 6.28 (d, $^4J_{Hp}$ = 5.8 Hz, 6H, *m*-ArH_2), 3.88 (s, 9H, *p*-OCH_3) 3.61 ppm (s, 18H, *o*-OCH_3).

$^{13}C\{^1H\}$ NMR (CD_3CN): δ 167.5 (s, *p*-ArC), 165.1 (d, $^2J_{CP}$ = 1.6 Hz, *o*-ArC), 133.1 (d, $^4J_{CP}$ = 2.3 Hz, *o*-C_6H_5), 131.8 (s, *p*-C_6H_5), 129.9 (s, *m*-C_6H_5), 121.3 (d, $^3J_{CP}$ = 4.9 Hz, *ipso*-C_6H_5), 102.9 (d, $^2J_{CP}$ = 36.6 Hz, P-C≡C), 93.0 (d, $^3J_{CP}$ = 7.5 Hz, *m*-ArC), 92.1 (d, $^1J_{CP}$ = 126.8 Hz, *ipso*-ArC), 77.9 (d, $^1J_{CP}$ = 205.5 Hz, P-C≡C), 57.1 (s, *o*-OCH_3), 56.7 ppm (s, *p*-OCH_3).

IR (KBr pellet): ν 3181 (w), 3001 (m), 2940 (s), 2840 (m), 2186 (vs, C≡C), 2080 (w), 1937 (w), 1604 (vs), 1466 (vs), 1412 (vs), 1340 (vs), 1301 (m), 1234 (vs), 1208 (vs), 1161 (vs), 1127 (vs), 1098 (vs), 1024 (s), 949 (m), 917 (m), 858 (m), 816 (s), 762 (m), 735 (w), 693 (vs), 646 (w), 588 (w), 535 (m), 482 (vs), 444 cm^{-1} (m).

1.2.7 Synthesis of 3 + Ring-closed isomers – 4a,b

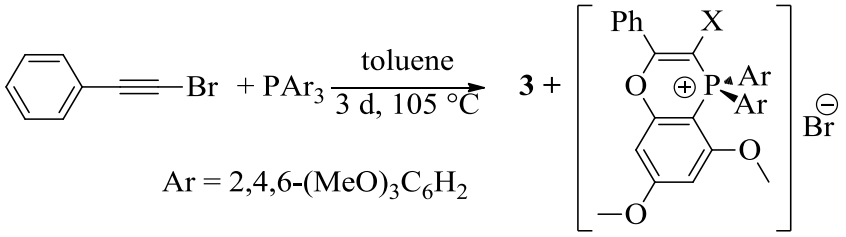

4; **(a)** X = H, **(b)** Me

Following the same procedure as for synthesis of **3** using instead toluene as the solvent, the reaction was repeated at 105 °C using 0.300 g (1.66 mmol, 1 eq.) of 1-bromo-2-phenylacetylene and 0.853 g (1.60 mmol, 0.96 eq.) of tris(2,4,6-trimethoxyphenyl)phosphine. The pale yellow coloured reaction mixture was left to sit for three days without stirring. After this time, a red coloured reaction mixture was present with red coloured crystals on the side of the flask. These were analysed by X-ray diffraction and were revealed to be cyclised by-products. The red coloured supernatant was decanted off, and the red coloured crystals were washed with 3 x 15 mL portions of pentane and dissolved in 20 mL of acetonitrile. The red coloured acetonitrile mixture was filtered through Celite, and the solvent was removed *in vacuo* to produce a brown coloured semi-solid that was triturated with 10 mL of pentane to produce a brown coloured powder containing a mixture of **3**, **4a** and **4b**.

Yield: 0.76 g (in a 2.7:2.5:1 ratio from the ^{31}P NMR spectrum for **3**:**4a**:**4b**)

$^{31}P\{^{1}H\}$ NMR (CD_3CN): δ **4a** -21.9 (s); **4b** 0.0 ppm (s).

1.2.8 Synthesis of [PhC≡CP(iPr)Ph$_2$]Br – 5

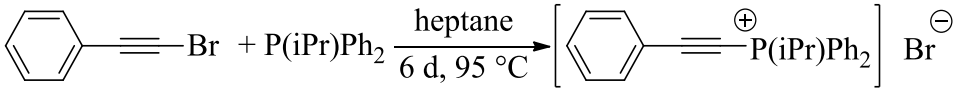

In a 100 mL sealed reaction vessel, 0.593 g (2.60 mmol) of colourless isopropyldiphenylphosphine were suspended in 25 mL of heptane. To this suspension, 0.437 g (2.41 mmol, 0.93 eq.) of pale yellow coloured 1-bromo-2-phenylacetylene were added, producing a pale yellow coloured mixture. This mixture was warmed to 95 °C and left to stir for six days to ensure reaction completion, but showed no visible changes after the first day. The stirring was stopped and the contents of the flask were allowed to settle, producing a pale yellow coloured mixture. The heptane was decanted before suspending the contents of the flask in *ca.* 10 mL of pentane and transferring to a vial. The pentane was decanted, and the residual solid was washed with 3x15 mL portions of toluene and dried *in vacuo* to afford a colourless powder. Long needle-like colourless crystals suitable for X-ray analysis were obtained by dissolving the phosphonium salt in a 5:1 mixture of toluene and acetonitrile and allowing the mixture to slowly evaporate.

Yield: 0.32 g (32 %)

EA: Calc. for $C_{23}H_{22}PBr$: C: 67.49 %, H: 5.42 %, N: 0.00 %. Found: C: 66.82 %, H: 5.25 %, N: 0.04 %.

m.p. (°C): 151.9–152.3.

$^{31}P\{^{1}H\}$ NMR (CD_2Cl_2): δ 24.0 ppm (s).

^{1}H NMR (CD_2Cl_2): δ 8.35 (dd, $^{3}J_{HP}$ = 14.0 Hz, $^{3}J_{HH}$ = 7.6 Hz, 4H, *o*-C_6H_5), 7.86 (d, $^{3}J_{HH}$ = 7.6 Hz, 2H), 7.80–7.66 (m, 7H), 7.57 (t, $^{3}J_{HH}$ = 7.6 Hz 2H), 4.84 (oct, $^{3}J_{HH}$ = 7.0 Hz, 1H, C*H*(CH_3)$_2$), 1.39 ppm (dd, $^{2}J_{HP}$ = 21.5 Hz, $^{3}J_{HH}$ = 6.9 Hz, 6H, CH(C*H*$_3$)$_2$).

$^{13}C\{^{1}H\}$ NMR (CD_2Cl_2): δ 135.3 (d, $^{4}J_{CP}$ = 3.1 Hz, *p*-Ph_2), 133.7 (d, $^{4}J_{CP}$ = 2.2 Hz, *o*-C_6H_5), 133.4 (s, *p*-C_6H_5) 133.1 (d, $^{2}J_{CP}$ = 11.8 Hz, *o*-Ph_2), 130.6 (d, $^{3}J_{CP}$ = 13.8 Hz, *m*-Ph_2), 129.5 (s, *m*-C_6H_5), 118.5 (d, $^{1}J_{CP}$ = 93.4 Hz, *ipso*-Ph_2), 118.1 (d, $^{2}J_{CP}$ = 26.3 Hz, P-C≡C), 117.5 (d, $^{3}J_{CP}$ = 4.5 Hz, *ipso*-C_6H_5), 66.3 (d, $^{1}J_{CP}$ = 170.8 Hz, P-C≡C), 25.7 (d, $^{1}J_{CP}$ = 51.2 Hz, CH), 16.1 ppm (s, CH_3).

IR (KBr pellet): ν 3052 (m), 2974 (m), 2930 (m), 2834 (m), 2176 (vs, C≡C), 2098 (w), 1596 (m), 1485 (m), 1462 (m), 1439 (s), 1413 (w), 1388 (w), 1339 (w), 1265 (w), 1232 (m), 1208 (w), 1162 (m), 1110 (s), 1044 (w), 1025 (w), 997 (w), 871 (s), 811 (w), 762 (s), 725 (m), 692 (s), 626 (w), 542 (m), 519 (s), 480 cm^{-1} (w).

1.2.9 Synthesis of $[Bu_3PC{\equiv}C(C_6H_4)C{\equiv}CPBu_3]Br_2$ – 6

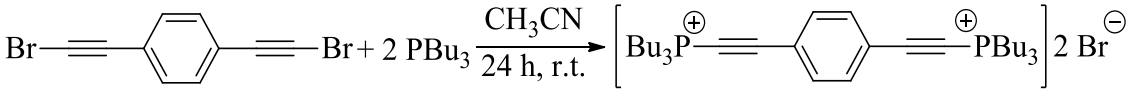

In a 20 mL scintillation vial, 0.166 g (0.584 mmol) of pale yellow coloured 1,4-di(bromoethynyl)benzene powder were combined with 5 mL of acetonitrile producing a pale yellow coloured mixture. To this mixture, 0.30 mL (1.20 mmol, 2.1 eq.) of colourless tributyl phosphine were added *via* syringe to produce an orange coloured mixture. After *ca.* 10 minutes, the colour of the reaction mixture changed to black and was left to stir overnight. The following day an aliquot was removed for $^{31}P\{^{1}H\}$ NMR spectroscopy and showed multiple signals with a small trace of the starting tributyl phosphine. Storage of a mixture of acetonitrile/diethyl ether (5 mL:5 mL) placed in a -35 °C freezer overnight produced oily, black coloured crystals suitable for X-ray crystallography. Subsequent washings with pentane produced a black coloured crystalline powder, however various by-products were still detected in the $^{31}P\{^{1}H\}$ NMR spectrum.

Yield: 0.07 g (16 %).

EA: Calc. for $C_{34}H_{58}P_2Br_2$: C: 59.31 %, H: 8.49 %, N: 0.00 %. Found: C: 59.45 %, H: 8.54 %, N: 0.07 %.

m.p. (°C): 112.4–113.0.

$^{31}P\{^1H\}$ NMR (CD_2Cl_2): δ 18.5 ppm (s, 2P).

^1H NMR (CD_2Cl_2): δ 7.73 (s, 4H, C_6H_4), 2.87–2.78 (m, 12H), 1.74–1.66 (m, 12H), 1.60–1.48 (sextet, $^3J_{HH}$ = 7.3 Hz, 12H), 0.96 ppm (t, $^3J_{HH}$ = 7.3 Hz, 18H).

$^{13}C\{^1H\}$ NMR (CD_2Cl_2): δ 133.5 (d, $^4J_{CP}$ = 2.2 Hz, *o*-(C_6H_4)), 121.5 (d, $^3J_{CP}$ = 4.4 Hz, *ipso*-(C_6H_4)), 111.5 (d, $^2J_{CP}$ = 22.7 Hz, P-C≡C), 73.5 (d, $^1J_{CP}$ = 146.1 Hz, P-C≡C), 24.5 (d, $^2J_{CP}$ = 6.1 Hz, CH_2), 24.0 (d, $^3J_{CP}$ = 16.8 Hz, CH_2), 22.3 (d, $^1J_{CP}$ = 52.8 Hz, CH_2), 13.5 ppm (s, CH_3).

IR (KBr pellet): ν 2959 (vs), 2931 (vs), 2869 (vs), 2362 (w), 2182 (vs, C≡C), 1584 (m, br), 1498, (m), 1462 (s), 1402 (s), 1383 (s), 1344 (m), 1315 (w), 1230 (s, br), 1128 (w), 1096 (vs), 1006 (m), 967 (m), 916 (vs), 851 (vs), 815 (s), 725 (s), 560 (m), 477 cm^{-1} (m, br).

1.2.10 Synthesis of $[Ph_3PC{\equiv}C(C_6H_4)C{\equiv}CPPh_3]Br_2$ – 7

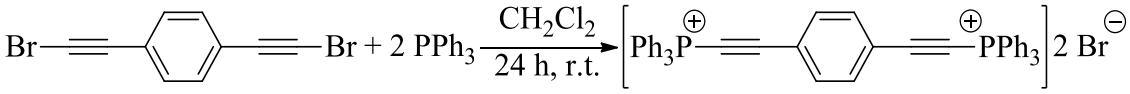

In a 20 mL scintillation vial, 0.352 g (1.24 mmol) of pale yellow coloured 1,4-di(bromoethynyl)benzene powder were dissolved in 10 mL of dichloromethane producing a pale yellow coloured solution. To this solution, 0.651 g (2.48 mmol, 2.00 eq.) of colourless triphenylphosphine granules were added, producing a pale yellow coloured

mixture. After *ca.* 10 minutes, the mixture changed to a blue coloured solution. This mixture was left to stir overnight. The following day an orange coloured solution remained. To this orange coloured solution, 10 mL of pentane were added to facilitate the precipitation of the product. After stirring for *ca*. 10 minutes, the solvent was decanted and the solid was dried *in vacuo* to afford the product as a yellow coloured powder, which was recrystallised from dichloromethane (3 mL) layered with pentane (15 mL) to produce pale yellow coloured crystals.

Yield: 0.97 g (97 %).

EA: Calc. for $C_{46}H_{34}P_2Br_2$: C: 68.33 %, H: 4.24 %, N: 0.00 %. Found: C: 67.93 %, H: 4.17 %, N: 0.02 %.

m.p. (°C): 106.0–106.8 (slight darkening), 210 (turns black, decomposes).

$^{31}P\{^1H\}$ NMR (CD_2Cl_2): δ 7.1 ppm (s, 2P).

^1H NMR (CD_2Cl_2): δ 8.23 (s, 4H), 7.95–7.85 (m, 12H), 7.84–7.76 ppm (m, 18H).

$^{13}C\{^1H\}$ NMR (CD_2Cl_2): δ 136.5 (d, $^4J_{CP}$ = 3.2 Hz, *p*-Ph_3) 134.7 (d, $^4J_{CP}$ = 2.2 Hz, *o*-(C_6H_4)), 133.8 (d, $^2J_{CP}$ = 12.4 Hz, *o*-Ph_3), 131.2 (d, $^3J_{CP}$ = 14.0 Hz, *m*-Ph_3), 121.5 (d, $^3J_{CP}$ = 4.7 Hz, P-C≡C-C), 117.9 (d, $^1J_{CP}$ = 100.1 Hz, *ipso*-Ph_3), 116.2 (d, $^2J_{CP}$ = 30.3 Hz, P-C≡C), 72.7 ppm (d, $^1J_{CP}$ = 184.0 Hz, P-C≡C).

IR (KBr pellet): ν 3046 (m), 3004 (m), 2687 (w), 2580 (w), 2465 (w), 2317 (w), 2177 (vs, C≡C), 1615 (m, br), 1582 (m), 1480 (m), 1438 (vs), 1400 (w), 1360 (m), 1312 (w), 1282 (m), 1238 (w), 1184 (w), 1109 (vs), 1018 (w), 996 (m), 934 (w), 857 (vs), 754 (s), 727 (vs), 688 (vs), 616 (w), 561 (m), 526 cm^{-1} (vs).

1.3 Results and Discussion

1.3.1 Mono(ethynyl)phosphonium Salts

Reaction between 1-bromo-2-phenylacetylene and tributylphosphine or triphenylphosphine yielded the previously known ethynylphosphonium salts **1** and **2** (Figure 1.4) from pentane in high to moderate yields (84% and 56%, respectively). Pentane was chosen as the reaction medium to facilitate direct precipitation of the product. This method worked well for **2**, however **1** produced an oil that required multiple triturations with pentane before yielding a brown coloured powder.

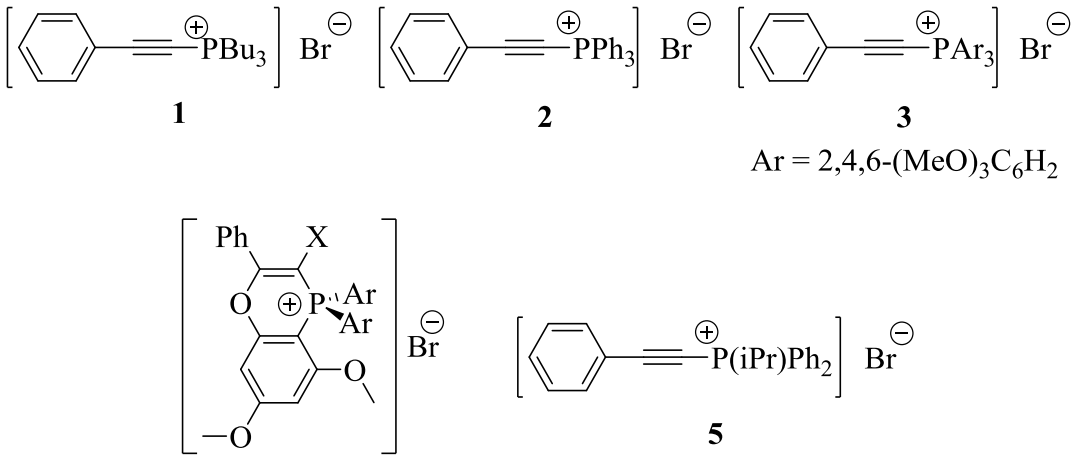

1 **2** **3**

4; **(a)** X = H, **(b)** Me
Ar = 2,4,6-$(MeO)_3C_6H_2$

5

Figure 1.4. Compounds synthesised that will be discussed in this section.

After extensively searching the literature, it was apparent that **1** has only been characterised by ^{1}H NMR spectroscopy with vague peak assignments (e.g. 7.55 ppm is reported for *all* aromatic peaks for **1** as a multiplet, and multiplicities were not provided for the butyl resonances), IR spectroscopy with only the acetylenic vibration reported, melting point, and by elemental analysis.[2] It has not been previously characterised by $^{13}C\{^{1}H\}$ and $^{31}P\{^{1}H\}$NMR spectroscopy or structurally by X-ray crystallography. Taking

into consideration that publication standards have changed since **1** and **2** were initially reported,[15] and that the objective of the earlier reports was to evaluate the kinetics of the formation of **1**,[2] it seemed appropriate to reinvestigate and expand upon the characterisation data available. More characterisation data is available for **2**: ^{1}H, ^{13}C{^{1}H}, and ^{31}P{^{1}H} NMR spectroscopic properties have been studied,[18,22] and have often been supplemented by IR spectroscopy and melting point,[2,18,22] and one cyclic voltammetry study has been done as well.[29] These data will be combined and compared to our own but will not be discussed in detail. Discussion will be limited only to the new structural information obtained through single crystal X-ray diffraction.

The ^{1}H NMR spectrum of **1** collected in CD_2Cl_2 displayed no unusual characteristics and was similar to previous reports in $CDCl_3$.[2] The sample was collected in CD_2Cl_2 to compare spectroscopic properties with the related trimethylphosphine derivative [PhC≡CPMe$_3$]Br, which was also measured in CD_2Cl_2.[17] The methylene bound directly to phosphorus was detected as a multiplet in the ^{1}H NMR spectrum (δ 2.87–2.78 ppm, $^{2}J_{HP}$ = 14.6 Hz) and is similar to that of the methyl groups found in [PhC≡CPMe$_3$]Br (δ 2.57 ppm, $^{2}J_{HP}$ = 15.2 Hz).[17] The remaining methylene resonances appear as a multiplet (δ 1.79–1.65 ppm), and as a sextet (δ 1.56 ppm, $^{3}J_{HH}$ = 7.2 Hz) while the terminal methyl group was identified as a triplet (δ 0.99 ppm, $^{3}J_{HH}$ = 7.2 Hz). In the aromatic region the *o*-ArH (δ 7.65 ppm, $^{3}J_{HH}$ = 7.8 Hz), *m*-ArH (δ 7.48 ppm, $^{3}J_{HH}$ = 7.5 Hz), and *p*-ArH (δ 7.59 ppm, $^{3}J_{HH}$ = 7.6 Hz) resonances are visible as multiplets and appear in a 2:1:2 ratio. These were assigned on the basis of their integration values as well as the degree of coupling observed. Resonances for the acetylenic carbon resonances appear as two sets of doublets (δ 114.2 ppm, $^{2}J_{CP}$ = 23.2 Hz and 69.5 ppm, $^{1}J_{CP}$ = 149.5 Hz)

in the $^{13}C\{^{1}H\}$ NMR spectrum. These are similar to other reported ethynylphosphonium salts such as [PhC≡CPMe$_3$]Br (72.9 ppm, $^{1}J_{CP}$ = 163.7 Hz and 112.5 ppm, $^{2}J_{CP}$ = 29.2 Hz) and [PhC≡CPPh$_3$]Br (68.7 ppm, $^{1}J_{CP}$ = 187.0 Hz and 118.5 ppm, $^{2}J_{CP}$ = 31.2 Hz).[17,22] Peak assignments for the remaining resonances were made based on the magnitude of their J_{CP} values,[22] and using the $^{13}C\{^{1}H\}$ DEPTQ experiment. The acetylenic vibration (ν 2179 cm^{-1}) matches the literature,[2] while the melting point (71.7–72 °C) was considerably higher than previously reported (57–59 °C). The $^{31}P\{^{1}H\}$ NMR spectrum of **1** displayed a singlet resonance (δ 21.5 ppm). Other phosphorus-containing impurities could be seen near the baseline, but could not be identified on the basis of their ^{31}P chemical shifts. The ethynylphosphonium salt **1** is known to react with another equivalent of tributylphosphine to afford the α,β-bis(tributylphosphonium) styrene dibromide (Scheme 1.6) which may be what is observed in the $^{31}P\{^{1}H\}$ NMR spectrum.[2] Unfortunately ^{31}P chemical shifts were not reported, and no explanation of the extra equivalent of "HBr" was provided other than from the reactants and medium. The presence of these impurities after multiple pentane washings indicates that these contaminates are poorly soluble in pentane, suggesting that any remaining impurities are likely some form of ionic species such as a bisphosphonium salt. Mass spectrometry may be useful in determining the identity of some of these by-products.

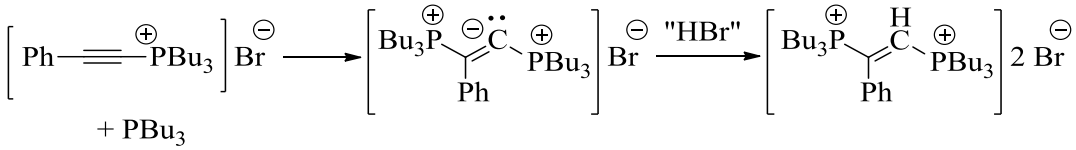

Scheme 1.6. Possible by-product observed during the synthesis of **1**.

In the powder form, **1** could not be crystallised using routine techniques. Crystals of **1** were instead obtained by slow reagent diffusion in pentane (see Experimental section 1.2.4 for details). Compound **1** crystallises in the monoclinic space group $P2_1/c$ as colourless rectangular blocks, and features only one molecule in the asymmetric unit. The structure of **1** (Figure 1.5) is consistent with the observed spectroscopic data and features a tetra-coordinated phosphorus cation with a bromide anion nested between three butyl groups. The P1-C1 and C1-C2 bond lengths were found to be 1.739(2) Å and 1.197(3) Å, respectively, and are similar to the measurements found in [PhC≡CPMe_3]Br (1.739(3) Å and 1.202(4) Å, respectively),[17] and [PhC≡CP(*o*-An)Ph_2][BF_4] (1.719(2) Å and 1.190(2) Å).[5]

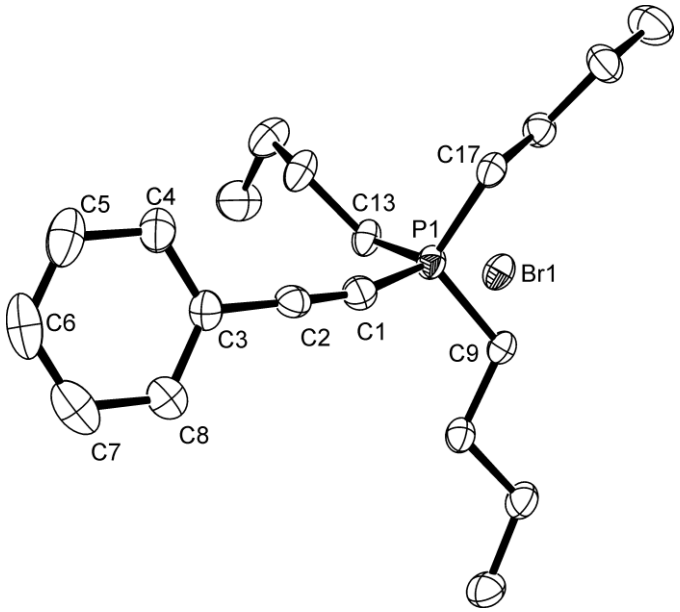

Figure 1.5. Molecular structure of **1**. Ellipsoids are shown at the 50% probability level. Hydrogen atoms have been omitted for clarity. Selected bond lengths (Å) and angles (°): P1-C1 1.732(3), P1-C9 1.791(3), P1-C13 1.792(3), P1-C17 1.776(3), C1-C2 1.200(4), C2-

C3 1.445(4), C1-C2-C3 176.4(3), C2-C1-P1 163.3(3), C1-P1-C9 110.83(13), C1-P1-C13 105.89(14), C1-P1-C17 108.30(14).

Crystals of **2** were obtained by layering a concentrated dichloromethane solution with pentane. Compound **2** crystallises as colourless rectangular blocks in the orthorhombic space group *P*bca, and features only one molecule in the asymmetric unit. The structure of **2** (Figure 1.6) is also consistent with spectroscopic data and is structurally similar to **1**. The P1-C1 and C1-C2 bond lengths were found to be 1.727(2) Å and 1.200(3) Å respectively. Recent evidence suggests that the phenylacetylene fragment in **2** is responsible for anticancer activity,[12-14] so the overall length of the phenylacetylene fragment determined by the distance between P1-C6 was measured and found to be 7.106(2) Å. When the same measurement is done for **1** it is found that the distance between P1-C6 is 7.045(3) Å, indicating that modification of the groups attached to phosphorus can cause significant structural differences.

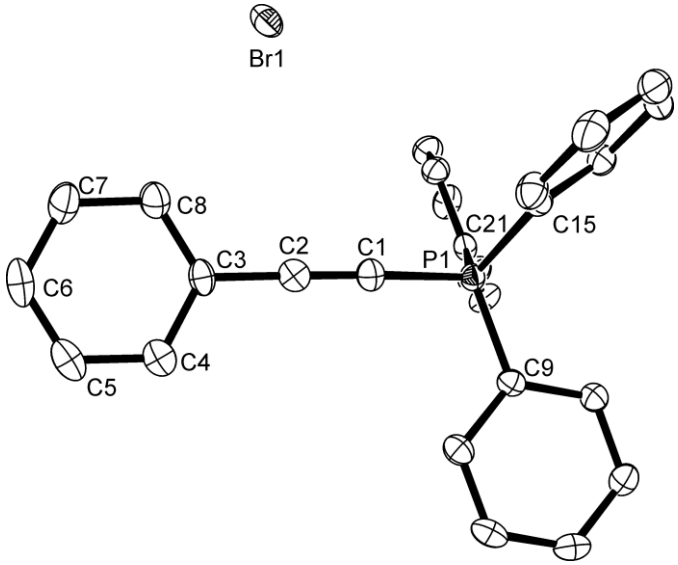

Figure 1.6. Molecular structure of **2**. Ellipsoids are shown at the 50% probability level. Hydrogen atoms have been omitted for clarity. Selected bond lengths (Å) and angles (°):

P1-C1 1.727(2), P1-C9 1.786(2), P1-C15 1.7923(19), P1-C21 1.785(2), C2-C1 1.200(3), C2-C3 1.437(3), C1-C2-C3 179.2(2), C2-C1-P1 168.6(2), C1-P1-C9 107.96(10), C1-P1-C15 109.11(10), C1-P1-C21 107.60(9).

Several attempts were made at expanding the library of known derivatives of **2** with varied aryl substituents, however many of these were unsuccessful. Reactions involving sterically hindered or electron deficient phosphines ($PMes_3$ (Mes = 2,4,6-trimethylphenyl), $P(o\text{-Tol})_3$ (*o*-Tol = 2-methylphenyl), $P(C_6F_5)_3$) were attempted at 60 °C in either toluene or heptane, and with or without silver triflate added to abstract the bromide, but were unsuccessful in producing the desired ethynylphosphonium salts; reactivity was observed in the form of a colour change from pale yellow to brown, but the products could not be unambiguously identified. Reaction of the electron-rich tris(2,4,6-trimethoxyphenyl)phosphine (TMPP) was also attempted due to the majority of related examples possessing methoxy substituents. This reaction did not proceed at room temperature, presumably due to the steric demands of the phosphine. Varied modes of reactivity, however, were observed at elevated temperatures.

When TMPP was combined with 1-bromo-2-phenylacetylene in heptane and heated to 80 °C for 3 days, the ethynylphosphonium salt **3** was obtained in only 8% isolated yield. Compound **3** was characterised by multinuclear NMR and IR spectroscopies, as well as by melting point determination and X-ray crystallography. Analogous to triarylphosphines, the $^{31}P\{^1H\}$ chemical shift of **3** is considerably lower in frequency than related ethynylphosphonium salts, appearing as a singlet (δ -27.7 ppm) when measured in CD_3CN. Collectively, the resonances in the ^1H NMR spectrum attributed to the TMPP moiety are

shifted to a slightly higher frequency than the parent phosphine,[55] while the acetylenic carbon resonances appear as two sets of doublets (δ 102.9 ppm, $^{2}J_{CP}$ = 37.0 Hz and 77.9 ppm, $^{1}J_{CP}$ = 205.5 Hz). Further evidence for a carbon-carbon triple bond is given by a strong signal in the IR spectrum (ν 2186 cm^{-1}), which is significantly different from **2** (ν 2167 cm^{-1}). When compared to the parent compound **2**, modification of the aryl groups on phosphorus with more electron donating substituents significantly changed the electronic properties of the ethynyl fragment, however the consequences of this have yet to be evaluated.

Large colourless block-shaped crystals of **3** were obtained by dissolving the phosphonium salt in a 5:1 mixture of toluene and acetonitrile and allowing the solution to slowly evaporate. Compound **3** crystallises in the cubic space group $Pa\bar{3}$ and features only one and a third of a molecule in the asymmetric unit. The structure of **3** (Figure 1.7) is consistent with spectroscopic data and is structurally similar to **2**. The P1-C1 and C1-C2 bond lengths were found to be 1.752(2) Å and 1.194(3) Å, respectively. The overall length of the phenylacetylene fragment determined by the distance between P1-C6 was measured and found to be 7.141(3) Å. The steric demands of the 2,4,6-methoxyphenyl rings are clearly much greater than the simple phenyl rings in **2** however, and prevent a direct comparison. The C2-C1-P1 bond angle (174.6(2)°) deviates slightly from linearity, and is less than what is observed for both **1** and **2**. The phosphorus-C_{ipso} bond lengths are all quite similar with bond lengths of 1.785(2) Å, 1.797(2) Å, and 1.788(2) Å between C9, C18, and C27, respectively. A larger bond angle is observed for C1-P1-C9 (108.93(10)°) compared to C1-P1-C18 (105.84(10)°) and C1-P1-C27 (104.14(9)°) and is most likely required to reduce steric repulsion with the phenylacetylene group.

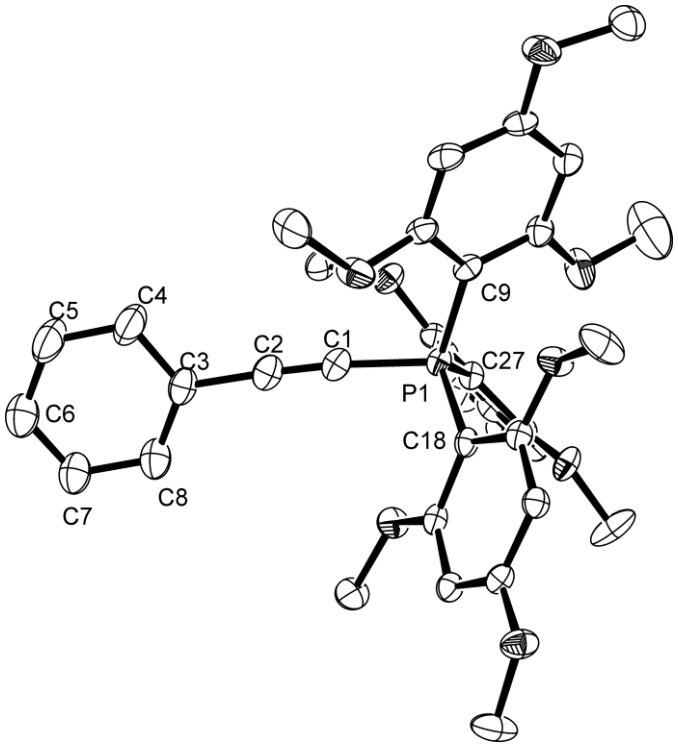

Figure 1.7. Molecular structure of the cation of **3**. Ellipsoids are shown at the 50% probability level. Hydrogen atoms and the bromide anion have been omitted for clarity. Selected bond lengths (Å) and angles (°): P1-C1 1.752(2), P1-C9 1.785(2), P1-C18 1.797(2), P1-C27 1.788(2), C1-C2 1.194(3), C2-C3 1.450(3), C1-C2-C3 176.2(2), C2-C1-P1 174.6(2), C1-P1-C9 108.93(10), C1-P1-C18 105.84(10), C1-P1-C27 104.14(9).

It was speculated that poor solubility was the reason for such a slow conversion, so to accelerate the reaction toluene was chosen as the reaction medium for its higher boiling point and solvent polarity. When the same reaction was performed in toluene at 105 °C for 3 days, the initial formation of the ethynylphosphonium salt **3** occurred and partially underwent an intramolecular cyclisation to form two additional products. The phosphoniapyrans **4a** and **4b** were first identified crystallographically and co-crystallised in a 3:1 ratio, and were later identified with similar ratios (2.5:1) using ^{31}P and $^{31}P\{^{1}H\}$ NMR spectroscopies (**4a** δ -21.9 ppm, **4b** δ 0.0 ppm).

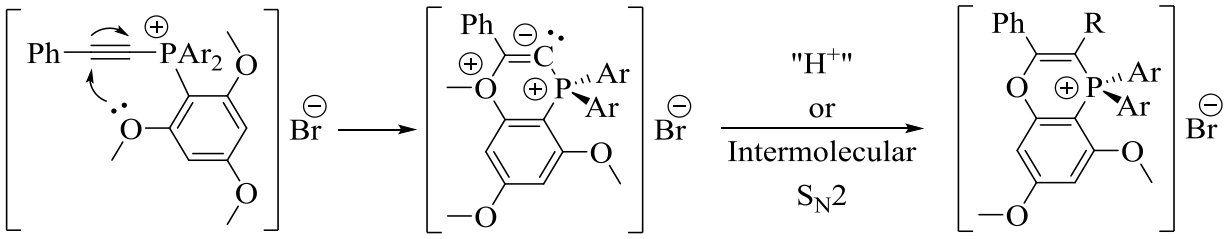

3 **4**; **(a)** R = H, **(b)** Me

Scheme 1.7. Proposed formation of **4a,b** from **3**. Ar = 2,4,6-trimethoxyphenyl.

The most probable source of **4b** is the initial formation of **3**, followed by an intramolecular cyclisation *via* nucleophilic attack at the β-carbon of the acetylene by a methoxy group in the *ortho* position. Intermolecular nucleophilic attack at the oxonium centre may transfer the methyl group to the vinylic position. Nucleophilic reactions at the β-carbon have been studied extensively,[3,6,7,18] and such a reaction would be possible given the orientation of the methoxy groups of the C9-containing aromatic ring in the structure of **3** (Figure 1.7). The intermediate reacting with the medium would also be analogous to what was observed in reactions of additional equivalents of tertiary phosphines in which the products of these reactions seemingly acquire an additional equivalent of HBr.[2] Attempts at elucidating the pathway leading to the formation of **4a** have been unsuccessful thus far; an initial hypothesis was that **4a** formed after an intermediate reacted with the solvent. To test this, the reaction was repeated in deuterated toluene, however no deuterium incorporation into **4a** or **4b** was evident thereby eliminating the solvent as a possible reactant for the formation of **4a**. The fate of the methyl group has yet to be determined also; given the lack of deuterium incorporation it may be the source of a proton, and escape in the form of a simple gas such as ethylene or methane, but no evidence for this has been

found based on ^{1}H NMR spectroscopy after repeating the reaction in a sealed NMR sample tube.

Structurally **4a** and **4b** differ by only a hydrogen atom or methyl group attached to C1 (Figure 1.8) and crystallise in the monoclinic space group $P2_1/n$ as yellow rectangular blocks. The phosphorus centre deviates significantly from an ideal tetrahedral geometry, with the most acute angles being between C1-P1-C27 (101.42(13)°) and C1-P1-C9 (105.87(13)°). The phosphorus-carbon bond lengths are all similar, however a slight shortening was noted for P1-C1 (1.763(3) Å) and P1-C27 (1.766(3) Å) when compared to P1-C9 (1.798(3) Å) and P1-C18 (1.790(3) Å) of the non-cyclised aryl rings. These measurements are similar to those found in the only other structurally characterised phosphoniapyran in the literature.[56]

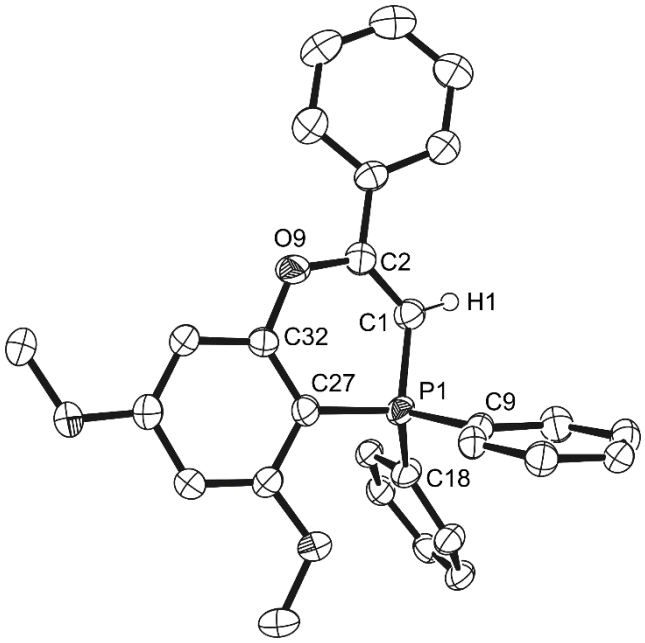

Figure 1.8. Molecular structure of the cation of **4a**. Ellipsoids are shown at the 50% probability level. Hydrogen atoms (excluding H1) and the bromide anion have been omitted for clarity. Methoxy groups of the non-cyclised tris(2,4,6-trimethoxyphenyl)

substituents have been removed for clarity. Selected bond lengths (Å) and angles (°): C1-C2 1.348(4), P1-C1 1.763(3), P1-C9 1.798(3), P1-C18 1.790(3), P1-C27 1.766(3), O9-C2 1.356(3), O9-C32 1.374(3), C1-P1-C9 105.87(13), C1-P1-C18 111.72(13), C1-P1-C27 101.42(13), C2-C1-P1 122.2(2), C1-C2-O9 125.1(3), C2-O9-C32 123.7(2), O9-C32-C27 124.2(2), C32-C27-P1 121.6(2).

The final objective of the project was to attempt to expand the library of mixed alkyl/aryl ethynylphosphonium salts as these may also exhibit different properties from either alkyl or aryl analogues. The mixed alkyl/aryl ethynylphosphonium salt **5** was prepared in 32 % isolated yield by reacting isopropyldiphenylphosphine with 1-bromo-2-phenylacetylene in heptane at 95 °C for six days. Compound **5** was characterised by multinuclear NMR and IR spectroscopies, as well as by melting point determination and X-ray crystallography. The chemical shift as measured by $^{31}P\{^{1}H\}$ NMR spectroscopy of **5** is higher in frequency than **1** or **2**, appearing as a singlet (δ 24.0 ppm) when measured in CD_2Cl_2. An intense signal appearing at 2176 cm^{-1} in the IR spectrum provides strong evidence of the acetylene fragment, and is supplemented by resonances in the $^{13}C\{^{1}H\}$ NMR spectrum, appearing as two sets of doublets (δ 118.1 ppm, $^{2}J_{CP}$ = 26.3 Hz and 66.3 ppm, $^{1}J_{CP}$ = 170.8 Hz). Resonances for the isopropyl group are clearly visible in the ^{1}H NMR spectrum, with the methyl groups appearing as a doublet of doublets (δ 1.39 ppm, $^{3}J_{HP}$ = 21.8 Hz, $^{3}J_{HH}$ = 6.9 Hz) and the methine as an octet (δ 4.84 ppm, $^{3}J_{HH}$ = 7.0 Hz). The magnitude of the $^{2}J_{HP}$ coupling could not be determined with certainty. Most likely, the coupling due to phosphorus overlaps with the signals observed for $^{3}J_{HH}$ coupling. For both **1** and $[PhC{\equiv}CPMe_3]Br$[17] the $^{2}J_{HP}$ observed is *ca*. 15 Hz, which is slightly more than twice as much as typical $^{3}J_{HH}$ values, which are roughly 7 Hz in magnitude. It is also unlikely

that ^{31}P NMR would be able to determine the $^{2}J_{HP}$ because of overlap with the $^{3}J_{HP}$ observed for the *ortho*-phenyl environments, which appear at 8.35 ppm in the ^{1}H NMR spectrum as a doublet of doublets ($^{3}J_{HP}$ = 14.0 Hz, $^{3}J_{HH}$ = 7.6 Hz). The remaining resonances in the aromatic region of the ^{1}H NMR spectrum could not be unambiguously identified, but the sum of the integration values (2+7+2 = 11) match with what is left unassigned for the product.

Long colourless needle-shaped crystals of **5** were obtained by dissolving the phosphonium salt in a 5:1 mixture of toluene and acetonitrile and allowing the solution to slowly evaporate. Compound **5** crystallises in the orthorhombic space group *Pbca* and contains three molecules in the asymmetric unit in an alternating head-to-tail arrangement. In the molecular structure of **5** (Figure 1.9) the P1-C1 bond length of 1.733(3) Å is much longer when compared to other ethynylphosphonium salts while the C2-C1-P1 fragment is bent significantly at an angle of 170.0(3)°, possibly due to the steric demands of the aryl groups attached to phosphorus or due to crystal packing forces.

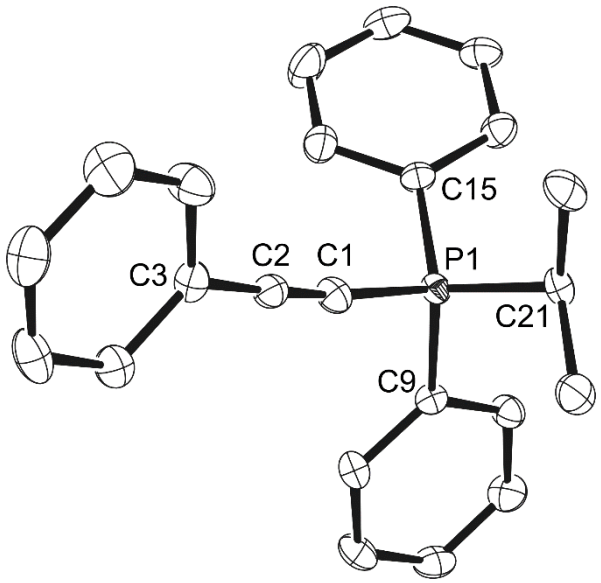

Figure 1.9. Molecular structure of the cation of **5**, only one third of the asymmetric unit is shown. Ellipsoids are shown at the 50% probability level. Hydrogen atoms and the bromide anion have been omitted for clarity. Selected bond lengths (Å) and angles (°): P1-C1 1.733(3), P1-C9 1.786(3), P1-C15 1.786(3), P1-C21 1.812(3), C1-C2 1.198(4), C2-C3 1.432(4), C1-C2-C3 177.6(4), C2-C1-P1 170.0(3), C1-P1-C9 108.63(14), C1-P1-C15 107.89(15), C1-P1-C21 107.63(15).

The significant deviations of the P-C≡C angle in the solid state structures of the ethynyl phosphonium salts prompted a further computational investigation of energetic impact of the P-C≡C angle when it deviates from linearity. These angles range from 163.3(3)° for **1** to 175.9(3)° for **7** and even in the solid state structure for compound **7**, the three independent molecules in the asymmetric unit have P-C≡C angles that range from 167.1(3)° to 175.9(3)°. A scan of the P-C≡C angles in the model cation, $[Ph\text{-}C{\equiv}C\text{-}PMe_3]^+$, shows that decreasing the P-C≡C angle from the fully optimised angle (B3LYP/6-31G(d)) of 179.57° to 139.57 (40° total) there is only a 4.7 kcal mol^{-1} (19.7 kJ mol^{-1}) penalty for

this deviation, reinforcing that in the solid state these angles are impacted by crystal packing forces (Figure 1.10).

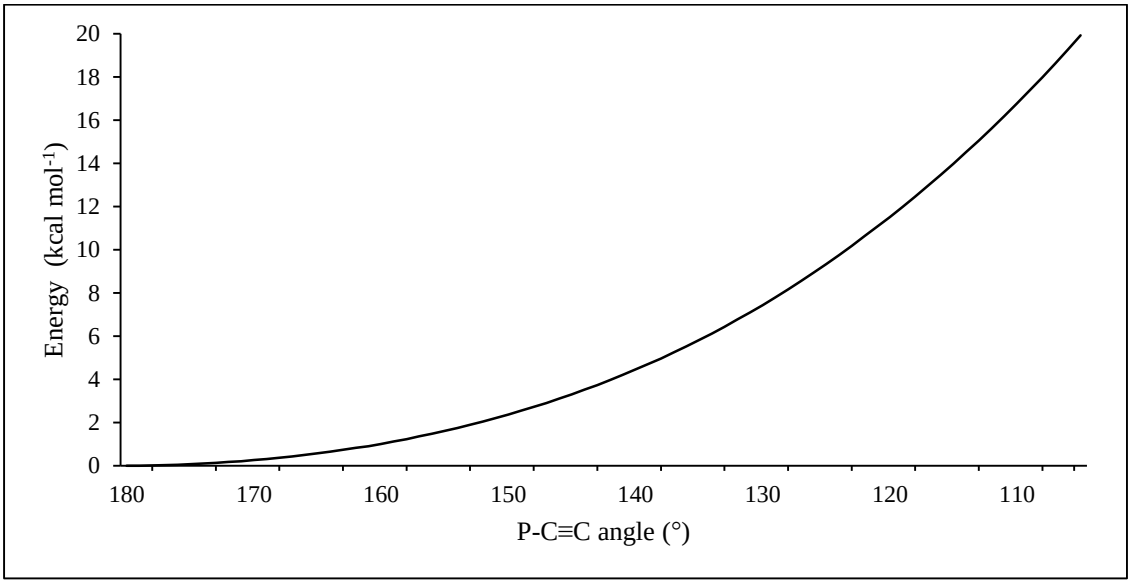

Figure 1.10. The relative energies of the P-C≡C angle in the model cation, $[Ph\text{-}C{\equiv}C\text{-}PMe_3]^+$, scanned over 75° from the optimised angle of 179.57°. Calculations performed at the B3LYP/6-31G(d) level of theory. The P-C≡C bond angle was scanned in 1° increments while the remaining bond lengths and angles were allowed to optimise freely to a minimum along the potential energy surface.

1.3.2 Bis(ethynylphosphonium) salts

For reasons previously stated, current synthetic routes for bis(ethynylphosphonium) salts are undesirable. An alternative, atom-economical approach was found by reacting the tertiary phosphines PBu_3 and PPh_3 with 1,4-(dibromo-ethynyl)benzene in either acetonitrile or dichloromethane, giving the new bis(ethynylphosphonium) salts $[R_3PC{\equiv}C(C_6H_4)C{\equiv}CPR_3]Br_2$ (R = Bu, **6**; Ph, **7**) in 16% and 97% isolated yields, respectively. Both **6** and **7** were fully characterised using multinuclear

NMR spectroscopy, IR spectroscopy, X-ray crystallography, cyclic voltammetry, melting point determination, and elemental analysis. These molecules displayed similar spectroscopic properties and structural parameters as their analogous monophenylethynyl derivatives **1** and **2**.

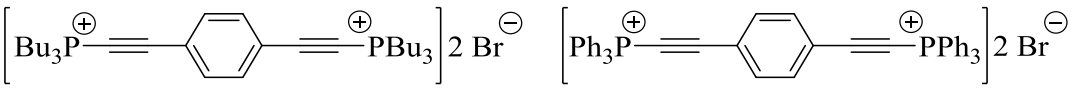

6 **7**

Figure 1.11. Bis(ethynylphosphonium) salts synthesised and are discussed in this section.

All attempts at the synthesis of **6** with dichloromethane produced a complex mixture of phosphorus-containing products that could not be identified by ^{31}P NMR spectroscopy. Acetonitrile produced a similar mixture but yielded higher amounts of **6** and was chosen as the solvent for this reason. These impurities could not be completely removed by multiple pentane washings or by recrystallization and efforts to obtain high purity material severely impacted the isolated yield and are likely similar to those found in **1**. The ^{31}P{^{1}H} NMR spectrum of **6** displayed a singlet resonance (δ 18.5 ppm) in CD_2Cl_2. In the ^{1}H NMR spectrum the central aromatic ring also exhibited singlet resonance (δ 7.79 ppm), while the butyl methylene resonances displayed complex multiplet patterns (δ 2.87–2.78 ppm, $^{2}J_{HP}$ = 14.6 Hz, 1.74–1.62 ppm, and 1.60–1.48 ppm) and a characteristic triplet (δ 0.96 ppm, $^{3}J_{HH}$ = 7.2 Hz) was observed for the terminal methyl groups. The integration values for these peaks did not match the expected structure, however, this is most likely caused from the multiple impurities clearly present in both the ^{1}H and ^{31}P{^{1}H} NMR spectra. The butyl groups could still be assigned reliably based on characteristics similar to **1.** The acetylenic carbons were identified by two doublets in the ^{13}C{^{1}H} NMR spectrum

(δ 111.5 ppm, $^{2}J_{CP}$ = 22.7 Hz and 73.5 ppm, $^{1}J_{CP}$ = 146.1 Hz), and also by a strong vibration in the IR spectrum (ν 2182 cm^{-1}).

Long, yellow coloured needle-shaped crystals of **6** suitable for X-ray diffraction were obtained by dissolving the black coloured powder in a 1:1 mixture of acetonitrile and diethyl ether and storing in a -35 °C freezer overnight. Compound **6** crystallises in the monoclinic space group $P2_1/c$ and features one half of the molecule in the asymmetric unit. In the structure of **6** (Figure 1.12) the P1-C13 and C13-C14 bond lengths were found to be 1.735(6) Å and 1.208(6) Å, respectively, and are similar to the related monoethynyl species **1** and **2**, and those of the literature.[5,17] No structurally characterised bis(ethynylphosphonium) salts were available for comparison, however these parameters were found to be similar to **7**. Considerably more disorder was encountered in the butyl groups of **6** relative to **1** and resulted in some C-C bond lengths being inaccurate. This was most likely caused by using different methods of crystallisation, and had little effect on the bond lengths of interest. The butyl groups were disordered and different components of the disorder were separated using the PART command. Site occupancies were allowed to freely refine and rigid bond restraints were applied using the RIGU command. For the butyl groups, P-C bond lengths, 1,2-distances, and 1,3-distances were restrained appropriately using the DFIX command. The C14-C13-P1 bond angle (178.2(5)°) is much more linear than the related bond angle found in **1** (163.3(3)°), possibly due to increased amount of conjugation in the molecule from an additional ethynyl substituent.

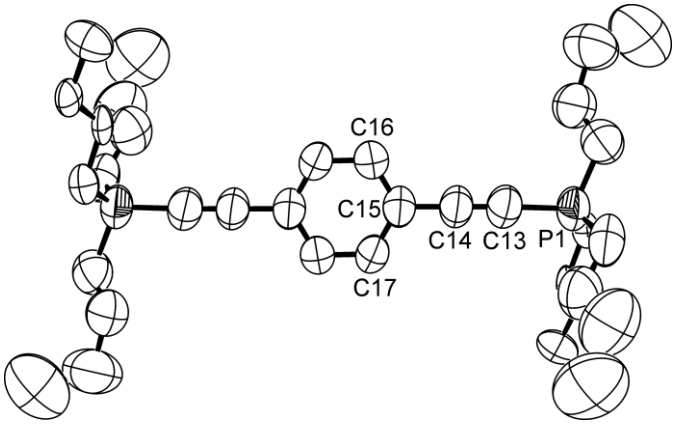

Figure 1.12. Molecular structure of the dication of **6**. Ellipsoids are shown at the 50% probability level. Hydrogen atoms and bromide anions have been omitted for clarity. One component of the butyl disorder has been omitted for clarity. Selected bond lengths (Å) and angles (°): P1-C13 1.735(6), C13-C14 1.208(6), C14-C15 1.434(7), C14-C13-P1 178.2(5).

The synthesis of **7** was much more straightforward and allowed for the use of dichloromethane as the solvent followed by the addition of pentane to facilitate precipitation. Spectroscopically **7** is similar to **6** with a strong diagnostic acetylenic vibration in the IR spectrum (ν 2177 cm^{-1}). When measured in CD_2Cl_2 resonances related to the acetylenic carbons were also identified as doublets in the $^{13}C\{^1H\}$ NMR spectrum (δ 116.2 ppm, $^2J_{CP}$ = 30.3 Hz and 72.7 ppm, $^1J_{CP}$ = 184.0 Hz), while a singlet is observed in the $^{31}P\{^1H\}$ NMR spectrum (δ 7.1 ppm) indicating only one unique phosphorus environment. The bridging aromatic ring was clearly visible as a singlet in the ^1H NMR spectrum (δ 8.23 ppm), however the remaining aromatic resonances could not be unambiguously assigned due to their complexity.

Crystals of **7** suitable for X-ray diffraction were obtained by layering a concentrated dichloromethane solution with pentane. Compound **7** crystallises in the monoclinic space group $P2_1/c$ and features one half of the molecule in the asymmetric unit. In the structure of **7** (Figure 1.13) the P1-C1 and C1-C12 bond lengths were found to be 1.743(5) Å and 1.196(7) Å, respectively. Interestingly, the P1-C1 distance is significantly longer than found in **2** (1.727(2) Å), while the related distances in **1** and **6** are much more similar but show the reverse trend. The phosphorus-C_{ipso} bond lengths are all quite similar with bond lengths of 1.790(5) Å, 1.781(5) Å, and 1.780(5) Å between C6, C12, and C18, respectively. The geometry at phosphorus is almost tetrahedral (C1-P1-C6 109.9(3)°, C1-P1-C12 107.1(3)°, C1-P1-C18 108.0(2)°) while the C2-C1-P1 bond angle (175.8(5)°) is slightly larger than the analogous bond found in **2** (168.6(2)°). Similarly to **1** and **6**, this is possibly due to the increased amount of conjugation from an additional ethynyl substituent, however the effect is much more subtle and may also be a consequence of crystal packing.

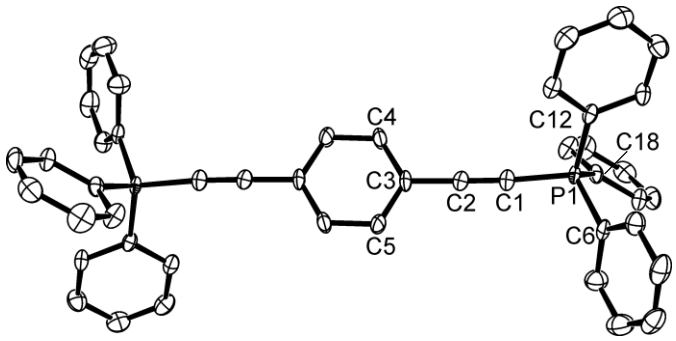

Figure 1.13. Molecular structure of the dication of **7**. Ellipsoids are shown at the 50% probability level. Hydrogen atoms and bromide anions have been omitted for clarity. Selected bond lengths (Å) and angles (°): P1-C1 1.734(5), P1-C6 1.790(5), P1-C12

1.781(5), P1-C18 1.780(5), C1-C2 1.196(8), C2-C3 1.432(7), C1-C2-C3 177.4(5), C2-C1-P1 175.8(5), C1-P1-C6 109.9(3), C1-P1-C12 107.1(3), C1-P1-C18 108.0(2).

1.3.3 Summary of Crystal Tables and Relevant Data

Table 1.1. Summary of relevant characterisation data for compounds 1−7.

Compound	^{31}P NMR (ppm)	^{13}C{^{1}H} NMR (C≡C) (δ, ppm**;** J_{CP}, Hz)	IR (C≡C) (cm^{-1})	P-C≡C angle (°)
1	21.5	69.5**;***149.5*, 114.2**;***23.2*	2179	163.3(3)
2	6.5	69.0**;***188.0*, 118.7**;***31.4*	2167	168.6(2)
3	-27.7	77.9**;** *205.5*, 102.9**;***36.6*	2186	174.6(2)
4a/b	-21.9 **(a)**, 0.0 **(b)**			
5	24.0	66.3**;***170.8*, 118.1**;***26.3*	2176	170.0(3)
6	18.5	73.5**;***146.1*, 111.5**;***22.7*	2182	178.2(5)
7	7.1	72.7**;***184.0*, 116.2**;***30.3*	2177	175.8(7)

Table 1.2. Summary of crystallographic data for compounds 1−7.

Compound reference	1	2	3	4ab	5	6	7
Chemical formula	$C_{20}H_{32}BrP$	$C_{26}H_{20}BrP$	$C_{147}H_{160}Br_4O_{36}P_4$	$C_{34.25}H_{36.50}BrO_9P$	$C_{23}H_{22}BrP$	$C_{34}H_{58}Br_2P_2$	$C_{48}H_{38}Br_2Cl_4P_2$
Formula Mass	383.33	443.30	2946.26	703.01	409.28	688.56	978.34
Crystal system	Monoclinic	Orthorhombic	Cubic	Monoclinic	Orthorhombic	Monoclinic	Monoclinic
a/Å	10.8535(18)	16.9774(12)	30.2286(16)	8.6131(13)	11.7797(10)	11.680(7)	8.3143(8)
b/Å	12.907(2)	14.1780(10)	30.2286(16)	28.993(4)	19.4453(17)	17.067(10)	10.2810(9)
c/Å	14.799(2)	17.9615(13)	30.2286(16)	13.087(2)	53.906(5)	10.080(6)	25.844(2)
α/°	90	90	90	90	90	90	90
β/°	90.604(2)	90	90	102.416(2)	90	102.178(8)	90.1960(10)
γ/°	90	90	90	90	90	90	90
Unit cell volume/Å^3	2073.0(6)	4323.4(5)	27622(4)	3191.7(8)	12347.6(19)	1964(2)	2209.2(3)
Temperature/K	125(2)	125(2)	125(2)	125(2)	125(2)	125(2)	125(2)
Space group	*P*21/*c*	*Pbca*	$Pa\bar{3}$	*P*21/*n*	*Pbca*	*P*21/*c*	*P*21/*c*
No. of formula units per unit cell, *Z*	4	8	8	4	24	2	2
No. of reflections measured	14799	31900	338038	24668	126861	17450	14711
No. of independent reflections	4521	4720	11397	6944	12122	3163	4024
R_{int}	0.0410	0.0330	0.1190	0.0395	0.0931	0.0501	0.0257
Final R_1 values ($I > 2\sigma(I)$)	0.0341	0.0292	0.0369	0.0426	0.0434	0.0560	0.0698
Final $wR(F^2)$ values ($I > 2\sigma(I)$)	0.0698	0.0731	0.0734	0.0960	0.0884	0.1392	0.2316
Final R_1 values (all data)	0.0599	0.0406	0.0657	0.0634	0.0564	0.1240	0.0825
Final $wR(F^2)$ values (all data)	0.0780	0.0790	0.0829	0.1050	0.0925	0.1732	0.2430

1.4 Conclusions

The ethynylphosphonium salts **1** and **2** were reinvestigated and the newly reported structural information indicated that exchanging alkyl and aryl groups bound to phosphorus leads to significant structural differences in the phenylacetylene fragment. Several attempts at diversifying the steric or electronic properties of the phosphorus were also made, but were mostly unsuccessful in producing the desired ethynylphosphonium salts. At room temperature the reaction between 1-bromo-2-phenylacetylene and the electron-rich, sterically hindered tris(2,4,6-trimethoxyphenyl)phosphine was also unsuccessful, but varied reactivity was observed at elevated temperatures. In hot heptane, only a minimal amount of **3** could be isolated after three days, while a mixture of **3** with the cyclised by-products **4a** and **4b** were isolated from the same reaction when hot toluene was used as the reaction medium. IR spectroscopy demonstrated similarities in the acetylenic vibrations between **1** and **2** and **5**, however **3** demonstrated a significant difference indicating that modification of the aryl rings with electron-donating substituents may influence the properties of the acetylene fragment. The consequences of this observation still require further study.

A new, greener synthetic route to the related bis(ethynylphosphonium) salts has also been discovered and the newly synthesised derivatives **6** and **7** have been reported. These compounds exhibit similar spectroscopic and structural properties to their related mono-substituted derivatives, and are the first bis(ethynylphosphonium) salts to be structurally characterised using X-ray crystallography.

1.5 Future Work

The unique reactivity observed for the ethynylphosphonium salt **3** provided an exciting new synthetic route to the phosphoniapyrans **4a** and **4b**. The intermediate proposed for this rearrangement involves a transient ylidene, which reacts with the medium to produce **4a** as the major product. Future work with this molecule will be directed towards synthesising **4a** exclusively, and attempting to generate the corresponding ylidene from the addition of a strong base (Scheme 1.8). Alternatively acyclic ylidenes may be targeted using other nucleophiles and the ethynylphosphonium salts **2**, with the preference given for **2** due to its ease of synthesis and previous reactivity studies with nucleophiles. A cyclic ylidene derived from **4a** would be expected to be more stable than acyclic derivatives of **2** due to more steric protection from the 2,4,6-trimethoxyphenyl substituents and possibly push-pull interactions as well. Therefore it may be necessary to generate the acyclic ylidene *in situ* at low temperatures and trap them using a metal complex. These ylidenes could then be used as ligands for metal centres.

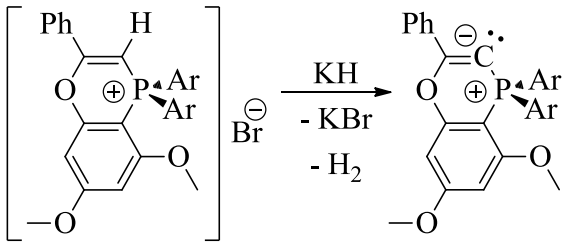

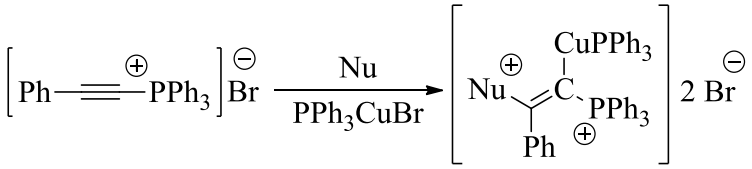

Scheme 1.8. Ylidene synthesis from **4a** and **2**. Nu is any nucleophile.

Another avenue that has yet to be pursued is the reactivity of the ligands bound to phosphorus in these systems. The ethynylphosphonium salt **5** is a particularly interesting molecule in that it has the potential to form a phosphonium ylide following deprotonation of the isopropyl group (Scheme 1.9). Reactions of ethynylphosphonium salts *with* phosphorus ylides have been studied,[RW.ERROR - Unable to find reference:189] however to date no such ethynylphosphonium ylides have been prepared. These compounds would be expected to participate in reactions that are typical of other phosphorus ylides such as the Wittig reaction, but the unique electronic properties that are likely possessed by these molecules are much more interesting. These molecules are expected to be highly electron rich, and would likely exhibit unique chemical properties due to the proximity of the alkyne moiety next to the phosphorus centre. One pursuit that should be investigated in the future is the synthesis and characterisation of such a species and its corresponding radical anion, and evaluating the reactivity of both compounds.

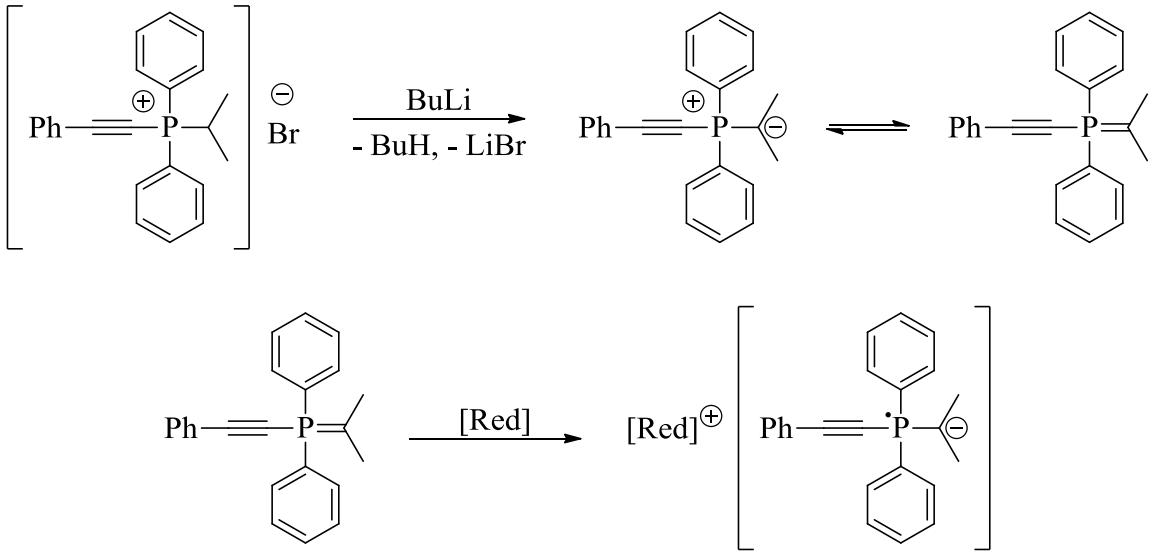

Scheme 1.9. Proposed reactivity of **5** that should be further explored. [Red] is a reducing agent.

Another aspect of these molecules that should be explored in the future is the potential of these molecules to act as starting materials for new derivatives of classical ligands such as *N*-heterocyclic carbenes. Using a copper catalysed cross-coupling reaction, the ethynylbismuthonium salt [*t*BuC≡CBi(*p*-An)$_3$][BF$_4$] has been shown to react with cyclic imides such as succinimide to yield the corresponding ynimides.[39] Using similar chemistry, it may be possible to extend this synthesis to ethynylphosphonium salts, and use it to synthesise *N*,*N*'-phenylethynyl substituted imidazolium salts, which can then be converted to their respective carbenes using a strong base such as potassium hydride ().

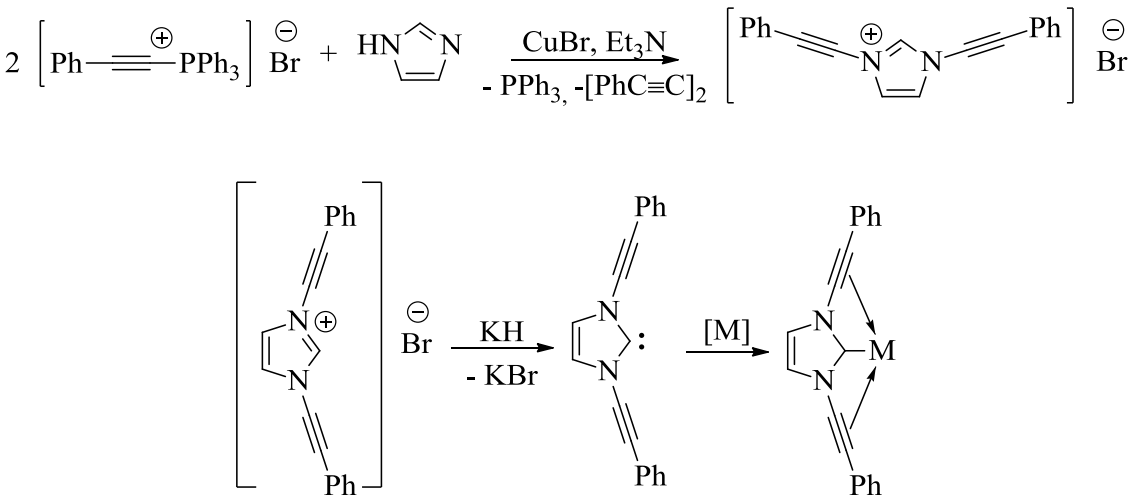

Scheme 1.10. Possible synthetic route to *N,N'*-phenylethynyl imidazolium salts and carbenes.

These carbene ligands are of interest as they could function as hemilabile ligands by coordinating to metal centres using the acetylenic π-bonds of the flanking phenylethynyl groups. These interactions would be weak enough to be easily displaced by incoming substrates, but could be strong enough to stabilise any reactive intermediates. Unfortunately the reaction between ethynylbismuthonium salts and imides was shown to

yield the dimeric acetylene species $[PhC{\equiv}C]_2$,[39] and so a similar by-product would be expected in this case as well.

1.6 References

1. Hoffmann, H.; Förster, H. *Tetrahedron Lett.* **1964**, *5*, 983-987.

2. Dickstein, J. I.; Miller, S. I. *J. Org. Chem.* **1972**, *37*, 2168-2175.

3. Morita, N.; Dickstein, J. I.; Miller, S. I. *J. Chem. Soc., Perkin Trans. 1* **1979**, 2103-2106.

4. Morita, N.; Moriyama, S.; Toyota, K.; Watanabe, M.; Kikuchi, S.; Ito, S.; Fujimori, K. *Heterocycles* **2011**, *82*, 1283-1296.

5. Reichl, K. D.; Radosevich, A. T. *Chem. Commun.* **2014**, *50*, 9302-9305.

6. Bagdasaryan, G. B.; Pogosyan, P. S.; Panosyan, G. A.; Indzhikyan, M. G. *Russ. J. Gen. Chem.* **2007**, *77*, 866-870.

7. Bagdasaryan, G. B.; Pogosyan, P. S.; Panosyan, G. A.; Asratyan, G. V.; Indzhikyan, M. G. *Russ. J. Gen. Chem.* **2006**, *76*, 1324-1326.

8. Mohebat, R.; Anary-Abbasinejad, M.; Hajmohammadi, S.; Hassanabadi, A. *Synth. Commun.* **2013**, *43*, 2833-2840.

9. Viehe, H. G.; Franchimont, E. *Chem. Ber.* **1962**, *95*, 319-327.

10. Tasior, M.; Gryko, D.; Pielacińska, D.; Zanelli, A.; Flamigni, L. *Chem. Asian J.* **2010**, *5*, 130-140.

11. Sun, Q.; Ma, S.; Dai, Z.; Meng, X.; Xiao, F. *J. Mater. Chem. A* **2015**, *3*, 23871-23875.

12. Leu, J. I. -.; Zhang, P.; Murphy, M. E.; Marmorstein, R.; George, D. L. *ACS Chem. Biol.* **2014**, *9*, 2508-2516.

13. Bailey, C. K.; Budina-Kolomets, A.; Murphy, M. E.; Nefedova, Y. *Cancer Biol. Ther.* **2015**, *16*, 1422-1426.

14. Stetz, G.; Verkhivker, G. M. *J. Chem. Inf. Model.* **2016**, *56*, 1490-1517.

15. Miller, S. I.; Orzech, C. E.; Welch, C. A.; Ziegler, G. R.; Dickstein, J. I. *J. Am. Chem. Soc.* **1962**, *84*, 2020-2021.

16. Hoffmann, H.; Diehr, H. J. *Angew. Chem. Int. Ed Engl.* **1964**, *3*, 737-746.

17. Schuster, O.; Schmidbaur, H. *Z. Naturforsch. B* **2006**, *61*, 961-967.

18. Zhou, P.; Blumstein, A. *Polymer* **1997**, *38*, 595-604.

19. Bestmann, H. J.; Kloeters, W. *Angew. Chem. Int. Ed. Engl.* **1977**, *16*, 45-46.

20. Stang, P. J.; Tykwinski, R.; Zhdankin, V. V. *J. Org. Chem.* **1992**, *57*, 1861-1864.

21. Jürgen Bestmann, H.; Kisielowski, L. *Tetrahedron Lett.* **1990**, *31*, 3301-3304.

22. Bestmann, H. J.; Kisielowski, L. *Chem. Ber.* **1983**, *116*, 1320-1326.

23. Xu, X.; Fröhlich, R.; Daniliuc, C. G.; Kehr, G.; Erker, G. *Chem. Commun.* **2012**, *48*, 6109-6111.

24. Colebatch, A. L.; Cade, I. A.; Hill, A. F.; Bhadbhade, M. M. *Organometallics* **2013**, *32*, 4766-4774.

25. Sünkel, K.; Birk, U. *Polyhedron* **1999**, *18*, 3187-3197.

26. Westenberg, H.; Slootweg, J. C.; Hepp, A.; Kösters, J.; Roters, S.; Ehlers, A. W.; Lammertsma, K.; Uhl, W. *Organometallics* **2010**, *29*, 1323-1330.

27. Möbus, J.; Bonnin, Q.; Ueda, K.; Fröhlich, R.; Itami, K.; Kehr, G.; Erker, G. *Angew. Chem. Int. Ed.* **2012**, *51*, 1954-1957.

28. Mobus, J.; Kehr, G.; Daniliuc, C. G.; Frohlich, R.; Erker, G. *Dalton Trans.* **2014**, *43*, 632-638.

29. Peregudova, S.; Denisovich, L.; Ustynyuk, N.; Leont'eva, L.; Vinogradova, V.; Filatova, T. *Russ. Chem. Bull.* **1995**, *44*, 1973-1975.

30. Miller, S. I.; Ziegler, G. R.; Wieleseck, R. *Org. Synth.* **1965**, *45*, 86.

31. Li, M.; Li, Y.; Zhao, B.; Liang, F.; Jin, L. *RSC Adv.* **2014**, *4*, 30046-30049.

32. Albright, T. A.; Freeman, W. J.; Schweizer, E. E. *J. Am. Chem. Soc.* **1975**, *97*, 2946-2950.

33. Mann, B. E. *J. Chem. Soc., Perkin Trans. 2* **1972**, 30-34.

34. Miller, S. I.; Tanaka, R. *J. Org. Chem.* **1971**, *36*, 3856-3861.

35. Ivanova, N. R.; Panfilovich, Z. U.; Lipatova, I. P.; Kuz'min, K. I. *Metalloorg. Khim.* **1990**, *3(2)*, 346-351.

36. Nagaoka, T.; Sueda, T.; Ochiai, M. *Tetrahedron Lett.* **1995**, *36*, 261-264.

37. Hartmann, H.; Kühl, G. *Z. anorg. allg. Chem.* **1961**, *312*, 186-194.

38. Matano, Y. *Chem. Commun.* **2000**, 2233-2234.

39. Sueda, T.; Oshima, A.; Teno, N. *Org. Lett.* **2011**, *13*, 3996-3999.

40. Dickstein, J. I.; Miller, S. I. *J. Org. Chem.* **1972**, *37*, 2175-2180.

41. Becke, A. D. *J. Chem. Phys.* **1993**, *98*, 5648-5652.

42. Lee, C.; Yang, W.; Parr, R. G. *Phys. Rev. B* **1988**, *37*, 785.

43. Vosko, S. H.; Wilk, L.; Nusair, M. *Can. J. Phys.* **1980**, *58*, 1200-1211.

44. Stephens, P. J.; Devlin, F. J.; Chabalowski, C. F.; Frisch, M. J. *J. Phys. Chem.* **1994**, *98*, 11623-11627.

45. Ditchfield, R.; Hehre, W. J.; Pople, J. A. *J. Chem. Phys.* **1971**, *54*, 724-728.

46. Gaussian 09, Revision A.02, M. J. Frisch, G. W. Trucks, H. B. Schlegel, G. E. Scuseria, M. A. Robb, J. R. Cheeseman, G. Scalmani, V. Barone, G. A. Petersson, H. Nakatsuji, X. Li, M. Caricato, A. Marenich, J. Bloino, B. G. Janesko, R. Gomperts, B. Mennucci, H. P. Hratchian, J. V. Ortiz, A. F. Izmaylov, J. L. Sonnenberg, D. Williams-Young, F. Ding, F. Lipparini, F. Egidi, J. Goings, B. Peng, A. Petrone, T. Henderson, D. Ranasinghe, V. G. Zakrzewski, J. Gao, N. Rega, G. Zheng, W. Liang, M. Hada, M. Ehara, K. Toyota, R. Fukuda, J. Hasegawa, M. Ishida, T. Nakajima, Y. Honda, O. Kitao, H. Nakai, T. Vreven, K. Throssell, J. A. Montgomery, Jr., J. E. Peralta, F. Ogliaro, M. Bearpark, J. J. Heyd, E. Brothers, K. N. Kudin, V. N. Staroverov, T. Keith, R. Kobayashi, J. Normand, K. Raghavachari, A. Rendell, J. C. Burant, S. S. Iyengar, J. Tomasi, M. Cossi, J. M. Millam, M. Klene, C. Adamo, R. Cammi, J. W. Ochterski, R. L. Martin, K. Morokuma, O. Farkas, J. B. Foresman, and D. J. Fox, Gaussian, Inc., Wallingford CT, 2009.

47. GaussView, Version 5.0.8, Dennington, Roy; Keith, T.; Millam, John. Semichem Inc., Shawnee Mission, KS, 2009.

48. Fulmer, G. R.; Miller, A. J.; Sherden, N. H.; Gottlieb, H. E.; Nudelman, A.; Stoltz, B. M.; Bercaw, J. E.; Goldberg, K. I. *Organometallics* **2010**, *29*, 2176-2179.

49. SAINT, v. 7. 6.; Bruker AXS Inc., Madison, WI, 2008.

50. SAINT, v. 8. 3.; Bruker AXS Inc, Madison, WI, 2015.

51. Sheldrick, G. M. *Acta Cryst. A* **2015**, *71*, 3-8.

52. Hübschle, C. B.; Sheldrick, G. M.; Dittrich, B. *J. App. Cryst.* **2011**, *44*, 1281-1284.

53. Sheldrick, G. M. *Acta Cryst. C* **2015**, *71*, 3-8.

54. Farrugia, L. J. *J. App. Cryst.* **2012**, *45*, 849-854.

55. Dunbar, K. R.; Haefner, S. C. *Polyhedron* **1994**, *13*, 727-736.

56. Guilhem, J. *Cryst. Struct. Commun.* **1974**, *3*, 227.

2 *m*-Terphenyl Substituted Cyclopentadienyl Ligands

2.1 Overview

Cyclopentadiene is an organic molecule with the molecular formula C_5H_6. In terms of hydrocarbon molecules, the cyclopentadiene molecule is unusually acidic (pK_a *ca.* 15)[1,2] and is readily deprotonated by strong bases such as alkali metal hydrides or amides to produce the aromatic cyclopentadienyl anion ($C_5H_5^-$, abbreviated as Cp) (Figure 2.1).

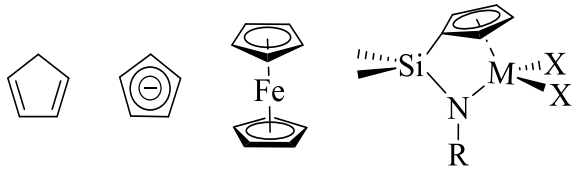

Figure 2.1. Cyclopentadiene (left), the cyclopentadienyl anion (middle left), the first metallocene complex, ferrocene (middle right), and a typical cyclopentadienyl-amido complex (right).

Since the serendipitous discovery of ferrocene (Figure 2.1) by Pauson and Kealy in 1951,[3] and elucidation of its structure and bonding the following year,[4] the Cp ligand has become one of the most fundamental ligands in organometallic chemistry. Complexes incorporating cyclopentadienyl ligands are known for most main group elements, all abundant transition metals, and most accessible *f*-block elements. Cyclopentadienyl ligands have demonstrated excellent utility in catalytic processes: particularly those incorporating chelating cyclopentadienyl-amido ligands bound to Group IV metals for olefin polymerisation reactions (Figure 2.1; M = Ti, Zr, or Hf).[5-10] The importance of cyclopentadienyl ligands and their respective complexes have also been highlighted in various review articles[11-14] and have rich potential in asymmetric catalysis.[15]

One of the most attractive features of cyclopentadienyl ligands is that they are easily modified, which allows for specific tailoring of their combined steric and electronic properties. The permethylated analogue ($C_5Me_5^-$, abbreviated as Cp*) is an excellent example and has remained a popular ligand in organometallic chemistry due to its (often beneficial) properties in comparison to the parent unsubstituted Cp complexes. These properties include increased steric hindrance at the metal centre, superior electron donating capabilities, and improved solubility in organic solvents.[16-18] Cyclopentadienyl ligands incorporating even bulkier substituents have demonstrated their usefulness in accessing unprecedented or unusual molecular structure, spin states, or reactivity.[16,19-24]

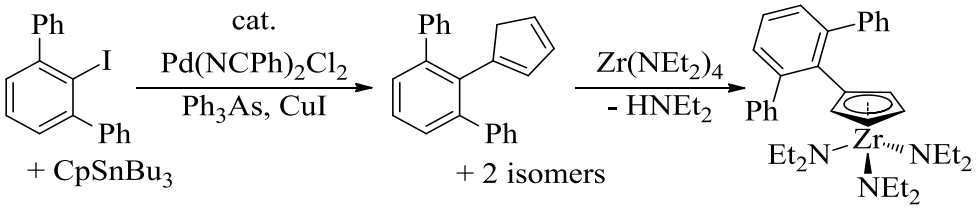

Scheme 2.1. Solitary synthetic route for *m*-terphenyl cyclopentadienyl ligand precursors and its only known metal complex.

Presently, examples of free *m*-terphenyl substituted Cp ligands and their corresponding metal complexes are extremely limited in the literature. The bulky cyclopentadienyl ligand precursor $Ter^{Ph}CpH$ (Ter^{Ph} = C_6H_2-2,6-Ph_2) synthesised through a Pd-catalysed cross-coupling reaction, and a corresponding Zr complex (Scheme 2.1) are the only examples.[25] It was hypothesised and highly anticipated that by expanding the library of known *m*-terphenyl substituted Cp ligands, a new class of hemilabile, bidentate cyclopentadienyl ligands would emerge that are capable of binding to metal centers through both cyclopentadienyl and aryl substituents. Furthermore, an improvement in

solubility and simplification of ^{1}H and $^{13}C\{^{1}H\}$ NMR spectra is expected from the addition of substituents to the *m*-terphenyl ligand thereby increasing the utility of these molecules in organometallic chemistry.

2.1.1 Sterically Hindered Cyclopentadienyl Ligands

The description for a "bulky Cp" ligand is poorly defined in the literature and is often dependent on the authors' perspective. For example, a mono *tert*-butyl substituted Cp ligand may be considered as sterically demanding in some situations. The most recent review on the subject (1991)[26] offered the clearest description and included only cyclopentadienyl ligands with three or more substituents larger than a methyl group − an arbitrary decision meant to limit the size of the article. Under these criteria the *m*-terphenyl Cp molecules synthesised over the course of this project would not be considered as bulky cyclopentadienyl ligands. However, the *m*-terphenyl Cp molecules synthesised in this project will be treated as bulky ligands due to the already well-established opinion that *m*-terphenyl ligands are sufficiently large to allow the isolation of novel molecular structures that are otherwise inaccessible.[27-31]

The use of sterically hindered cyclopentadienyl ligands has followed closely in line with how convenient the ligands are to prepare. The coordination chemistry of polyarylated cyclopentadienyl ligands was the first to be developed due to convenient synthetic routes, and used relatively inexpensive, commercially available starting materials. Synthetic routes to tri- and tetraphenylcyclopentadiene were first described in 1898,[32,33] while the initially reported synthesis of pentaphenylcyclopentadiene occurred in 1925.[34] Development of the coordination chemistry of polyalkylated cyclopentadienyl ligands

occurred much later due to the increased difficulty in obtaining the parent dienes: which often require organometallic reagents or techniques such as sequential metalation/alkylation (e.g. Scheme 2.4). Unsurprisingly, many developments involving these ligands were made by organometallic chemists themselves in their search for new ligands, as is exemplified by molecules such as tetra- and penta(isopropyl) cyclopentadiene,[35,36] or 1,2,4-tri(isopropyl)-3,5-dimethyl cyclopentadiene.[37]

As mentioned earlier, the chemistry of sterically hindered cyclopentadienyl ligands is significantly influenced by the availability of economical, high yielding, large scale synthetic routes to the precursor dienes or their bromine derivatives. While economical and high yielding are relative terms, large scale synthetic routes on the order of tens or hundreds of grams are essential for bulky cyclopentadienyl ligands due to their inherently low mole/mass ratio. Unfortunately most sterically demanding cyclopentadienyl ligands are not commercially available or are prohibitively expensive for routine use. Therefore under most circumstances the synthesis of the bulky cyclopentadiene precursor is an important first step before the exploration of any coordination chemistry can begin.

Three general synthetic routes[26] are available for the synthesis of sterically demanding cyclopentadienes: (1) construction of the C_5 ring from a combination of C_3, C_2, or C_1 fragments in which the bulky substituents are already attached; (2) through replacement of hydrogen atoms of the parent cyclopentadiene, C_5H_6, with bulky groups or (3) by modifying an already sterically demanding C_5 system. Some conventional organic and organometallic routes to sterically hindered cyclopentadienes are given below (many

of these routes are also applicable to non-bulky dienes), but these are by no means a comprehensive list.

Method 1: Assembly of the C_5 ring system

Tetra- and pentaphenylcyclopentadiene can be synthesised *via* the homocoupling of diphenylacetylene with elemental lithium followed by the subsequent reaction of the dilithiated intermediate with either methylene bromide or benzal chloride (Scheme 2.2).[38] Yields for the corresponding dienes are 51% and 66%, respectively. Amounts were not specified, but the dilithiated intermediate was produced on a 2 g scale. The main setback this route suffers from is the tendency for the dilithiated intermediate to undergo dimerisation yielding 1,2,3-triphenylnapthalene.[39] To circumvent this issue the conversion was only allowed to reach 60% (determined by quenching the intermediate with methanol and weighing the tetraphenylbutadiene) before the addition of dihalogenated reagents.[38]

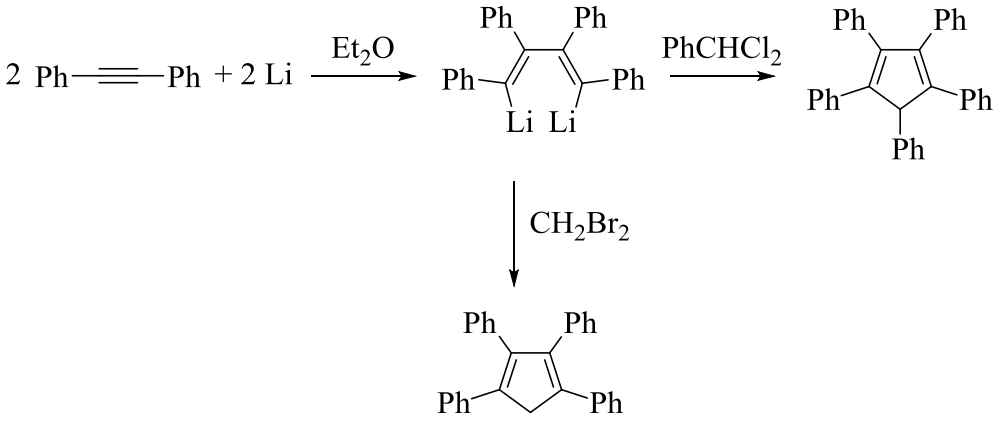

Scheme 2.2. Synthetic route to tetra- and pentaphenylcyclopentadienes using diphenylacetylene.

Tetraphenyl cyclopentadiene derivatives can also be synthesised through the coupling of substituted phenylacetophenones with formaldehyde *via* a base-catalysed

condensation reaction.[40] Subsequently the 1,5-diketone can be reductively cyclised with zinc in acetic acid to produce the corresponding 1,2-diol, which affords the corresponding tetraaryl cyclopentadiene following an acid-catalysed dehydration.[40] Reaction scales ranged between 3.8 g and 28.8 g with yields ranging between 32 % and 94%.

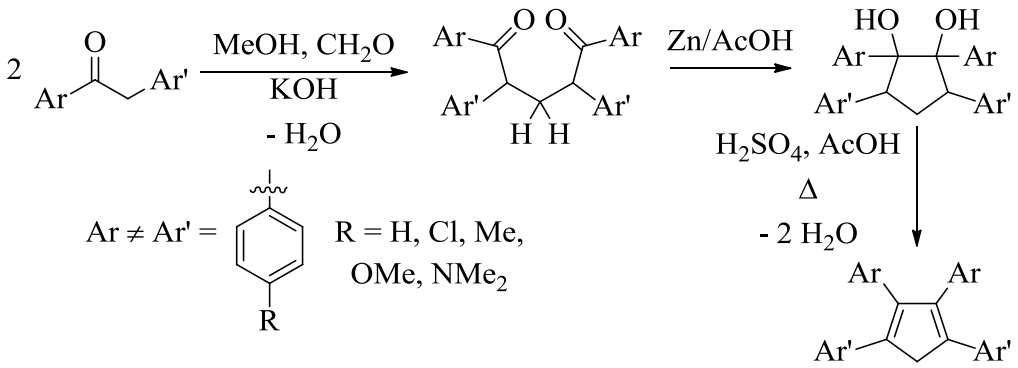

Scheme 2.3. Synthesis of tetraaryl cyclopentadienes from phenylacetophenone derivatives.

Method 2: Hydrogen atom replacement

Reaction of the cyclopentadienyl anion with alkyl halides affords polyalkylated cyclopentadienes. The primary advantage of this route over others is that it allows for the specific tailoring of steric properties through the stepwise addition of groups. However, it lacks selectivity and leads to the production of non-acidic isomers that require removal and lower overall yields. This route is also applicable to ethyl (up to pentasubstitution),[26] *tert*-butyl,[36] and trimethylsilyl[41] (up to trisubstitution) with minimal modification.

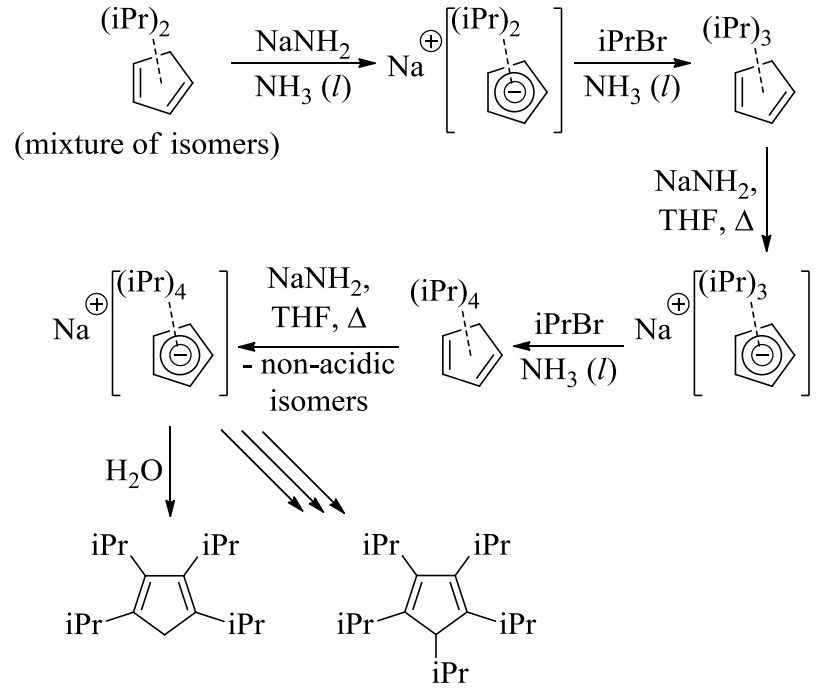

Scheme 2.4. Stepwise synthesis of polyalkylated cyclopentadienyl ligands. Triisopropylcyclopentadiene is obtained in a 4:1 ratio of 1,2,4- and 1,2,3-substituted isomers.[35] Non-acidic isomers dialkylated at the 5,5' position and are removed by evaporation *in vacuo*.

This route is largely inapplicable for aryl halides as they are resistant to nucleophilic substitution reactions, however, special cases are known. Sodium cyclopentadienide has been shown to react with an excess of hexafluorobenzene and sodium hydride to give either mono- or di-substituted,[42] or a mixture of mono-, di-, and triaryl substituted pentafluorophenyl cyclopentadiene products and their respective isomers in a one-pot reaction.[43,44] This reaction is believed to occur *via* a series of S_NAr reactions, and is therefore analogous to Scheme 2.4. Purification of this mixture by column chromatography afforded the respective dienes albeit in low individual yields relative to sodium cyclopentadienide (2–26% in dimethoxyethane at 85 °C).[44] Longer reaction times

at higher temperatures increase the degree of substitution, allowing for the isolation of the tetrasubstituted isomer as the dominant product (57% in diglyme at 110 °C for two days).[44] The pentasubstituted cyclopentadiene could not be obtained from this reaction even with higher temperatures or longer reaction times.

Method 3: Modification of a Preassembled, Sterically Hindered C_5 system

Modification of a preassembled sterically congested C_5 system is often the most direct route to bulky cyclopentadienes. The first reported synthesis of pentaphenylcyclopentadiene followed this method;[34] the reaction between tetracyclone and phenyl lithium produces pentaphenylcyclopentadienol following aqueous work up. This can be isolated directly or reduced to produce the respective cyclopentadiene (Scheme 2.5). This route is highly effective due to the relatively low cost of tetracyclone (or the benzil and dibenzyl ketone required to synthesise tetracyclone[45]), and the moderate to high yields (50–70%) on reaction scales between 50 and 100 grams.[34,46]

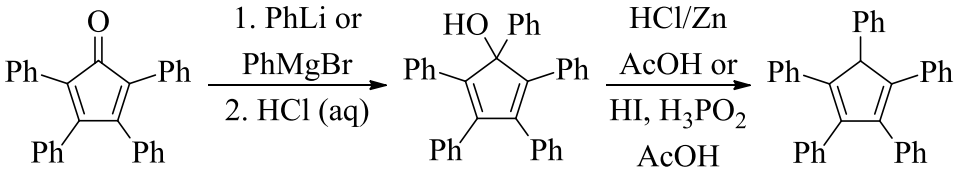

Scheme 2.5. Synthesis of pentaphenylcyclopentadiene from tetracyclone.

This reaction is only applicable for highly substituted cyclopentadienones; those with smaller or fewer substituents may undergo dimerization *via* 4+2 cycloaddition.[47] This can be prevented by using cyclopentenones instead of cyclopentadienones and have led to the isolation of significantly substituted cyclopentadienes such as 1,2,4-tri(isopropyl)-3,5-dimethyl cyclopentadiene (Scheme 2.6).[37] The parent cyclopentenone can be prepared on

the scale of several hundred grams with a yield of 77%, while the cyclopentadiene is prepared on a 20 g scale in 72% yield from commercially available isopropylmagnesium chloride.[37]

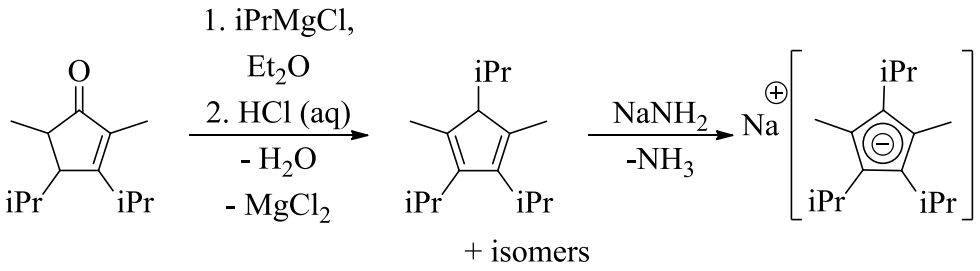

Scheme 2.6. Synthesis of sterically hindered cyclopentadienes from cyclopentenones.

While this route is very general,[14] a caveat is that it is limited to moderately substituted cyclopentenones. While this seems like a harmless condition if highly substituted molecules are desired, it does provide a challenge during the initial substitution reactions particularly when metallated arenes are used as nucleophiles. Two deviant reactions are particularly problematic (Scheme 2.7); (i) nucleophilic attack may occur at the β-carbon resulting in a 1,4-addition, followed by tautomerisation after hydrolysis to yield a formal 3,4-addition product or (ii) deprotonation of the ketone may occur by the carbanion, which regenerates the starting ketone upon hydrolysis.[14,48] Additives capable of suppressing these side reactions are known for Grignard reagents such as $CeCl_3$,[49] which functions by lowering the basicity of Grignard reagents while activating the carbonyl group due to the high oxophilicity of cerium, however these are not always effective at mediating the reaction.[50]

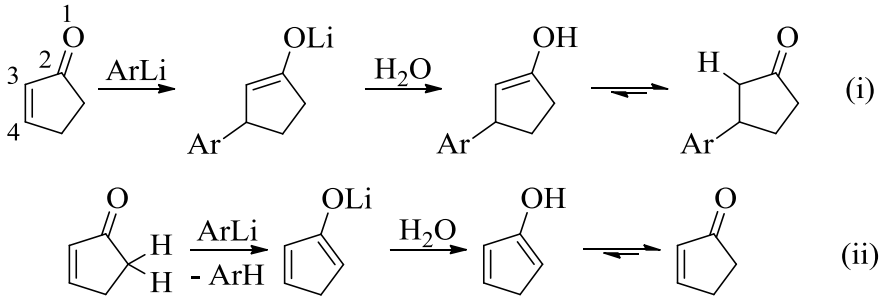

Scheme 2.7. Deviant reaction pathways of S_N2 reactions with cyclopetenones.

As previously stated, this is only an outline of a small number of the conventional syntheses; more comprehensive reviews on sterically hindered,[26] aryl substituted,[14] and chiral[15] cyclopentadienyl ligands are given in the literature and provide less common examples such as the synthetic route used for the synthesis of the *m*-terphenyl cyclopentadienyl ligands described in this project using cobaltocenium salts (refer to section 2.3.1.2 of the Results and Discussion section for a detailed explanation).

2.1.2 Preparation of Cyclopentadienyl Metal Complexes

Many of the conventional synthetic routes used to make typical unhindered Cp complexes are also compatible with the bulkier analogues. The three reactions most frequently used are (i) salt metathesis, (ii) oxidative addition, and (iii) metalation/deprotonation (Scheme 2.8).

$$CpM + M'X \longrightarrow CpM' + MX \quad (i)$$

$$CpX + M^{m+}L_n \longrightarrow CpM^{(m+2)+}L_{n-a}X + a\ L \quad (ii)$$

$$2\ CpH + 2\ M \longrightarrow 2\ CpM + H_2 \quad (iii)$$

Scheme 2.8. General reaction schemes for the preparation of Cp metal complexes using conventional synthetic routes.[26] For process (i) M is typically an alkali metal salt, M' is any other metal, and X is a halide, (ii) X is a halide (typically Br), M^{m+} is often a low

oxidation state metal (m = 0–2), and L is typically CO and in (iii) M is typically a Group I metal.

The latter is particularly useful as it allows the direct synthesis of alkali metal salts of Cp ligands from their respective elements (e.g. NaCp or KCp from CpH and Na or K metals).[37,51] Their respective hydrides or amides are also acceptable reagents. Transition metal amides have also been used to prepare cyclopentadienyl complexes from the parent dienes.[14,25] Salt metathesis was the first to be discovered for complexes beyond alkali metal salts (e.g. ferrocene[3]) and is frequently used to prepare the majority of new Cp complexes, while oxidative addition reactions are typically reserved for low oxidation state metals and require the bromine derivative of a highly substituted cyclopentadienyl ligand.[26] Bromine derivatives are preferred for these reactions due to their compatibility with low oxidation state metals (*c.f.* soft-hard acid base theory) and their higher stability in comparison to CpI derivatives, while multiple substituents reduce the rate of nucleophilic substitution reactions that occur on the Cp ring.[52,53]

Methods (i) and (iii) are the most relevant for discussing the new molecules synthesised over the duration of this project, however it is expected that (ii) will become increasingly important in the near future for targeting electron-rich metals such as Cu or Pd. There are other synthetic routes that have been developed out of fundamental interest,[54-56] but these are far too specific to discuss and irrelevant to the methods used in this work.

2.1.3 Concepts for Using Bulky Cyclopentadienyl Ligands

Four main conceptual areas for using bulky cyclopentadienyl ligands were outlined in the most recent review[26] and have persisted as general areas of research and interest in the field of cyclopentadienyl chemistry.[16,19-24]

The first and arguably most fundamental idea is the use of bulky ligands to provide kinetic inertness to thermodynamically unstable species. This is a well-established concept in the field of molecular chemistry and is governed by the idea that unstable species can be isolated by using large substituents to shield highly reactive sites. These substituents act as a protective barrier, lowering the rate of decomposition through homomolecular collisions in solution or by reacting with small molecules such as water or oxygen.

A second concept of perpetual interest is the use of sterically hindered cyclopentadienyl ligands to invoke new and unusual molecular geometry. Significantly different molecular geometry is often facilitated by extremely bulky ligands by shifting the balance of steric and electronic properties. This shift often allows the isolation of molecules that lie in local minima along the potential energy surface that are otherwise inaccessible using smaller ligands. This concept was applied to isolate the first terminal cerium hydride Ce[C_5H_2(*t*Bu)$_3$]H.[57] These molecules have a tendency to dimerise or oligomerise when less sterically demanding substituents are employed such as Cp*,[58] but are isolable if the ligands employed are large enough to block low-lying vacant orbitals at the metal centre (Figure 2.2).

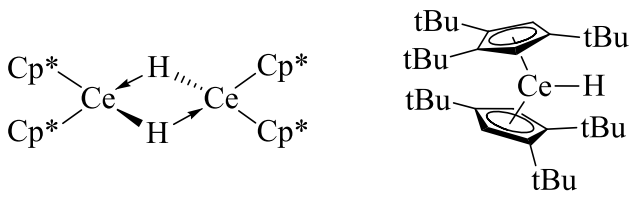

Figure 2.2. Steric influence of Cp ligands in cerium(III) hydride complexes.

The third and fourth concepts are closely related, and are focused on the rotation dynamics and chirality of the organometallic complexes. In the most trivial cases, chirality will be present if a chiral substituent is present on the Cp ring (Figure 2.3, i), or if two or more different substituents are present on the Cp ring (Figure 2.3, ii). Another common example of chirality is when rotation is prevented in achiral substituents (Figure 2.3, iii). Lastly, sterically crowded cyclopentadienyl rings are more likely to experience reduced rotation about the metal centre due to repulsive forces between the bulky substituents bound to each ring. While this makes rotation dynamics much easier to study in-depth, chirality is frequently encountered even with achiral substituents if rotation is completely inhibited (Figure 2.3, iv).

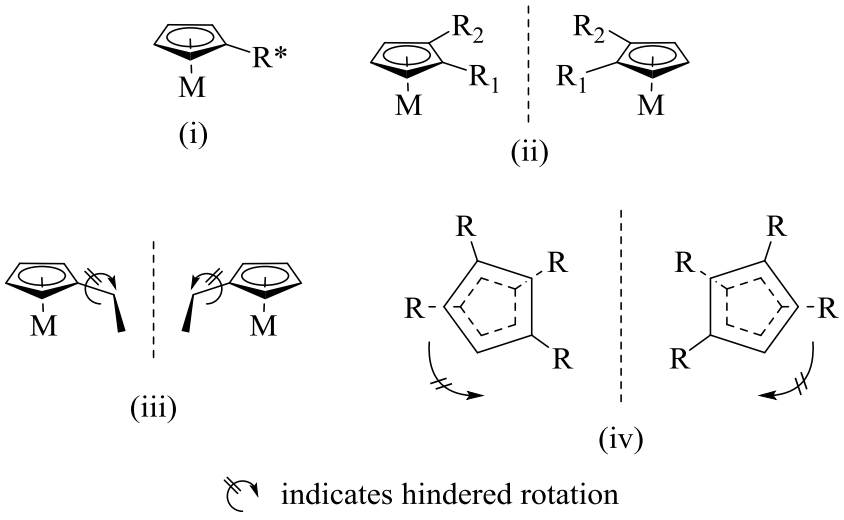

Figure 2.3. Possible configurations for chiral cyclopentadienyl complexes; (i) chirality will occur if R* is a chiral substituent, (ii) if R_1 and R_2 are different chirality will occur, (iii)

chirality will occur if rotation is prevented for a substituent and (iv) chirality will occur if the orientation of the Cp rings are fixed in place (note that this is only a schematic representation to illustrate the principal).

The primary purpose for targeting *m*-terphenyl substituted cyclopentadienyl ligands is to investigate the bonding properties of both cyclopentadienyl and aryl substituents, therefore the first two concepts are the most relevant to this project. If both the cyclopentadienyl and aryl rings participate in bonding with the metal centre, then it is likely that rotation dynamics will not be applicable as rotation about the Cp-M axis would be locked. However, chirality may become important as this project progresses, particularly if other substituents are added to the cyclopentadienyl ring in the future.

2.2 Experimental

All manipulations were carried out under an inert atmosphere of dry nitrogen or argon gas using either standard Schlenk techniques or in an mBraun inert atmosphere glovebox unless otherwise stated. Calculations (B3LYP,[59-62] 6-31G(d)[63]) were completed using the Gaussian 09W suite of programs[64] and visualised using the program GaussView.[65] Glassware was dried for a minimum of four hours in a 150 °C oven prior to use. Alumina and 4 Å molecular sieves were pre-dried in an oven at 150 °C for one day prior to drying at 300 °C *in vacuo*. Celite® and silica gel were dried by storing in a 150 °C oven for a minimum of three days prior to use. NMR solvents were purchased from Cambridge Isotope Laboratories, Inc. and stored over 4 Å molecular sieves for a minimum of one day prior to use. NMR spectra were recorded at 298 K on a 300 MHz spectrometer unless otherwise indicated and are reported in ppm. ^{1}H NMR spectra are collected in

deuterated (^{2}H, defined as D) solvents and referenced[66] internally to either residual protio (^{1}H) solvents relative to tetramethylsilane, TMS (δ = 0 ppm), or using an internal TMS standard ($CDCl_3$ only). The $^{13}C\{^1H\}$ NMR spectra were referenced[66] internally to the deuterated solvents in which they were collected relative to TMS (δ = 0 ppm). ^{31}P NMR chemical shifts are referenced to an external standard of 85% phosphoric acid (δ = 0 ppm). Coupling constants are reported in Hz and are given as absolute values. IR spectra were collected as KBR pellets using an ALPHA FT-IR spectrometer (Bruker) unless otherwise indicated. UV-Vis absorption spectra were collected in 1 cm quartz cuvettes using a Cary 50 Bio spectrophotometer (Agilent) unless otherwise indicated. Melting points were recorded on an Electrothermal MEL-Temp 3.0 using glass capillaries sealed under inert conditions. Elemental analysis was performed by the Centre for Environmental Analysis and Remediation (CEAR) facility at Saint Mary's University using a Perkin Elmer 2400 II series Elemental Analyser. Deionised water was used in synthetic procedures unless otherwise indicated. Dichloromethane (Caledon Laboratory Chemicals), diethyl ether (ACP Chemicals Inc.), THF (Caledon Laboratory Chemicals), toluene (Caledon Laboratory Chemicals), and pentane (Fisher Scientific) were dried using an alumina-based solvent purification system from Vacuum Atmospheres. Diethyl ether, THF, toluene, and pentane were further dried using KH followed by filtration through alumina and stored over 4 Å molecular sieves in the glovebox. Dichloromethane was stored over 4 Å molecular sieves for a minimum of three days prior to use. Acetonitrile (Fisher Scientific) was used without further purification. All reagents were purchased from Sigma-Aldrich and used as received, unless otherwise noted. Sodium hydride and potassium hydride were purchased as mineral oil dispersions (60% and 30% respectively) from Sigma-Aldrich and washed

three times with an appropriate amount of pentane, and dried *in vacuo* until a free-flowing powder was obtained. Cobalt(II) chloride hexahydrate (ACP Chemicals Inc.) was ground into a fine powder and dried in a 150 °C oven until uniformly blue in colour and used without further purification.

2.2.1 X-ray crystallography

Under inert conditions, crystals were prepared for mounting by suspending them in paratone-N oil on a microscope slide. Crystals were attached to the tip of an appropriate sized MiTeGen loop with paratone-N oil and cooled to 125 K. Measurements were made on a Bruker APEX2 CCD equipped diffractometer (30 mA, 50 mV) using monochromated Mo Kα radiation (λ = 0.71073 Å) at 125 K. The initial orientation and unit cell were indexed[67] using a least-squares analysis of a random set of reflections collected from three series of 0.5° wide scans, 10 seconds per frame and 12 frames per series that were well distributed in reciprocal space. For data collection, four ω-scan frame series were collected with 0.5° wide scans and 366 frames per series at varying φ angles (φ = 0°, 90°, 180°, 270°). The frame length was adjusted between 10 s and 60 s to provide an expected resolution limit below 0.8 Å. The crystal to detector distance was set to 6 cm and a complete sphere of data was collected. Cell refinement and data reduction were performed with the Bruker SAINT software,[68] which corrects for beam inhomogeneity, possible crystal decay, Lorentz and polarization effects. Data processing and a multi-scan absorption correction was applied using APEX3 software package.[68] Structures were solved using direct[68] or intrinsic methods[69] and all non-hydrogen atoms were refined anisotropically using the ShelXLE[70] graphical user interface and SHELXL.[71] Hydrogen atoms were included at geometrically idealized positions and were fixed (Ar-H, C-H, CH_2) or, in the case of methyl

groups, the dihedral angle of the idealized tetrahedral CH_3 fragment was allowed to refine, and coupled with isotropic temperature factors. Figures were made using ORTEP-3 for Windows.[72]

During the refinement of the homocoupled dimer **9'**, some disorder was encountered in the central cyclopentadiene. This was modelled using a combination of SIMU and DELU restraints.

During the refinement of the lithium cyclopentadienide **10**, two-site lithium disorder was encountered Different components of the disorder were separated using the PART command. Site occupancies were allowed to freely refine.

During the structure refinement of $[Na(THF)Ter^{Mes}Cp{\cdot}NaCp(THF)]_\infty$, some disorder was present in one of the coordinated THF molecules and could not be modelled, so bond lengths and angles have been excluded. This structure has been included to show connectivity.

During the structure refinement of $[KTer^{Mes}Cp]_2[KN(SiMe_3)_2]_2$ (**12'**) disorder was encountered in a molecule of co-crystallised pentane. Different components of the disorder were separated using the PART command. Site occupancies were allowed to freely refine. The C-C distances for the molecule of pentane were restrained to be approximately equal using the SADI command, and restrained using a combination of SIMU, DELU, and ISOR commands.

Multiple (>7) non-coordinating solvent molecules were visible during the structure refinement of the caesium cyclopentadienide **14**, some of which were disordered and could not be modelled properly. To remedy this, the residual electron density attributed to these

molecules was removed by implementing PLATON's squeeze command,[91] removing a total electron density of 347 electrons per unit cell, which corresponded to *ca.*8.5 molecules of THF.

During the structure refinement of the cobaltocene **16** disorder was encountered in a molecule of co-crystallised pentane. Different components of the disorder were separated using the PART command. Site occupancies were allowed to freely refine. The C-C distances for the molecule of pentane were restrained to be approximately equal using the SADI command, and restrained using a combination of SIMU and DELU commands.

During the structure refinement of the bismuth complex **19**, the orientation of the hydrogen atoms in the methyl groups C19 and C20 were modelled as disordered between two positions. Site occupancies were allowed to freely refine.

During the refinement of the Ter^{Dipp} cobalt intermediate **20** and cyclopentadiene **21**, significant disorder was encountered that could not be modelled. These structures have been included for connectivity.

2.2.2 Synthesis of $Ter^{Mes}I$

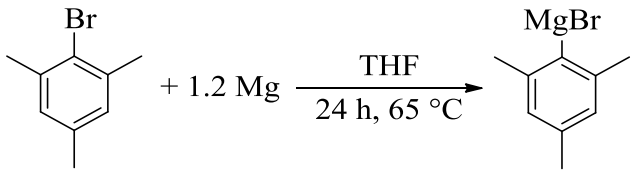

Following a similar procedure as those reported in the literature,[73,74] magnesium powder (7.21 g, 296 mmol, 1.18 eq.) and a PTFE-coated magnetic stir bar were added to a 250 mL, 3-necked round bottom flask equipped with a 100 mL pressure-equalising dropping funnel capped with a rubber septum, and a reflux condenser capped with a gas

adaptor. A glass stopper was added to the remaining neck, and 10 mL of THF were added to the magnesium through the dropping funnel to produce a slurry. The magnesium slurry was heated to 60 °C before adding *ca*. 100 mg of I_2 to activate the magnesium. The slurry became slightly green and the THF began to boil. In the dropping funnel, 2-bromomesitylene (50.0 g, 251 mmol, 1 eq.) and 40 mL of THF were combined to produce a 1:1 MesBr:THF solution, which was then added dropwise to the magnesium slurry, producing a dark brown coloured mixture. The dropping funnel was rinsed with an additional 60 mL of THF, and the reaction mixture was left to reflux for 6 h. The reaction mixture was adjusted to just below reflux temperature (*ca.* 65 °C) and left to stir overnight. The following day the mixture was left to cool to room temperature before being used in the next reaction.

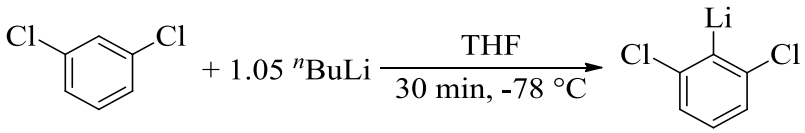

The following day, a 1 L, 2-necked round bottom flask equipped with a PTFE-coated magnetic stir bar, a reflux condenser fitted with a gas adaptor and a 125 mL pressure-equalising dropping with a rubber septum was assembled. To the dropping funnel, pale yellow coloured 1,3-dichlorobenzene (14.7 g, 99.8 mmol, 1 eq.) were added and transferred to the round bottom flask. The contents of the flask were diluted by rinsing the dropping funnel with 150 mL of THF, producing a pale yellow coloured solution. The reaction flask was then cooled to -78 °C using a liquid nitrogen/isopropanol bath. To the dropping funnel, 42.5 mL of a pale yellow coloured solution of BuLi (2.5 M in hexanes, 106 mmol, 1.06 eq.) were added *via* syringe. While maintaining a temperature of -78 °C, the pale yellow coloured solution of BuLi was added dropwise to the pale yellow coloured solution of 1,3-

dichlorobenzene to produce a peach coloured mixture. After the addition was complete, the dropping funnel was rinsed with 10 mL of THF and the reaction mixture was left to stir for 30 minutes at -78 °C. During this time, the brown coloured MesMgBr Grignard solution was transferred to the 125 mL dropping funnel *via* cannula.

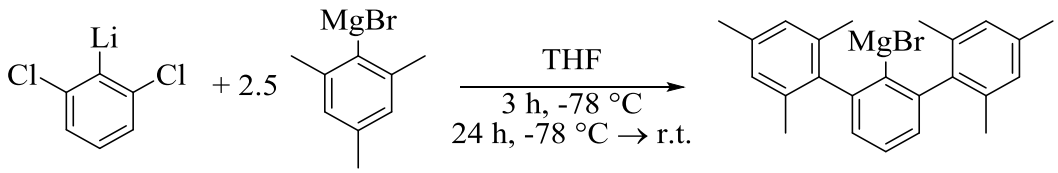

The MesMgBr Grignard solution was then added dropwise to the peach coloured reaction mixture over a period of 3h while maintaining a temperature of -78 °C. Over the course of the addition, the colour of the reaction mixture changed from an initial peach colour, to yellow, then orange, then reddish-orange, before finally reaching a reddish-brown colour. After the addition was complete, the reaction mixture was left to warm up to room temperature overnight.

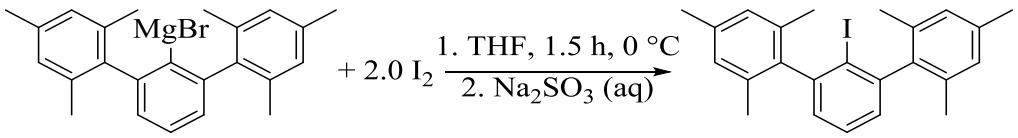

The following day, the dark brown coloured mixture of Ter^{Mes}MgBr was cooled to 0 °C using an ice-water bath. The reflux condenser was removed and dropping funnel was replaced with a gas adaptor, leaving the centre neck open to the atmosphere. Using a funnel, violet coloured I_2 crystals (50.9 g, 201 mmol, 2.01 eq.) were slowly added to the flask, and the colour of the reaction mixture changed to dark reddish-brown. This mixture was left to stir in the ice-water bath for 1.5 h. Excess I_2 was then quenched using 500 mL of a 1 M aqueous solution of Na_2SO_3. Addition of the colourless solution of Na_2SO_3 to the reddish-

brown coloured reaction mixture produced a bright yellow coloured mixture that was left to warm up to room temperature and stir overnight.

The following day, the yellow coloured mixture was left to separate into a bright yellow coloured top organic layer and a pale yellow coloured bottom aqueous layer, with some colourless precipitate in the bottom of the flask. The reaction mixture was transferred into a 1 L separatory funnel and the yellow coloured organic fraction was collected and washed once with 200 mL of a saturated aqueous solution of NaCl. The yellow coloured organic fraction was then dried with $MgSO_4$ for 20 minutes before removing the solids by vacuum filtration. The yellow coloured filtrate was transferred to a 1 L round bottom flask and the volatiles were removed *in vacuo* to yield a yellow coloured solid.

The yellow coloured solid was broken up with a spatula, and *ca*. 500 mL of methanol were added to the 1 L round bottom flask. A reflux condenser with a balloon covering the top was attached to the flask and the yellow coloured mixture was refluxed for 4h. The precipitate was then separated *via* hot vacuum filtration, washed with cold methanol, and dried *in vacuo* to yield a pale yellow coloured powder. A portion of the yellow coloured methanol filtrate was collected, the solvent removed *in vacuo*, and a ^{1}H NMR spectrum was collected of the filtrate; a negligible quantity of $Ter^{Mes}I$ remained so the filtrate was discarded without further purification.

Yield: 19.41 g (44 % yield)

^{1}H NMR ($CDCl_3$): δ 7.45 (t, $^3J_{HH}$ = 7.5 Hz, 1H, *p*-C_6H_3), 7.07 (d, $^3J_{HH}$ = 7.5 Hz, 2H, *m*-C_6H_3), 6.95 (s, 4H, *m*-$C_6H_2(CH_3)_3$), 2.35 (s, 6H, *p*-CH_3), 1.98 ppm (s, 12H, *o*-CH_3).

$^{13}C\{^{1}H\}$ NMR ($CDCl_3$): δ 147.3, 142.2, 137.3, 135.5, 129.0, 128.2, 127.9, 107.8, 21.4, 20.4 ppm.

2.2.3 Synthesis of $Ter^{Mes}Li$

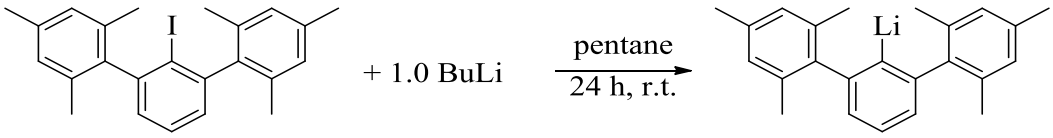

Following a similar procedure as reported in the literature,[75] to a 125 mL Erlenmeyer flask equipped with a PTFE-coated magnetic stir bar, 10.36 g (23.5 mmol, 1.0 eq.) of pale yellow $Ter^{Mes}I$ were suspended in 40 mL of pentane to produce a pale yellow mixture. To this mixture, 14.75 mL of a pale yellow coloured BuLi solution (1.6 M in hexanes, 23.6 mmol, 1.0 eq.) were added to produce a bright yellow coloured mixture. This mixture was left to stir overnight. The following day, the stir bar was removed and the bright yellow coloured mixture was filtered through a coarse glass frit, washed with a minimal amount of cold pentane, and dried *in vacuo* to yield a colourless powder.

Yield: 5.95 g (79 % yield)

^{1}H NMR (C_6D_6): δ 7.23 (t, $^{3}J_{HH}$ = 7.6 Hz, 1H, *p*-C_6H_3), 6.84 (s, 4H, *m*-$C_6H_2(CH_3)_3$), 6.82 (d, $^{3}J_{HH}$ = 7.5 Hz, 2H, *m*-C_6H_3), 2.17 (s, 6H, *p*-CH_3), 1.83 ppm (s, 12H, *o*-CH_3).

2.2.4 Synthesis of $Ter^{Dipp}I$

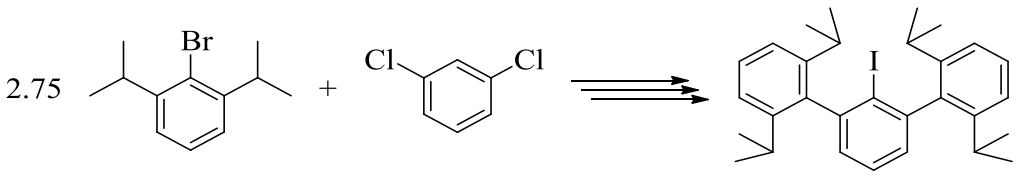

$Ter^{Dipp}I$ was synthesised following a similar method as the synthesis of $Ter^{Mes}I$ using 50.0 g (207 mmol, 2.5 eq.) of 1-bromo-2,6-diisopropylbenzene, 5.54 g (228 mmol, 2.75

eq.) magnesium, 57 mL of a BuLi solution (1.6 M in hexanes, 91.2 mmol 1.1 eq), 12.19 g (82.9 mmol, 1 eq.) of 1,3-dichlorobenzene, and 42.28 g (167 mmol, 2.0 eq.) of iodine. The product was isolated as a viscous brown coloured oil that could not be purified by refluxing in methanol. This was due to a large amount of 1-iodo-2,6-diisopropylbenzene that was recovered as a pale yellow coloured liquid from the reaction between unreacted Grignard reagent and iodine, and was removed *via* short-path vacuum distillation. Afterwards the product was crystallised from ethanol and washed with 3 x 15 mL portions of cold ethanol to produce pale yellow coloured crystals.

Yield: 5.19 g (12 %)

^{1}H NMR ($CDCl_3$): δ 7.42 (m, $^{3}J_{HH}$ = 7.3 Hz, 3H, *p*-C_6H_3, *p*-$C_6H_3(iPr)_2$), 7.22 (d, $^{3}J_{HH}$ = 7.6 Hz, 4H, *m*-$C_6H_3(iPr)_2$), 7.15 (d, $^{3}J_{HH}$ = 7.5 Hz, 2H, *m*-C_6H_3), 2.53 (sept, $^{3}J_{HH}$ = 7.1 Hz, 4H, iPr-C*H*), 1.22 (d, $^{3}J_{HH}$ = 7.1 Hz, 12H, iPr-CH_3), 1.09 ppm (d, $^{3}J_{HH}$ = 7.1 Hz, 12H, iPr-CH_3).

^{13}C{^{1}H} NMR ($CDCl_3$): δ 146.6, 146.2, 142.8, 128.6, 128.3, 127.6, 123.0, 110.3, 31.0, 25.0, 23.4 ppm.

While it may seem that the ^{13}C{^{1}H} NMR spectrum possesses an extra peak, it is in fact correct. The isopropyl groups contain chemically inequivalent methyl groups and will produce three resonances instead of two (also evident by the ^{1}H NMR spectrum).

2.2.5 Synthesis of Ter^{Dipp}Li

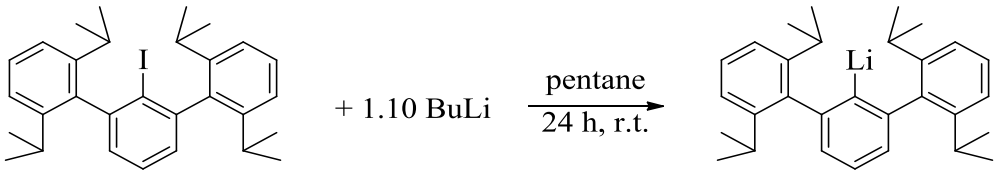

To a 20 mL scintillation vial equipped with a PTFE-coated magnetic stir bar, 0.971 g (1.85 mmol, 1 eq.) of pale yellow coloured $Ter^{Dipp}I$ were dissolved in 10 mL of pentane to produce a pale yellow coloured mixture. To this mixture, 0.80 mL of a pale yellow coloured solution of BuLi (2.5 M in hexanes, 2.0 mmol, 1.1 eq.) were added and a colourless precipitate began to form. This mixture was left to stir overnight. The following day, the stir bar was removed and the pale yellow coloured mixture was left to settle before decanting off the pale yellow coloured supernatant. The colourless precipitate was washed three times with *ca*. 2 mL of cold pentane, and dried *in vacuo* to afford a colourless powder.

Yield: 0.70 g (94 %)

^{1}H NMR (C_6D_6): δ 7.31 (t, $^3J_{HH}$ = 7.6 Hz, 1H, *p*-C_6H_3, *p*-C_6H_3(iPr)$_2$), 7.20 (d, 4H, $^3J_{HH}$ = 7.4 Hz, *m*-$C_6H_2(CH_3)_3$), 7.10 (d, $^3J_{HH}$ = 7.5 Hz, 2H, *m*-C_6H_3), 3.22 (sept, $^3J_{HH}$ = 6.9 Hz, 2H, iPr-C*H*), 2.91 (sept, $^3J_{HH}$ = 6.9 Hz, 4H, iPr-C*H*), 1.14 (d, $^3J_{HH}$ = 6.9 Hz, 12H, iPr-CH_3), 1.13 ppm (d, $^3J_{HH}$ = 6.8 Hz, 12H, iPr-CH_3).

2.2.6 Synthesis of $Ter^{Mes}H$ and $Ter^{Dipp}H$

These molecules were synthesised by adding methanol to *ca*. 50 mg of their respective lithium salts, extracting the mixture with pentane, and removing the solvent *in vacuo*. These compounds were desired to verify the presence of $Ter^{Mes}H$ and $Ter^{Dipp}H$ during the synthesis of their respective cobalt(I) intermediates **8** and **20**. Their respective ^{1}H NMR spectra were used frequently as reference standards during the synthesis of these compounds and are included for future reference.

<u>$Ter^{Mes}H$</u>

^{1}H NMR (C_6D_6): δ 7.25 (t, $^3J_{HH}$ = 7.6 Hz, 1H, *p*-C_6H_4), 6.99 (dd, $^3J_{HH}$ = 7.6 Hz, $^4J_{HH}$ = 1.6 Hz 2H, *m*-C_6H_4), 6.87 (s, 4H, *m*-$C_6H_2(CH_3)_3$), 6.77 (t, $^4J_{HH}$ = 1.6 Hz, 1H, *i*-C_6H_4), 2.21 (s, 6H, *p*-CH_3), 2.07 ppm (s, 12H, *o*-CH_3).

^{1}H NMR (THF-d_8): δ 7.46 (t, $^3J_{HH}$ = 7.6 Hz, 1H, *p*-C_6H_4), 7.06 (dd, $^3J_{HH}$ = 7.6 Hz, $^4J_{HH}$ = 1.6 Hz 2H, *m*-C_6H_4), 6.88 (s, 4H, *m*-$C_6H_2(CH_3)_3$), 6.86 (t, $^4J_{HH}$ = 1.6 Hz, 1H, *i*-C_6H_4), 2.26 (s, 6H, *p*-CH_3), 2.01 ppm (s, 12H, *o*-CH_3).

<u>Ter^{Dipp}H</u>

^{1}H NMR (C_6D_6): δ 7.34 (m, $^3J_{HH}$ = 6.9 Hz, 3H, *p*-C_6H_4, *p*-C_6H_3(iPr)$_2$), 7.20 (d, $^3J_{HH}$ = 6.8 Hz, 4H, *m*-C_6H_3(iPr)$_2$), 7.10 (m, $^3J_{HH}$ = 7.5 Hz, 2H, *m*-C_6H_4), 7.04 (t, $^4J_{HH}$ = 1.5 Hz, 1H, *i*-C_6H_4), 2.90 (sept, $^3J_{HH}$ = 6.8 Hz, 4H, iPr-C*H*), 1.13 (d, $^3J_{HH}$ = 7.0 Hz, 12H, iPr-CH_3), 1.12 ppm (d, $^3J_{HH}$ = 6.9 Hz, 12H, iPr-CH_3).

2.2.7 Synthesis of NaCp

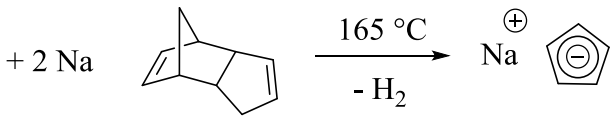

(large excess)

Following a similar procedure as reported in the literature[51], 5.16 g (224 mmol, 2 eq.) of gray coloured sodium metal were added in air to a 500 mL Schlenk flask containing a PTFE-coated magnetic stir bar and 200 mL (1500 mmol, 6.7 eq.) of pale yellow dicyclopentadiene. A Vigreux column was attached to the flask to serve as an air condenser and was equipped with a gas adaptor, and the reaction vessel was purged with a light flow of argon for 5 minutes. The reaction mixture was slowly heated to 165 °C for 6 hours, and the reaction mixture slowly became orange in colour and a copious amount of colourless

precipitate had formed. Once all of the sodium metal was consumed (as monitored by the evolution of hydrogen gas) the reaction mixture was cooled to *ca*. 50 °C before removing the orange coloured supernatant using a syringe. Alternatively it was found that similar assembly using a 2-necked flask with a cotton-plugged gas adaptor in the second neck to decant the supernatant directly into a beaker was also sufficient. The colourless precipitate was washed twice with 50 mL of pentane and transferred to the glovebox to collect *via* vacuum filtration, washing once more with 50 mL of pentane and drying *in vacuo* to afford the desired product as a colourless precipitate.

Yield: 16.5 g (87 %)

^{1}H NMR (THF-d_8): δ 5.66 ppm (s, 5H).

^{13}C{^{1}H} NMR (THF-d_8): δ 103.1 ppm.

2.2.8 Synthesis of Cp_2Co

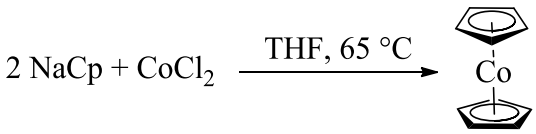

Similarly to a previously reported procedure[76], in a 500 mL Schlenk flask equipped with a PTFE-coated magnetic stir bar, 12.10 g (93.2 mmol, 1 eq.) of blue coloured $CoCl_2$ were suspended in 100 mL of THF producing a blue coloured mixture. Separately, 16.29 g (185 mmol, 1.98 eq.) of colourless NaCp were dissolved in 140 mL of THF producing a pale orange coloured solution. This solution was added directly to the suspension of $CoCl_2$, immediately producing an intensely violet coloured mixture. A condenser equipped with a gas adaptor was added to the flask, and the entire assembly was removed from the glovebox

and refluxed for two hours. The solvent was removed *in vacuo* and the violet coloured solid was purified by sublimation at 175 °C under dynamic vacuum yielding violet crystals.

Yield: 9.16 g (52 %)

2.2.9 Synthesis of [Cp_2Co][I]

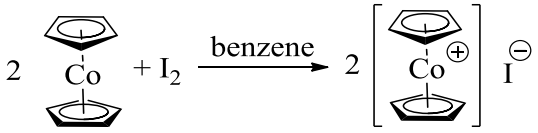

Similar to a previously reported procedure,[77] in a 250 mL round-bottom flask equipped with a PTFE-coated magnetic stir bar, 2.02 g (10.7 mmol, 1 eq.) of violet coloured cobaltocene were dissolved in 30 ml of benzene producing an intense violet coloured solution. Separately, 1.33 g (5.24 mmol, 0.49 eq.) of violet coloured iodine crystals were dissolved in 100 mL of benzene producing an intense reddish-violet coloured solution, and transferred to a 125 mL pressure-equalising dropping funnel. Dropwise-addition of the iodine solution to the cobaltocene solution immediately produced a bright yellow coloured precipitate. The reaction mixture was left to stir for two and a half hours before collecting the yellow coloured precipitate by vacuum filtration in air, and washing the product with 3 x 20 mL portions of pentane. The precipitate was dried *in vacuo* to afford the product as a bright yellow coloured powder.

Yield: 2.81 g (84%)

^{1}H NMR (CD_3CN): δ 5.73 ppm (s, 10H).

^{13}C{^{1}H} NMR (CD_3CN): δ 86.0 ppm.

2.2.10 Synthesis of $[Cp_2Co][PF_6]$

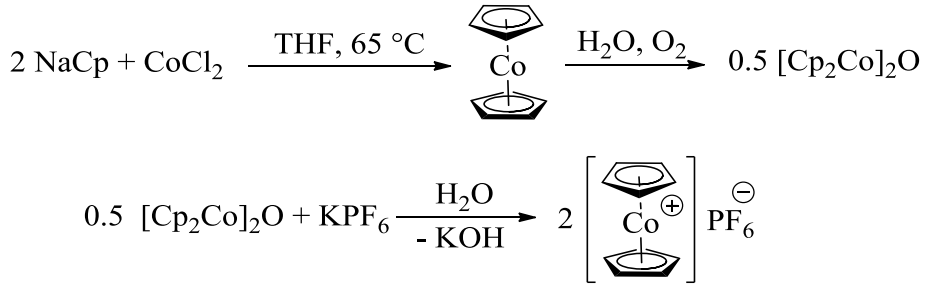

Following a similar procedure as previously reported,[76,78] Cp_2Co was synthesised using 17.66 g (0.20 mol, 2.0 eq.) of NaCp and 13.06 g (0.10 mol, 1.0 eq.) of $CoCl_2$. Instead of subliming the crude violet solids, 300 mL of boiling water were added and the dark brown reaction mixture was sparged with compressed air for 4 hours. The black coloured precipitate was separated by gravity filtration producing a greenish-yellow coloured solution, and the black coloured solids were extracted once with 100 mL of boiling water and filtered off again. The aqueous portions were combined, transferred to a 1 L separatory funnel, and washed twice with 100 mL of diethylether before reducing the volume to *ca*. 80 mL. To this yellow coloured solution, 250 mL of a 0.40 M solution of KPF_6 in water (0.10 mol, 1.0 eq.) were added, immediately producing an olive-green coloured precipitate. The greenish-yellow coloured reaction mixture was placed in an ice-water bath for 10 minutes before collecting the product by vacuum filtration using a medium porosity frit. The product was dried *in vacuo* overnight prior to use.

Yield: 6.35 g (19%)

^{1}H NMR (CD_3CN): δ 5.67 ppm (s, 10H).

$^{13}C\{^1H\}$ NMR (CD_3CN): δ 85.8 ppm.

2.2.11 Synthesis of Ter^{Mes}CpH(CoCp) – 8

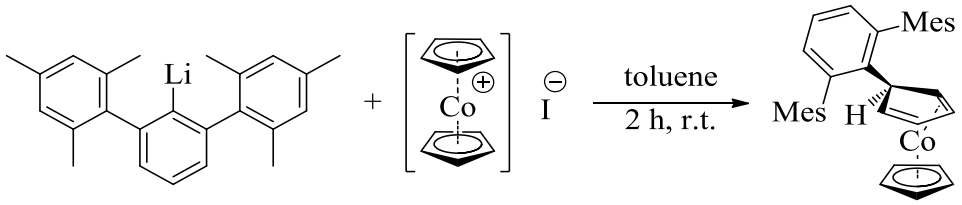

8

In a 20 mL scintillation vial, 0.502 g (1.57 mmol) of colourless Ter^{Mes}Li powder were dissolved in 10 mL of toluene to produce a pale yellow coloured mixture. This mixture was transferred to a 50 mL pressure-equalizing dropping funnel equipped with a PTFE stopcock and sealed with a rubber septum. In a separate 20 mL scintillation vial, 0.496 g (0.157 mmol, 1.00 eq) of bright yellow coloured [Cp_2Co][I] were measured and added to a 25 mL Schlenk flask equipped with a PTFE-coated magnetic stir bar. The [Cp_2Co][I] was suspended in 5 mL of toluene, producing a bright yellow coloured mixture. The Schlenk flask was fitted with the dropping funnel, and the entire apparatus was removed from the glovebox. The Schlenk flask was fitted with the dropping funnel, and the reaction vessel was removed from the glove box, connected to a Schlenk line, and the mixture of [Cp_2Co][I] was cooled to 0 °C using an ice-water bath. The pale yellow coloured Ter^{Mes}Li mixture was added dropwise to the bright yellow coloured [Cp_2Co][I] suspension to quickly produce a red-orange coloured mixture. Once the addition was complete, the dropping funnel was removed and the resultant mixture was transferred back to the glove box and left to stir overnight. The following day, an aliquot was removed for ^{1}H NMR analysis, which indicated that the reaction was complete and that approximately 20% of Ter^{Mes}H was produced as a by-product. The reddish-orange coloured mixture was filtered through silica gel to afford a cherry red coloured solution. Removal of the solvent *in vacuo*

yielded the crude product as a red coloured solid. Crystallization was achieved by dissolving the red colored solid in pentane and storing in a freezer at -30 °C overnight. The red coloured supernatant was decanted from the red coloured crystals, and the crystals were washed three times with *ca*. 1 mL portions of cold pentane.

The same procedure was suitable for $[Cp_2Co][PF_6]$ and was identical to $[Cp_2Co][I]$ in terms of ^{1}H NMR spectroscopy, and it was later found that cooling with an ice-water bath was not necessary however no isolated yields were recorded as **8** was generated and subsequently oxidised without isolation.

Yield: 0.53 g (66 %)

EA: Calc for $C_{34}H_{35}Co$: C: 81.25 %, H: 7.02 %, N: 0.00 %. Found: C: 81.48 %, H: 7.11 %, N: 0.08 %.

m.p. (°C): 138.8–140.1

UV (pentane): 327 (λ_{max}, ε = 1200 L mol^{-1} cm^{-1}), 390 nm (ε = 570 L mol^{-1} cm^{-1}).

1H NMR (C_6D_6): δ 7.03 (t, $^3J_{HH}$ = 7.5 Hz, 1H, *p*-C_6H_3), 6.92 (s, 4H, *m*-$C_6H_2(CH_3)_3$), 6.77 (d, $^3J_{HH}$ = 7.5 Hz, 2H, *m*-C_6H_3), 4.55 (m, $^4J_{HH}$ = 2.0 Hz, 2H, Cp-C*H*), 4.32 (s, 5H, C_5H_5), 4.18 (t, $^4J_{HH}$ = 2.6 Hz, 1H, Cp-C*H*), 2.50 (m, $^4J_{HH}$ = 2.5 Hz, $^4J_{HH}$ = 1.5 Hz, 2H, Cp-CH_2), 2.27 (s, 6H, *p*-CH_3) 2.10 ppm (s, 12H, *m*-CH_3).

$^{13}C\{^1H\}$ NMR (C_6D_6): δ 140.8, 140.0, 139.8, 136.2, 136.1, 129.8 (s, *m*-C_6H_3), 128.3 (*m*-$C_6H_2(CH_3)_3$), 126.7 (*p*-C_6H_3), 79.3 (C_5H_5), 75.3 (Cp-CH), 54.3 (Cp-CH), 44.5 (Cp-CH_2), 21.4 (*m*-CH_3), 21.3 ppm (*p*-CH_3).

Interestingly the cobalt(I) intermediate **8** is structurally different in solution (Figure 2.4), as indicated by the methylene resonance at 2.50 ppm in the ^{1}H NMR spectrum. Currently it is unknown which methylene isomer is present, HMBC data will be collected and should identify the nature of **8**.

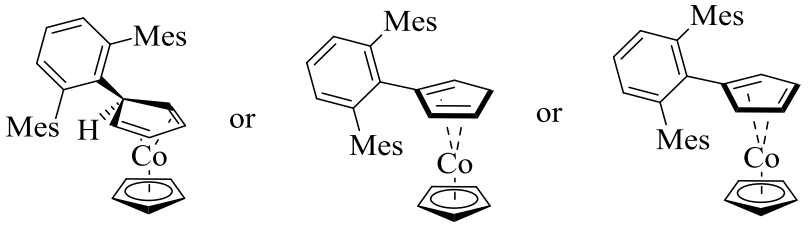

Figure 2.4. Possible isomers of the cobalt(I) intermediate **8**. The methine isomer has been confirmed in the solid state by X-ray crystallography, while in solution a methylene isomer is evident based on ^{1}H NMR spectroscopy.

2.2.12 Synthesis of Ter^{Mes}CpH – 9a+b

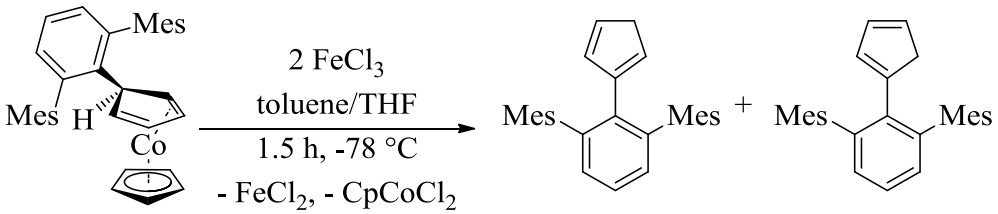

8 **9a** **9b**

Following a similar procedure for the synthesis of **8** (without isolation), 3.00 g (9.36 mmol) of colourless Ter^{Mes}Li powder were dissolved in 20 mL of toluene to produce a pale yellow coloured mixture. This mixture was transferred to a 125 mL pressure-equalising dropping funnel equipped with a PTFE stopcock, diluted with toluene to a total volume of 60 mL, and sealed with a rubber septum. Separately 3.14 g (9.40 mmol, 1.00 eq.) of yellow coloured [Cp_2Co][PF_6] were measured and transferred to a 250 mL Schlenk

flask equipped with a PTFE-coated magnetic stir bar. The $[Cp_2Co][PF_6]$ was suspended in 30 mL of toluene, producing a bright yellow colored mixture. The Schlenk flask was fitted with the dropping funnel, and the reaction vessel was removed from the glove box, connected to a Schlenk line, and cooled to 0 °C using an ice-water bath. The pale yellow coloured $Ter^{Mes}Li$ mixture was added dropwise to the bright yellow coloured $[Cp_2Co][PF_6]$ suspension to quickly produce a red-orange coloured mixture. Once the addition was complete, the dropping funnel was removed and the resultant mixture was transferred back to the glove box and left to stir overnight. The following day, an aliquot was removed for ^{1}H NMR spectroscopic analysis, which indicated that the reaction was complete and that *ca*.17% of $Ter^{Mes}H$ was produced as a by-product. The bright red coloured mixture was filtered through silica gel into a 500 mL Schlenk flask equipped with a PTFE-coated magnetic stir bar, and the flask was fitted with a 125 mL pressure-equalising dropping funnel. In a 20 mL scintillation vial, 2.54 g (15.4 mmol, 2.00 eq. scaled based on the yield determined by ^{1}H NMR spectroscopy) of dark green coloured $FeCl_3$ were measured out, and carefully dissolved in 20 mL of THF to produce a green colored solution. The green coloured solution of $FeCl_3$ was transferred to the 125 mL dropping funnel before sealing the reaction vessel with a rubber septum. The entire reaction vessel was removed from the glove box and connected to a Schlenk line before cooling the red colored solution of **8** to *ca*. -60 °C using a liquid nitrogen-isopropanol bath. Once cold, the green coloured solution of $FeCl_3$ was added dropwise over 30 minutes to immediately produce a bluish-green coloured mixture. The mixture was left to stir at between -60 and -70 °C for one hour and the temperature of the cold bath was monitored using a thermocouple. While cold, the blue-green coloured mixture was transferred to a column containing *ca*. 250 mL of silica gel

and toluene and eluted through the column using toluene in air. The initial bright yellow coloured fraction was collected into a 600-mL beaker (*ca*. 275 mL of toluene was used to isolate the product) while the slower eluting blue and red coloured fractions were discarded. The solvent was removed by evaporation to yield a yellow coloured solid that was found to contain a mixture of two isomers of the product, as well as $Ter^{Mes}H$ that could not be completely separated by crystallisation. In some instances, it was observed that one isomer was formed exclusively but would quickly equilibrate with the other isomer in solution within one week when monitored by ^{1}H NMR spectroscopy.

Yield: 2.90 g as a mixture of **9a**+**b** (83 %) and $Ter^{Mes}H$ (17 %) by ^{1}H NMR spectroscopy

EA: Calc for $C_{29}H_{30}$: C: 92.01 %, H: 7.99 %, N: 0.00 %. Found: C: 91.05 %, H: 7.78 %, N: 0.02 %.

m.p. (°C): 150.7–151.5.

UV (pentane): 270 nm (λ_{max}, ε = 4340 L mol^{-1} cm^{-1}).

^{1}H NMR (C_6D_6): δ 7.19 (dd, $^{3}J_{HH}$ = 8.2 Hz, $^{3}J_{HH}$ = 6.77 Hz, 1H, *p*-C_6H_3), 7.15 (dd, $^{3}J_{HH}$ = 8.3 Hz, $^{3}J_{HH}$ = 6.6 Hz, 1H, *p*-C_6H_3), 7.08-7.02 (m, $^{3}J_{HH}$ = 8.3 Hz, $^{3}J_{HH}$ = 7.9 Hz, 4H, *m*-C_6H_3 **a+b**), 6.79 (s, 4H, *m*-$C_6H_2(CH_3)_3$ **a+b**), 6.22 (dq, $^{3}J_{HH}$ = 5.1 Hz, $^{4}J_{HH}$ = 1.6 Hz, 1H, Cp-C*H*), 6.05-6.02 (m, 2H, Cp-C*H*), 5.90 (dq, $^{3}J_{HH}$ = 5.20 Hz, $^{4}J_{HH}$ = 1.53 Hz, 1H, Cp-C*H*), 5.84-5.78 (m, 2H, Cp-C*H*), 2.72 (q, $^{4}J_{HH}$ = 1.5 Hz, 2H, Cp-CH_2), 2.40 (q, $^{4}J_{HH}$ = 1.5 Hz, 2H, Cp-CH_2), 2.14-2.13 ppm (s (possibly overlapping), 24H, *o*-$C_6H_2(CH_3)_3$) 2.09 ppm (s, 6H, *p*-$C_6H_2(CH_3)_3$).

^{13}C {^{1}H} NMR (C_6D_6): δ 144.8, 144.2, 141.0, 140.8, 136.7, 136.3, 136.2, 136.0, 135.8, 132.9, 132.4, 132.3, 131.4, 131.0, 129.6, 129.4, 128.5, 128.2, 127.9, 127.6, 127.3, 43.6, 41.5, 21.1 (br, two overlapping signals), 21.0, 20.9 ppm.

2.2.13 Synthesis of Li(Ter^{Mes}Cp) – 10

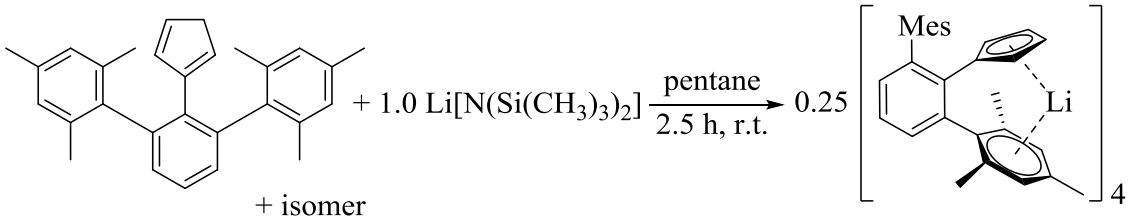

In a 20 mL scintillation vial equipped with a PTFE-coated magnetic stir bar, 0.500 g of a 5:1 mixture of **9a**+**b**:TerMesH (1.1 mmol) were dissolved in 10 mL of pentane to produce a pale yellow coloured mixture. Separately in another 20 mL scintillation vial, 0.182 g (1.1 mmol, 1.0 eq.) of lithium bis(trimethylsilyl)amide were dissolved in 5 mL of pentane to produce a colourless solution. Dropwise addition of the colourless lithium bis(trimethylsilyl)amide solution to the pale yellow mixture immediately produced an orange coloured mixture. This mixture was left to stir for 2.5 h before removal of the stir bar. The contents of the vial were left to settle before decanting off the orange coloured supernatant and washing the orange coloured precipitate three times with *ca*. 2 mL portions of pentane, yielding a yellow coloured powder. Crystals suitable for X-ray diffraction were isolated from evaporation of an NMR scale reaction completed in C_6D_6.

Yield: 0.17 g (40 %)

EA: Calc for $C_{29}H_{29}Li$: C: 90.59 %, H: 7.60 %, N: 0.00 %. Found: C: 88.02 %, H: 7.36 %, N: 0.14 %.

m.p. (°C): 292.4–294.8.

UV (THF): 313 nm (λ_{max}, ε = 4020 L mol^{-1} cm^{-1}).

^{1}H NMR (THF-d_8): δ 7.04 (m, $^{3}J_{HH}$ = 7.5 Hz, 1H, *p*-C_6H_3), 6.83 (d, $^{3}J_{HH}$ = 7.5 Hz, 2H, *m*-C_6H_3), 6.75 (s, 4H, *m*-$C_6H_2(CH_3)_3$), 5.26 (pseudo-t, $^{5}J_{HH}$ = 2.9 Hz, $^{5}J_{HH}$ = 2.5 Hz, 2H, Cp-C*H*), 5.21 (pseudo-t, $^{5}J_{HH}$ = 2.9 Hz, $^{5}J_{HH}$ = 2.5 Hz, 2H, Cp-C*H*), 2.23 (s, 6H, *p*-$C_6H_2(CH_3)_3$) 1.97 ppm (s, 12H, *o*-$C_6H_2(CH_3)_3$).

^{13}C{^{1}H} NMR (THF-d_8): δ 143.2, 140.6, 140.0, 136.3, 135.0, 129.7 (*m*-C_6H_3, $C^{(2)}$), 128.2 (*m*-$C_6H_2(CH_3)_3$, $C^{(11)}$), 123.6 (*p*-C_6H_3, $C^{(1)}$), 117.2, 106.9 (s, Cp-*C*H), 103.0 (s, Cp-*C*H), 21.0 (s, *p*-CH_3, $C^{(13)}$), 20.9 (s, *o*-CH_3, $C^{(10)}$) ppm.

While it may appear that resonances are missing in the ^{13}C{^{1}H} NMR spectrum of **10**, it is likely that coordinated THF molecules break up the tetrameric structure and produce a THF-saturated monomeric structure (Figure 2.5). This results in a total of 13 unique carbon environments, consistent with what is observed experimentally.

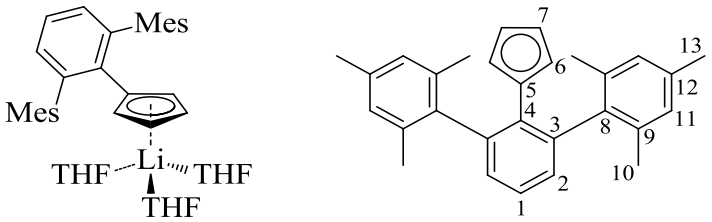

Figure 2.5. Proposed structure of **10** and unique carbon environments when dissolved in THF based on NMR spectroscopic data obtained in THF-d_8. Dashed bond indicates the THF may or may not be coordinated to the lithium ion.

2.2.14 Synthesis of Na(Ter^{Mes}Cp) – 11

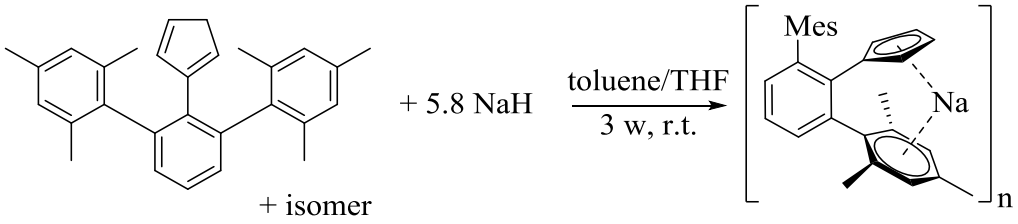

A 200 mL solution of a 5:1 mixture of **9a**+**b** isomers (*ca*. 6.4 mmol) and Ter^{Mes}H was prepared following the procedure described starting from 2.5 g (7.8 mmol) of Ter^{Mes}Li, and filtered through a silica gel column directly into 0.472 g (19.6 mmol, 3.0 eq.) of NaH suspended in 20 mL of toluene in a 500 mL Schlenk flask. This mixture was left to stir for one week, periodically monitoring the reaction progress by ^{1}H NMR spectroscopy. Only approximately 50% conversion based on starting material had been achieved after one week, so a further 0.429 g (17.9 mmol, 2.8 eq.) of NaH were added, and the dark brown coloured reaction mixture was left to stir for another two weeks. After a total reaction time of three weeks, the reaction was complete and the excess NaH was removed by vacuum filtration through Celite®. The solvent was then removed *in vacuo*, and the dark brown coloured residue was suspended in 50 mL of pentane. The solids were isolated *via* vacuum filtration, and the brown coloured solid was washed with pentane and dried *in vacuo* to afford the desired product as a grey coloured powder. Recrystallisation of a concentrated THF solution yielded crystals suitable for X-ray diffraction, however these were found to not correspond to the intended product. Alternatively, **11** could be synthesised in an analogous manner as **10** using 0.118 g (0.26 mmol, 1 eq.) of 83% purity of **9a**+**b**, and 0.045 g (0.245 mmol, 0.94 eq) of sodium bis(trimethylsilyl)amide.

Yield: 1.37 g (52 %) from NaH, 0.08 g (78%) from $NaN(SiMe_3)_2$

EA: Calc for $C_{29}H_{29}Na$: C: 86.96 %, H: 7.30 %, N: 0.00 %. Found: C: 87.46 %, H: 7.26 %, N: 0.05 %.

m.p. (°C): 367.0–369.0 (decomposes).

UV (THF): 322 nm (λ_{max}, ε = 4550 L mol^{-1} cm^{-1}).

^{1}H NMR (THF-d_8): δ 7.08 (t, $^3J_{HH}$ = 7.4 Hz, 1H, *p*-C_6H_3), 6.85 (d, $^3J_{HH}$ = 7.4 Hz, 2H, *m*-C_6H_3), 6.71 (s, 4H, *m*-$C_6H_2(CH_3)_3$), 5.27 (s, 4H, Cp-C*H*), 2.19 (s, 6H, *p*-$C_6H_2(CH_3)_3$), 2.02 ppm (s, 12H, *o*-$C_6H_2(CH_3)_3$).

^{13}C{^{1}H} NMR (THF-d_8): δ 143.9, 143.2, 141.1, 136.4, 135.0, 128.6 (*m*-C_6H_3, $C^{(2)}$), 127.9 (*m*-$C_6H_2(CH_3)_3$, $C^{(11)}$), 123.8 (*p*-C_6H_3, $C^{(1)}$), 118.0, 105.4 (Cp-*C*H), 103.0 (Cp-*C*H), 21.0 ppm (*m*-CH_3, $C^{(10)}$ and *p*-CH_3, $C^{(13)}$).

The solution-state structure of the sodium cyclopentadienide **11** is likely similar to the lithium salt **10**. Coordinated THF molecules produce a THF-saturated monomeric structure (Figure 2.6), resulting in a total of 13 unique carbon environments, consistent with what is observed experimentally.

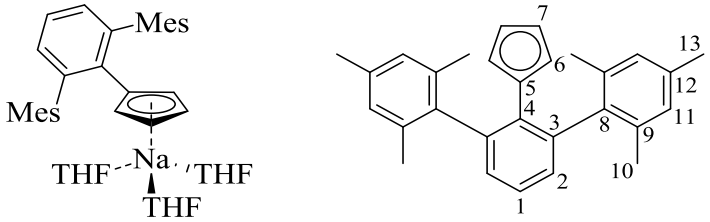

Figure 2.6. Proposed structure of **11** and unique carbon environments when dissolved in THF based on NMR spectroscopic data obtained in THF-d_8. Dashed bond indicates the THF may or may not be coordinated to the sodium ion.

2.2.15 Synthesis of K(Ter^{Mes}Cp) – 12

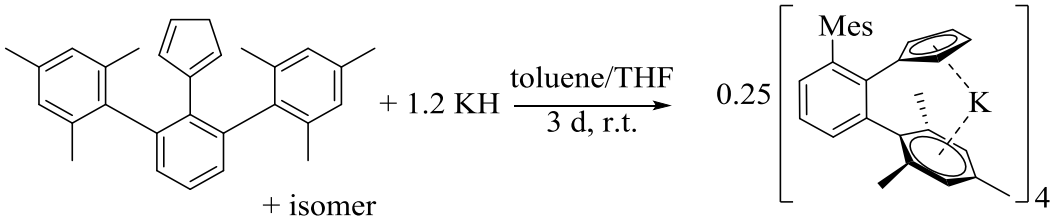

A 400 mL solution of a 5:1 mixture of **9a**+**b** isomers (*ca*. 13.3 mmol) and Ter^{Mes}H was prepared following the procedure described starting from 5.0 g (15.6 mmol) of Ter^{Mes}Li, and filtered through a silica gel column directly into 1.64 g (41.0 mmol, 3.1 eq) of KH suspended in 20 mL of toluene in a 1 L Schlenk flask. This was left to stir for 3 days, periodically monitoring the reaction progress by ^{1}H NMR spectroscopy. Once the reaction was complete, excess KH was removed by vacuum filtration through Celite®. The solvent was removed *in vacuo*, and the dark brown colored residue was suspended in 50 mL of pentane. The solids were isolated *via* vacuum filtration, and the brown colored solid was washed with pentane and dried *in vacuo* to afford the desired product as a gray colored powder. Crystals suitable for X-ray diffraction were obtained from pentane vapour diffusion into a concentrated toluene solution. It was later determined that the reaction could be completed with only 1.2 equivalents of KH instead.

Yield: 1.71 g (31 %)

EA: Calc for $C_{29}H_{29}K$: C: 83.60 %, H: 7.02 %, N: 0.00 %. Found: C: 83.36 %, H: 7.17 %, N: 0.03 %.

m.p. (°C): >400.

UV (THF): 325 nm (λ_{max}, ε = 5440 L mol^{-1} cm^{-1}).

^{1}H NMR (C_6D_6): δ 7.25 (t, $^{3}J_{HH}$ = 7.5 Hz, 1H, *p*-C_6H_3), 7.04 (s, 2H, *m*-$C_6H_2(CH_3)_3$), 6.92 (d, $^{3}J_{HH}$ = 7.5 Hz, 2H, *m*-C_6H_3), 6.55 (s, 2H, *m*-$C_6H_2(CH_3)_3$), 5.70 (s, br, 3H, Cp-C*H*), 5.63 (s, br, 1H, Cp-C*H*), 2.36 (s, 6H, *o*-CH_3), 2.27 (s, 6H, *o*-CH_3), 2.11 ppm (s, 6H, *p*-CH_3).

^{13}C{^{1}H} NMR (C_6D_6): δ 144.0, 143.1, 142.9, 136.6 (two partially overlapping signals), 134.7, 128.9 (s, *m*-$C_6H_3(CH_3)_3$, $C^{(13)}$ or $C^{(16)}$)), 127.9 (*m*-C_6H_3, $C^{(2)}$), 127.2 (*m*-$C_6H_3(CH_3)_3$, $C^{(13)}$ or $C^{(16)}$), 126.2 (*p*-C_6H_3, $C^{(1)}$), 120.7, 104.1 (Cp-*C*H), 103.8 (Cp-*C*H), 102.8 (Cp-*C*H), 102.7 (Cp-*C*H), 21.5 (br, *o*-*C*H_3, $C^{(12)}$ or $C^{(18)}$), 21.2 (br, *o*-*C*H_3, $C^{(12)}$ or $C^{(18)}$), 21.0 ppm (*p*-*C*H_3, $C^{(15)}$).

In the absence of a strong donor solvent, aryl interactions in the tetrameric structure of the potassium salt **12** remain intact, resulting in different ^{1}H and ^{13}C{^{1}H} NMR spectra. As confirmed by X-ray crystallography, the tetrameric structure of **12** consists of a large macrocyclic ring with chemically different inner and outer components. Therefore assignments are based according to Figure 2.7. The number of resonances in the ^{13}C{^{1}H} NMR spectrum match this proposal.

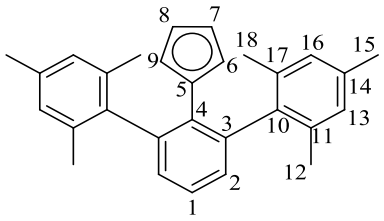

Figure 2.7. Unique carbon environments for **12** when dissolved in C_6D_6.

^{1}H NMR (THF-d_8): δ 7.07 (t, $^{3}J_{HH}$ = 7.5 Hz, 1H, *p*-C_6H_3), 6.80 (s, 4H, *m*-$C_6H_2(CH_3)_3$), 6.74 (d, $^{3}J_{HH}$ = 7.5 Hz, 2H, *m*-C_6H_3), 5.40 (s, 4H, Cp-C*H*), 2.20 (s, 6H, *p*-$C_6H_2(CH_3)_3$), 2.09 ppm (s, 12H, *o*-$C_6H_2(CH_3)_3$).

$^{13}C\{^{1}H\}$ NMR (THF-d_8): δ 144.3, 143.3, 139.7, 136.7, 135.9, 135.0, 129.1, 128.1 (*p*-C_6H_3, $C^{(1)}$ or *m*-$C_6H_3(CH_3)_3$, $C^{(11)}$), 128.0 (*m*-C_6H_3), 104.2 (Cp-*C*H), 103.4 (br, Cp-*C*H), 20.9 (*p*-*C*H_3, $C^{(13)}$), 20.8 ppm (*m*-*C*H_3, $C^{(10)}$).

The solution-state structure of the potassium cyclopentadienide **12** is likely similar to the other alkali metal salts when dissolved in THF. Coordinated THF molecules produce a THF-saturated monomeric structure (Figure 2.8), resulting in a total of 13 unique carbon environments, consistent with what is observed experimentally.

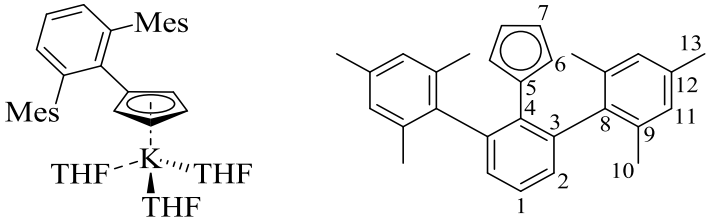

Figure 2.8. Proposed structure of **12** and unique carbon environments when dissolved in THF based on NMR spectroscopic data obtained in THF-d_8. Dashed bond indicates the THF may or may not be coordinated to the potassium ion.

2.2.16 Synthesis of Rb(Ter^{Mes}Cp) – 13

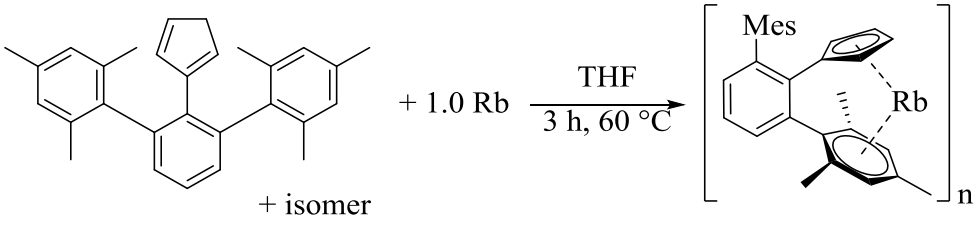

Using a heat gun, rubidium metal was melted and 0.25 g (2.93 mmol) of bluish-grey coloured rubidium metal were measured by difference and carefully added to a 100 mL sealed reaction vessel equipped with a PTFE-coated stir bar using a pipette. In a separate 20 mL scintillation vial, 1.356 g of a 5:1 mixture of **9a**+**b** isomers (*ca*. 2.97 mmol, 1.0 eq.) and Ter^{Mes}H were dissolved in 15 mL of THF to produce a yellow coloured solution and

added to the sealed reaction vessel. The reaction vessel was sealed with a PTFE stopcock and removed from the glove box and heated to 60 °C for 3 hours using an oil bath. After 30 minutes, a colourless precipitate began to form and the reaction mixture became pink in colour. After all of the rubidium was consumed, the reaction mixture was left to cool to room temperature before being transferred back into the glove box. The pink coloured reaction mixture was filtered through a coarse ground glass frit and the pink coloured precipitate was washed three times with 5 mL of pentane, to produce a pale pink, nearly colourless powder. This was dried *in vacuo* overnight and stored in the freezer as a precaution against potential decomposition.

Yield: 0.91 g (67 %)

EA: Calc for $C_{29}H_{29}Rb$: C: 75.23 %, H: 6.31 %, N: 0.00 %. Found: C: 74.41 %, H: 6.25 %, N: 0.02 %.

m.p. (°C): >400.

UV (THF): 326 nm (λ_{max}, ε = 4590 L mol^{-1} cm^{-1}), 357 nm (ε = 1410 L mol^{-1} cm^{-1}).

^{1}H NMR (THF-d_8): δ 6.75 (s, br, 5H, *p*-C_6H_3 and *m*-$C_6H_2(CH_3)_3$), 6.73 (d, $^{3}J_{HH}$ = 7.5 Hz, 2H, *m*-C_6H_3), 5.31 (s, 4H, Cp-C*H*), 2.19 (s, 6H, *p*-$C_6H_2(CH_3)_3$), 2.05 ppm (s, 12H, *o*-$C_6H_2(CH_3)_3$).

^{13}C{^{1}H} NMR (THF-d_8): δ 138.2, 137.0, 136.8, 128.7, 125.8, 21.3, 21.1 ppm.

Signals are missing from the ^{13}C{^{1}H} NMR spectrum due to the poor solubility of the rubidium complex **13**. Insufficient data was obtained after collecting over 24 hours, and so only a partial list of resonances are given for future reference.

2.2.17 Synthesis of Cs(Ter^{Mes}Cp) – 14

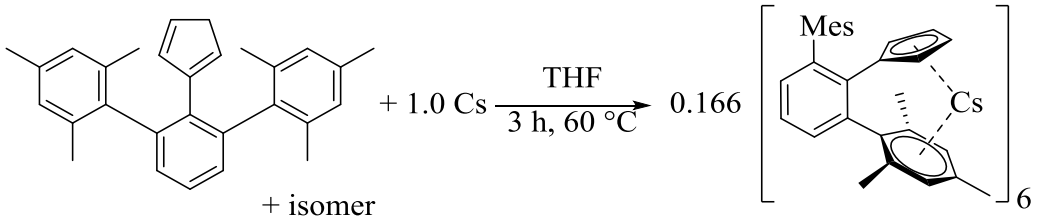

Using a heat gun, caesium metal was melted and 0.22 g (1.65 mmol) of yellow coloured caesium metal were measured by difference and carefully added to a 100 mL sealed reaction vessel equipped with a PTFE-coated stir bar using a pipette. In a separate 20 mL scintillation vial, 0.750 g of a 5:1 mixture of **9a**+**b** isomers (*ca*. 1.64 mmol, 1.0 eq.) and Ter^{Mes}H were dissolved in 15 mL of THF to produce a yellow coloured solution and added to the sealed reaction vessel. The reaction vessel was sealed with a PTFE stopcock and removed from the glove box and heated to 60 °C for 3 hours using an oil bath. After 30 minutes, a colourless precipitate began to form and the reaction mixture became reddish-pink in colour. After all of the caesium was consumed, the reaction mixture was left to cool back to room temperature before being transferred back into the glove box. The reddish-pink coloured reaction mixture was filtered through a coarse ground glass frit and the pink coloured precipitate was washed three times with 5 mL of pentane, to produce a pale pink, nearly colourless powder. This was dried *in vacuo* overnight and stored in the freezer as a precaution against potential decomposition. A small portion (*ca*. 20 mg) was recrystallised from 15 mL of a hot THF solution to yield crystals suitable for X-ray diffraction analysis.

Yield: 0.72 g (86 %)

EA: Calc for $C_{29}H_{29}Cs$: C: 68.24 %, H: 5.31 %, N: 0.00 %. Found: C: 65.76 %, H: 5.64 %, N: 0.04 %.

m.p. (°C): 388.0–391.0.

UV (THF): 323 nm (λ_{max}, ε = 5920 L mol^{-1} cm^{-1}), 355 nm (ε = 2510 L mol^{-1} cm^{-1}).

^{1}H NMR (THF-d_8): δ 6.97 (t, $^{3}J_{HH}$ = 7.6 Hz, 1H, *p*-C_6H_3), 6.76 (d, $^{3}J_{HH}$ = 7.5 Hz, 2H, *m*-C_6H_3), 6.71 (s, 4H, *m*-$C_6H_2(CH_3)_3$), 5.16 (s, 4H, Cp-C*H*), 2.19 (s, 6H, *p*-$C_6H_2(CH_3)_3$), 1.99 ppm (s, 12H, *o*-$C_6H_2(CH_3)_3$).

^{13}C{^{1}H} NMR (THF-d_8): δ 144.2, 144.0, 140.3, 137.1, 134.7, 129.5, 129.0, 128.7, 128.0, 125.8, 122.8, 109.7 (Cp-*C*H), 106.9 (Cp-*C*H), 21.2 (*p*-CH_3), 21.0 ppm (s, *o*-CH_3).

Signals are missing from the ^{13}C{^{1}H} NMR spectrum due to the poor solubility of the caesium complex **14**. Insufficient data was obtained after collecting over 24 hours, and so only a partial list of resonances are given. Based on X-ray diffraction data it is expected that 18 resonances would be visible in the ^{13}C{^{1}H} NMR spectrum, similar to **12**.

2.2.18 Synthesis of (Ter^{Mes}Cp)$_2$Fe – 15

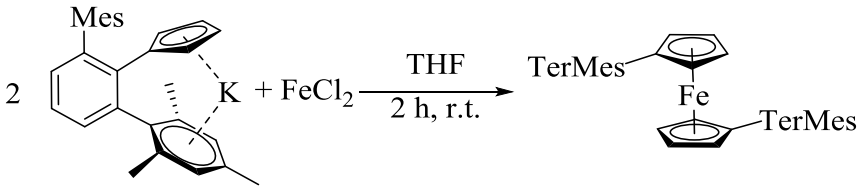

In a 20 mL scintillation vial equipped with a PTFE-coated magnetic stirring bar, 0.034 g (0.26 mmol, 1 eq.) of beige coloured anhydrous $FeCl_2$ were dissolved in 3 mL of THF. Separately, 0.206 g (0.496 mmol, 1.90 eq.) of gray coloured K(TerMesCp) powder were dissolved in 3 mL of THF producing an orange coloured solution. The orange

coloured solution of K(TerMesCp) was slowly added dropwise to the $FeCl_2$ suspension and immediately produced an intense orange coloured mixture. As more K(TerMesCp) was added, the reaction mixture gradually became an intense red colour. After the addition was complete, the reaction mixture was left to stir for 2 hours before removing the solvent *in vacuo* to produce a red coloured residue. This residue was dissolved in 10 mL of pentane, and filtered through Celite® to yield a red coloured solution, which when concentrated *in vacuo* yielded a red coloured semi-solid. The product was crystallised from a minimal amount of pentane by storing the concentrated solution at -35 °C overnight. The percent recovery was low, but the crystals that were obtained were washed carefully using 1 mL of cold pentane and dried *in vacuo*. Material suitable for elemental analysis and X-ray diffraction was obtained in this manner.

Yield: 0.20 g (88 %) – 56 mg (28 %) recovered from recrystallisation.

EA: Calc for $C_{58}H_{58}Fe$: C: 85.90 %, H: 7.21 %, N: 0.00 %. Found: C: 85.55 %, H: 7.05 %, N: 0.02 %.

m.p. (°C): 252.2–253.0.

UV (THF): 311 nm (λ_{max}, ε = 30600 L mol^{-1} cm^{-1}), 458 nm (ε = 60 L mol^{-1} cm^{-1}).

^{1}H NMR (C_6D_6): δ 7.02 (t, $^3J_{HH}$ = 7.5 Hz, 2H, *p*-C_6H_3), 6.88 (s, 8H, *m*-$C_6H_2(CH_3)_3$), 6.81 (d, $^3J_{HH}$ = 7.5 Hz, 4H, *m*-C_6H_3), 3.90 (pseudo-t, 4H, $^5J_{HH}$ = 2.1 Hz, Cp-C*H*), 3.78 (pseudo-t, 4H, $^5J_{HH}$ = 2.1 Hz, Cp-C*H*), 2.19 (s, 12H, *p*-$C_6H_2(CH_3)_3$), 1.99 ppm (s, 24H, *o*-$C_6H_2(CH_3)_3$).

$^{13}C\{^{1}H\}$ NMR (C_6D_6): δ 142.2, 140.9, 136.4, 135.9, 135.7, 131.3 (*m*-C_6H_3), 129.0 (*m*-$C_6H_3(CH_3)_3$), 126.0 (*p*-C_6H_3), 84.5 (Cp-*C*H), 71.0 (Cp-*C*H), 69.6 (Cp-*C*H), 21.2 ppm (*p*-CH_3 and *o*-CH_3).

Resonances in the ^{1}H NMR suggest symmetry, likely C_s configuration. Therefore the number of resonances in the $^{13}C\{^{1}H\}$ NMR spectrum should be 13 (Figure 2.9).

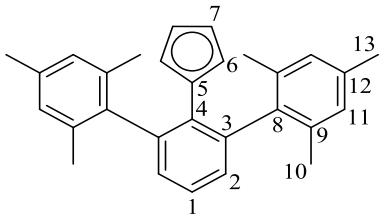

Figure 2.9. Unique carbon environments proposed for **15**.

IR (KBr pellet): ν 3146 (w), 3097 (w), 2946 (s), 2916 (vs), 2855 (m), 2730 (w), 1724 (w), 1610 (m), 1569 (w), 1483 (s), 1453 (vs), 1403 (s), 1377 (w), 1312 (w), 1249 (w), 1159 (w), 1085 (m), 1032 (m), 1013 (m), 879 (m), 849 (vs), 820 (s), 810 (s), 780 (w), 763 (vs), 748 (m), 710 (w), 650 (w), 601 (w), 586 (w), 578 (w), 556 (w), 532 (w), 501 (m), 486 (m), 470 (m), 427 cm^{-1} (w).

2.2.19 Synthesis of (TerMesCp)$_2$Co – 16

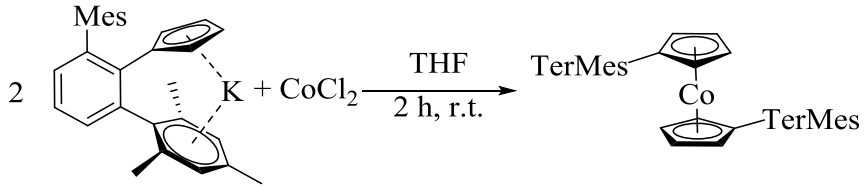

In a 20 mL scintillation vial equipped with a PTFE-coated magnetic stirring bar, 0.040 g (0.31 mmol, 1 eq.) of blue coloured anhydrous $CoCl_2$ were dissolved in 3 mL of THF. Separately, 0.254 g (0.613 mmol, 2.00 eq.) of gray coloured K(TerMesCp) powder were dissolved in 10 mL of THF producing an orange coloured solution. The orange

coloured solution of K(TerMesCp) was slowly added dropwise to the blue solution of $CoCl_2$ to produce a more intense blueish-violet coloured mixture. This was left to stir for 2 hours before removing the solvent *in vacuo* to produce a dark blue coloured oily residue. This residue was dissolved in 10 mL of pentane, and filtered through Celite® to yield a dark blue coloured solution, which when concentrated *in vacuo* yielded a dark blue coloured semi-solid.

Yield: 0.22 g (88 %) – 28 mg (11 %) recovered from recrystallisation.

m.p. (°C): 250.4–251.6.

UV (THF): 310 nm (λ_{max}, ε = 6430 L mol^{-1} cm^{-1}), 581 nm (ε = 2560 L mol^{-1} cm^{-1}).

^{1}H NMR (C_6D_6): δ 8.98 (s, br, 9.70–8.10 ppm, 6H), 7.14 (s, br, 8.10–5.70 ppm, 16H), 2.10 ppm (s, br, 3.80–0.00 ppm, 36H).

The product **16** is paramagnetic, resulting in the relative integrations in the ^{1}H NMR spectrum to be inaccurate.

IR (KBr pellet): ν 3141 (w), 2946 (s), 2915 (vs), 2855 (m), 2730 (w), 1723 (w), 1611 (m), 1578 (m), 1483 (m), 1454 (vs), 1400 (vs), 1375 (s), 1306 (w), 1261 (w), 1242 (w), 1231 (w), 1210 (w), 1171 (w), 1085 (m), 1061 (m), 1032 (m), 1011 (m), 883 (w), 867 (w), 849 (vs), 804 (m), 788 (s), 759 (vs), 748 (m), 714 (w), 678 (w), 630 (w), 599 (w), 586 (m), 554 (w), 503 (w), 461 cm^{-1} (w).

2.2.20 Synthesis of $(Ter^{Mes}Cp)_2Ni$ – 17

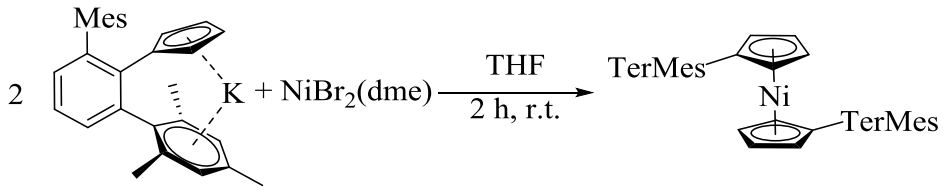

In a 20 mL scintillation vial equipped with a PTFE-coated magnetic stirring bar, 0.076 g (0.25 mmol, 1 eq.) of bright orange coloured $NiBr_2$(dme) were dissolved in 3 mL of THF producing a blue-violet coloured solution. Separately, 0.205 g (0.496 mmol, 1.98 eq.) of gray coloured K(TerMesCp) powder were dissolved in 3 mL of THF producing an orange coloured solution. The orange coloured solution of K(TerMesCp) was slowly added dropwise to the $NiBr_2$(dme) solution and immediately produced an intense brownish-orange coloured mixture. After the addition was complete, the reaction mixture was left to stir for 2 hours before removing the solvent *in vacuo* to produce a green coloured residue. This residue was dissolved in 10 mL of pentane, and filtered through Celite® to yield a brownish-yellow coloured solution, which when concentrated *in vacuo* yielded a green coloured semi-solid. The product was crystallised from a minimal amount of pentane by storing the concentrated solution at -35 °C overnight. The percent recovery was low, but the crystals that were obtained were washed carefully using 1 mL of cold pentane and dried *in vacuo*. Material suitable for X-ray diffraction was obtained in this manner.

Yield: 0.18 g (92 %) – 15 mg (8 %) recovered from recrystallisation.

m.p. (°C): 265.3–266.8.

UV (THF): 385 nm (λ_{max}, ε = 15700 L mol^{-1} cm^{-1}).

^{1}H NMR (C_6D_6): δ 8.70 (s, br, 9.10–8.30 ppm, 3H), 7.15 (s, br, 7.40–7.00 ppm, 5H), 6.78 (s, br, 7.00–6.50 ppm, 5H), 4.02 (s, br, 4.75–3.45 ppm, 11H) 2.39 ppm (s, br, 2.50–1.50 ppm, 18H).

The product **17** is paramagnetic, resulting in the relative integrations in the ^{1}H NMR spectrum to be inaccurate.

IR (KBr pellet): ν 3140 (w), 3114 w, 3103 (w), 2998 (m), 2968 (s), 2943 (s), 2914 (vs), 2854 (m), 2728 (w), 1930 (w), 1875 (w), 1729 (w), 1611 (m), 1570 (m), 1483 (m), 1454 (vs), 1410 (s), 1376 (vs), 1310 (w), 1260 (w), 1232 (w), 1212 (w), 1181 (w), 1159 (w), 1085 (m), 1065 (m), 1054 (m), 1030 (vs), 1009 (s), 890 (m), 848 (vs), 808 (s), 768 (vs), 758 (s), 743 (vs), 712 (m), 657 (w), 587 (m), 577 (m), 553 (w), 501 (w), 466 (w), 404 cm^{-1} (w).

2.2.21 Synthesis of $(Ter^{Mes}Cp)_nZrCl_{4-n}$ – 18a or 18b

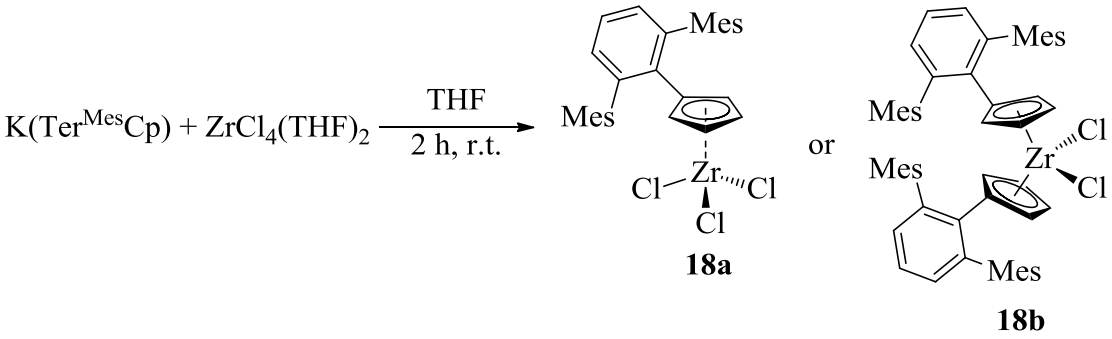

In a 20 mL scintillation vial equipped with a PTFE-coated magnetic stirring bar, 0.186 g (0.610 mmol, 1 eq.) of colourless $ZrCl_4(THF)_2$ were dissolved in 8 mL of THF producing a colourless solution. Separately, 0.255 g (0.612 mmol, 1.00 eq.) of gray coloured K(TerMesCp) powder were dissolved in 10 mL of THF producing an orange coloured solution. The orange coloured solution of K(TerMesCp) was slowly added

dropwise to the $ZrCl_4(THF)_2$ solution and immediately produced a pale orange coloured mixture. After the addition was complete, the reaction mixture was left to stir for 2 hours before removing the solvent *in vacuo* to produce a dark gray coloured residue. This residue was dissolved in 10 mL of toluene, and filtered through Celite® to yield an orange coloured solution, which when concentrated *in vacuo* yielded a dark gray coloured powder. The target molecule was the monosubstitution product $Ter^{Mes}CpZrCl_3$ (**18a**), however spectroscopic methods were unable to determine if the disubstituted product $Ter^{Mes}Cp_2ZrCl_2$ (**18b**) or a mixture thereof was isolated instead.

Yield: 0.176 g (51 % based on **18a**,64% based on **18b**).

EA: Calc for $C_{29}H_{29}ZrCl_3$: C: 60.56 %, H: 5.08 %, N: 0.00 %. Calc for $C_{58}H_{58}ZrCl_2$: C: 75.95 %, H: 6.37 %, N: 0.00 %. Found: C: 74.55 %, H: 5.87 %, N: 0.03 %.

m.p. (°C): 300 (irreversibly turns beige, remains like this >400).

UV (THF): 269 nm (λ_{max}, ε = 12900 (**18a**) or 20600 (**18b**) L mol^{-1} cm^{-1}), 340 nm (ε = 3260 (**18a**) or 5200 (**18b**) L mol^{-1} cm^{-1}).

^1H NMR (C_6D_6): δ 6.87–6.80 (m, 3H, *p*-C_6H_3, *m*-C_6H_3), 6.69 (s, 4H, *m*-$C_6H_2(CH_3)_3$), 6.11 (pseudo-t, $^5J_{HH}$ = 2.8 Hz, 2H, Cp-C*H*), 5.60 (pseudo-t, $^5J_{HH}$ = 2.8 Hz, 2H, Cp-C*H*), 2.07 (s, 12H, *o*-$C_6H_2(CH_3)_3$), 2.05 ppm (s, 6H, *p*-$C_6H_2(CH_3)_3$).

$^{13}C\{^1H\}$ NMR (C_6D_6): δ 141.7, 141.3, 140.9, 138.9, 137.2, 136.6, 136.0, 131.6 (*m*-C_6H_3), 129.2 (*m*-$C_6H_3(CH_3)_3$) 115.6 (Cp-*C*H), 112.6 (Cp-*C*H), 21.5 (*o*-CH_3), 21.1 ppm (*p*-CH_3).

IR (KBr pellet): ν 2950 (m), 2918 (m), 2857 (m), 1611 (m), 1570 (m), 1453 (m), 1379 (m), 1087 (vs, br), 851 (w), 792 (s), 767 (s), 619 (w), 474 cm^{-1} (w).

2.2.22 Synthesis of $Ter^{Mes}CpBiCl_2$ – 19

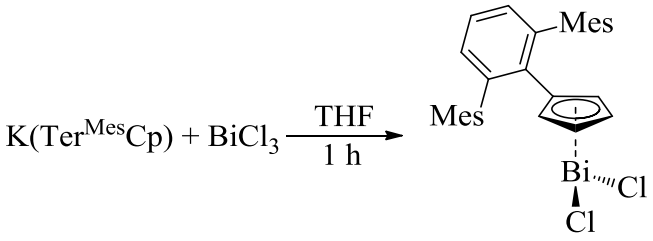

19

In a 20 mL scintillation vial equipped with a PTFE-coated magnetic stirring bar, 0.022 g (0.07 mmol, 1 eq.) of colourless $BiCl_3$ were dissolved in 1 mL of THF producing a colourless solution. Separately, 0.026 g (0.06 mmol, 0.86 eq.) of gray coloured K(TerMesCp) powder were dissolved in 1 mL of THF producing an orange coloured solution. The orange coloured solution of K(TerMesCp) was slowly added dropwise to the $BiCl_3$ solution and immediately produced a bright yellow coloured mixture that gradually changed to orange in colour. After the addition was complete, the reaction mixture was left to stir for 1 hour before removing the solvent *in vacuo* to produce an orange coloured residue. This residue was dissolved in 5 mL of pentane, and filtered through Celite® to yield an orange coloured solution, which when concentrated *in vacuo* yielded an orange coloured powder. Crystals suitable for X-ray diffraction were obtained by dissolving the compound in *ca*. 1 mL of pentane and storing in the freezer overnight at -35 °C.

Yield: 0.02 g (46 %).

^{1}H NMR (C_6D_6): δ 7.14–7.11 (m, 1H), 7.03–7.00 (m, 1H), 6.99 (d, $^3J_{HH}$ = 7.6 Hz, 1H), 6.77 (m, 2H), 6.65 (s, 2H, *m*-$C_6H_2(CH_3)_3$), 6.55 (pseudo-t, J_{HH} = 2.5 Hz, 1H, Cp-C*H*), 6.22 (pseudo-t, J_{HH} = 2.5 Hz, 1H, Cp-C*H*), 5.10 (pseudo-t, J_{HH} = 2.5 Hz, 1H, Cp-C*H*), 4.23

(pseudo-t, J_{HH} = 2.5 Hz, 1H, Cp-C*H*), 2.15–2.05 (m, 12H, $C_6H_2(CH_3)_3$) 1.89 ppm (s, 6H, $C_6H_2(CH_3)_3$).

Based on X-ray crystallography data, the cyclopentadienyl ligand adopts an η^3-coordination mode. Assuming this structure remains in solution, all cyclopentadienyl positions become chemically inequivalent, resulting in four resonances in the ^{1}H NMR spectrum. The mesityl rings are also inequivalent with overlapping resonances.

2.2.23 Synthesis of Ter^{Dipp}CpH(CoCp) – 20

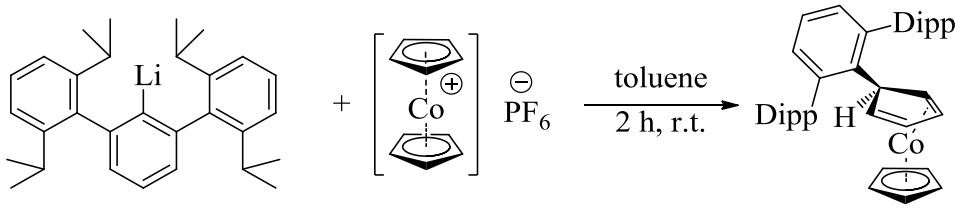

In a 20 mL scintillation vial, 0.498 g (1.23 mmol, 1 eq.) of colourless TerDippLi powder were dissolved in 10 mL of toluene to produce a pale yellow coloured mixture. Dropwise addition to a stirring suspension of 0.416 g (0.124 mmol, 1.01 eq) of yellow coloured $[Cp_2Co][PF_6]$ in 5 mL of toluene, producing an orange-red coloured mixture. The mixture was left to stir for 2 hours before filtration through a silica gel plug to produce a bright cherry-red coloured solution. Removal of the solvent *in vacuo* yielded the crude product as a red coloured semi-solid. Crystals suitable for X-ray diffraction studies and elemental analysis were obtained by dissolving the residue (approximately 700 mg in total mass) in 5 mL of pentane and storing in a freezer at -35 °C overnight.

Yield: 0.541 g (74 %) – 349 mg from recrystallization and an additional 192 mg from filtrate.

EA: Calc for $C_{40}H_{47}Co$: C: 81.88 %, H: 8.07 %, N: 0.00 %. Found: C: 81.90 %, H: 7.14 %, N: 0.04 %.

m.p. (°C): 186.6–188.0 (at elevated temperatures, the compound became blue).

UV (pentane): 327 (λ_{max}, ε = 1540 L mol^{-1} cm^{-1}), 391 nm (ε = 750 L mol^{-1} cm^{-1}).

^{1}H NMR (C_6D_6): δ 7.36 (t, $^3J_{HH}$ = 7.6 Hz, 2H, *p*-C_6H_3(iPr)$_2$), 7.22 (d, $^3J_{HH}$ = 7.6 Hz, 4H, *m*-C_6H_3(iPr)$_2$), 7.00–6.92 (m, 3H, *m*-C_6H_3, *p*-C_6H_3), 4.61 (m, $^4J_{HH}$ = 2.0 Hz, 2H, Cp-C*H*), 4.42 (t, $^4J_{HH}$ = 2.6 Hz, 1H, Cp-C*H*), 4.36 (s, 5H, C_5H_5), 2.70 (sept, $^3J_{HH}$ = 6.8 Hz, 4H, iPr-C*H*), 2.50 (m, $^4J_{HH}$ = 2.5 Hz, $^4J_{HH}$ = 1.6 Hz, 2H, Cp-CH_2), 1.36 (d, $^3J_{HH}$ = 6.9 Hz, 12H, iPr-CH_3) 1.03 ppm (d, $^3J_{HH}$ = 6.8 Hz, 12H, iPr-CH_3).

^{13}C{^{1}H} NMR (C_6D_6): δ 146.8, 140.7, 140.0, 138.9, 136.4, 131.0, (s, *m*-C_6H_3 or *p*-C_6H_3), 128.3 (s, *p*-C_6H_3(iPr)$_2$, *m*-C_6H_3(iPr)$_2$), 124.7 (s, *m*-C_6H_3 or *p*-C_6H_3), 122.8 (s, *p*-C_6H_3(iPr)$_2$, *m*-C_6H_3(iPr)$_2$), 79.2 (s, C_5H_5), 76.0, 54.3, 45.2 (s, Cp-*C*H_2), 31.1 (s, iPr-*C*H), 25.7 (s, iPr-*C*H_3), 23.0 ppm (s, iPr-*C*H_3).

The cobalt(I) intermediate **20** is also structurally different in solution (Figure 2.10), as indicated by the methylene resonance at 2.50 ppm in the ^{1}H NMR spectrum. Currently it is unknown which methylene isomer is present, HMBC data will be collected and should identify the nature of **20**. It was also noted that additional peaks are present in the ^{13}C{^{1}H} NMR spectrum. While it may seem that the ^{13}C{^{1}H} NMR spectrum possesses an extra peak, it is in fact correct. The isopropyl groups contain chemically inequivalent methyl groups and will produce three resonances instead of two (also evident by the ^{1}H NMR spectrum).

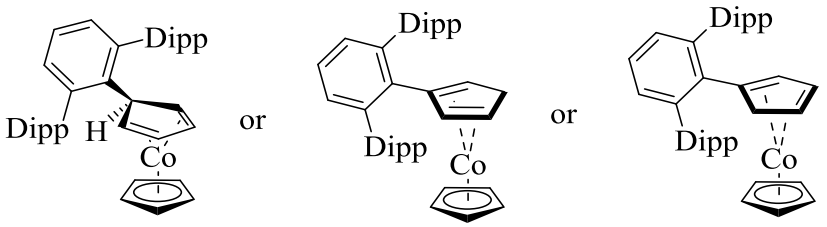

Figure 2.10. Possible isomers of the cobalt(I) intermediate **20**. The methine isomer has been confirmed in the solid state by X-ray crystallography, while in solution a methylene isomer is evident based on ^{1}H NMR spectroscopy.

2.3 Results and Discussion

2.3.1 Development of a Synthetic Route to Ter^{Mes}CpH

2.3.1.1 Unsuccessful Attempts

Prior to finding a viable synthetic route, two other approaches for synthesising cyclopentadienyl ligands were attempted and were unsuccessful at producing the desired *m*-terphenyl substituted cyclopentadienyl ligands. Attempts at reactions similar to the Pd-catalysed cross-coupling in THF-d_8 at 66 °C using the aryl halide (C_6H_2-2,4,6-Ph_3)Br failed to yield the corresponding cyclopentadiene compound. Another attempt using similar conditions was also unsuccessful with the biphenyl derivative *o*-MesPhI.

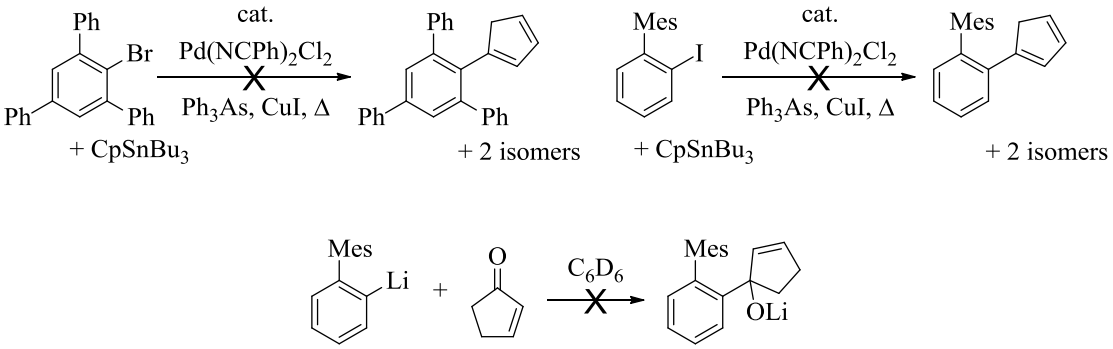

Scheme 2.9. Unsuccessful reactions attempted with biphenyl and *m*-terphenyl molecules.

Nucleophilic addition reactions to cyclopentenone have been well documented to produce substituted cyclopentadienyl derivatives, and avoid the oxidative addition step that was thought to be preventing the Pd-catalysed route from working. Unfortunately reaction attempts between cyclopentenone and the biphenyl *o*-MesPhLi were also unsuccessful. This route did not seem likely to work with the even more sterically hindered *m*-terphenyl systems that were the target of this project and so this synthetic route was also abandoned.

2.3.1.2 Synthesis of *m*-Ter^{Mes}CpH with Cobaltocenium Salts

The cobaltocenium cation is isoelectronic to ferrocene but it exhibits differing reactivity due to its cationic nature. It has been well documented that nucleophilic substitution reactions on unsaturated hydrocarbons (e.g. ethylene, butadiene, benzene) produce the corresponding *exo*-addition products when bound as ligands to cationic transition metal complexes.[14,79,80] Examples also include cyclopentadienyl ligands, and a commonly observed reaction in cobalt chemistry is the nucleophilic substitution reactions on the cyclopentadienyl ligands of cobaltocenium cations, $[Cp_2Co]^+$ (Figure 2.11).

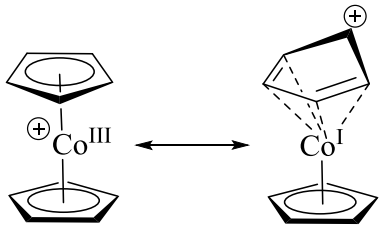

Figure 2.11. Canonical structures used to describe the cobaltocenium cation.

Nucleophilic substitution reactions to cobaltocenium cations were first reported in 1961,[81] and can be rationalised when the canonical structures of the cobaltocenium cation are considered (Figure 2.11). The cobaltocenium cation be considered as a Co^{III} complex substituted by two anionic cyclopentadienyl ligands, or as a $CpCo^{I}$ stabilised

cyclopentadienyl cation, $(C_5H_5)^+$.[80] When the latter description is considered, formally no redox chemistry occurs at the cobalt centre and it becomes perfectly reasonable to expect a nucleophilic substitution to occur at the cyclopentadienyl ring due to the highly electrophilic character and anti-aromaticity of the cyclopentadienyl cation. An alternative description is that a nucleophilic attack occurs at one of the η^5-bonded Cp rings, converting the ligand to an η^4-bonded cyclopentadiene ligand while the Co(III) centre is reduced to Co(I). Subsequent oxidation of the corresponding Co^I complex to Co^{III} then liberates the substituted cyclopentadienyl derivative following purification.

By following the same approach and reacting the organolithium reagent $Ter^{Mes}Li$ (Ter^{Mes} = C_6H_2-2,6-Mes_2, Mes = C_6H_2-2,4,6-Me_3) with $[Cp_2Co][I]$, the corresponding air-stable cobalt(I) (η^5-cyclopentadienyl)(η^4-cyclopentadiene) complex **8** was isolated in 66% yield following crystallisation from pentane (Scheme 2.10). Alternatively $[Cp_2Co][PF_6]$ may be used *in lieu* of the $[Cp_2Co][I]$ and is more convenient because its preparation avoids the tedious step of subliming cobaltocene.[78] However, **8** was used immediately without isolation following spectroscopic confirmation so no yield was recorded for reactions with $[Cp_2Co][PF_6]$. Aliquots collected from the crude reaction mixture of **8** synthesised using either cobaltocenium salt were nearly identical based on ^{1}H NMR spectroscopy. In each reaction there was a considerable amount of $Ter^{Mes}H$ present that was isolated along with **8**. The most logical source of this by-product is from $Ter^{Mes}Li$, however the cause of such significant contamination could not be definitively identified. Considerable formation was present even with rigorously dried solvents and glassware. After performing several NMR scale experiments in various solvents, it was determined that the formation of $Ter^{Mes}H$ was solvent dependent with the greatest proportion of $Ter^{Mes}H$ being formed when the reaction

was carried out in THF (*ca*. 50 %). Very little conversion to **8** or Ter^{Mes}H occurred at all when the reaction was carried out in diethyl ether. The least amount of Ter^{Mes}H, and highest yielding syntheses were when the conversion was carried out in benzene and toluene (*ca*. 20 %). Toluene was chosen over benzene because of its much lower freezing point, which is beneficial for recrystallisation, and a slightly better solubility of the starting materials.

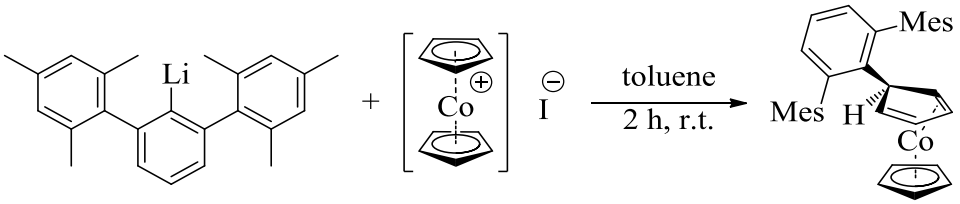

8

Scheme 2.10. Nucleophilic substitution of cobaltocenium iodide with Ter^{Mes}Li.

Crystals of **8** suitable for single crystal X-ray diffraction studies were grown by evaporation of a toluene solution. The structure of **8** (Figure 2.12) was found to be similar to related structures,[80] and features a cobalt atom 1.6745(11) Å from the Cp centroid and 1.6045(11) Å from the plane defined by C6-C9. The plane made up by the butadienyl fragment (C6-C9) is tilted 6.49(12)° away from the η^5-Cp fragment. The sp^3-hybridized C10 lies 0.597(3) Å above the butadiene plane causing the cyclopentadiene ring to pucker, and exhibits an angle of 34.74(17)° between the C6-C10-C9 and C6-C7-C8-C9 planes. The flanking mesityl groups are nearly parallel and twist out of the plane of the central aryl ring by 82.86(7)° and 80.72(6)°.

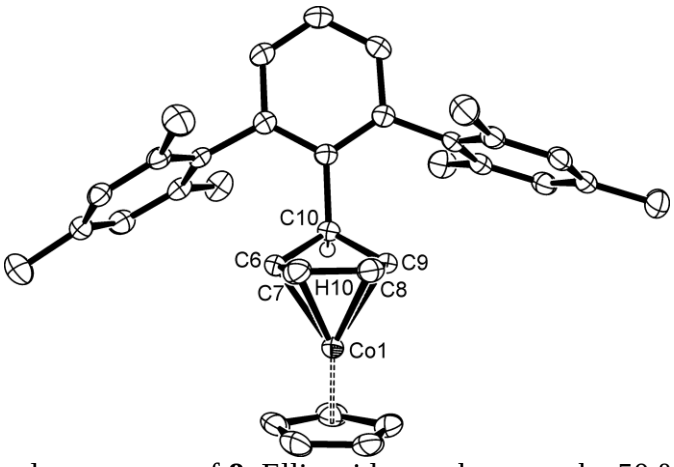

Figure 2.12. Molecular structure of **8**. Ellipsoids are shown at the 50 % probability level. Hydrogen atoms (except H10) have been removed for clarity. Selected bond lengths (Å) and angles (°) (note Cp_c denotes the ring centroid): Co1-C6 2.0023(17), Co1-C7 1.9627(19), Co1-C8 1.9649(19), Co1-C9 2.0181(17), Co1-Cp_c 1.6745(11).

Interestingly the cobalt(I) intermediate **8** is structurally different in solution (Figure 2.13), as indicated by the methylene resonance at 2.50 ppm in the ^{1}H NMR spectrum, which was confirmed to be part of the cyclopentadiene ring by examination of correlations between resonances at 4.18 ppm and 4.55 ppm in the ^{1}H-^{1}H COSY NMR spectrum. While the type of rearrangement is still unknown at this time, it is most likely required to accommodate the significant steric demand of the *m*-terphenyl ligand bound to the cyclopentadiene fragment.

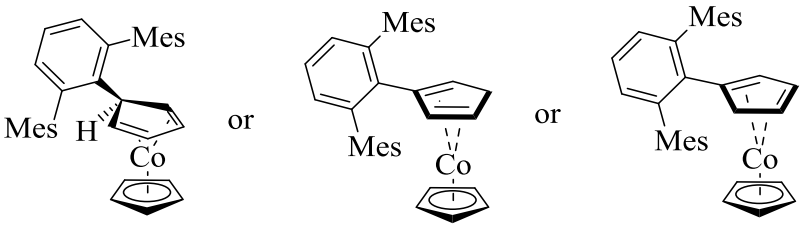

Figure 2.13. Possible isomers of the cobalt(I) intermediate **8**. The methine isomer has been confirmed in the solid state by X-ray crystallography, while in solution a methylene isomer is evident based on ^{1}H NMR spectroscopy.

Subsequent oxidation of **8** using two equivalents of $FeCl_3$, followed by column chromatography (silica gel, toluene) to remove all metal containing by-products yielded the desired cyclopentadienyl ligand precursors **9a+b** in 83 % isolated yield (Scheme 2.11) . The ^{1}H NMR spectrum in C_6D_6 revealed $Ter^{Mes}H$ as the major by-product carried through from the synthesis of **8**, which could not be completely removed by crystallization of either **8** prior to oxidation, or from **9a+b**. This prevented suitable elemental analysis data, so HRMS was also collected and confirmed the presence of **9a+b** from its corresponding $[M+H]^+$ peak (*m/z* = 379.2424). Initial preference for the formation of one isomer was observed by ^{1}H NMR spectroscopy immediately after isolation, but quickly reached a 1:1 equilibrium with its other isomer within one week. The initially formed product could not be determined from the coupling constants using a 300 MHz spectrometer and is still under investigation; likely the orientation of the methylene group remains unchanged from the Co(I) starting material **8**. Attempts at elucidating the structure of both **8** and the initial oxidation product **9** using NOESY NMR spectroscopy are planned in the future to verify this hypothesis. No evidence of the more sterically hindered allylic isomer **9c** could be detected in the ^{1}H NMR spectrum. This observation was investigated using DFT

calculations (B3LYP/6-31G(d)) and revealed that **9b** is only *ca.* 0.8 kJ mol^{-1} lower in energy than **9a**, and *ca.* 33 kJ mol^{-1} more stable than **9c**, consistent with experimental observations that a mixture of **9a** and **9b** are obtained without **9c**. No indication of the [4+2] Diels-Alder dimerisation product was observed after standing for a week both in the solid state and in solution and Cp-*H* resonances in the ^{1}H NMR spectrum were identified between 6.25 and 5.75 ppm and at 2.72 and 2.40 ppm, and are similar to the parent $Ter^{Ph}CpH$.[25]

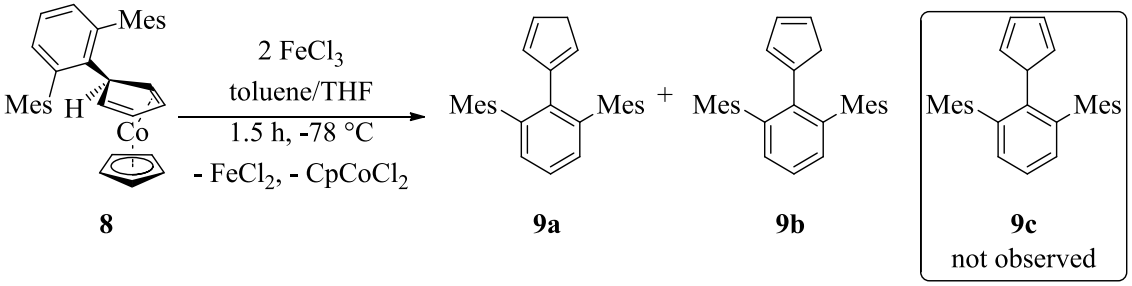

Scheme 2.11. Synthetic route to *m*-terphenyl substituted cyclopentadienyl compounds from the oxidative decomposition of **8**.

Crystals of **9a+b** were grown by evaporation of a C_6D_6 solution. Both **9a** and **9b** co-crystallise together as colourless blocks in the orthorhombic space group *Pbcn*. Structurally **9a+b** adopts a paddlewheel-type configuration about the C6-C11 aryl ring, with the mesityl groups relatively unchanged from **8**, while the cyclopentadiene ring twists 55.24(11)° out of the plane of the central aryl fragment to minimize steric interactions. The bond lengths and angles within the cyclopentadiene ring vary slightly, with the longest bonds and most acute angle occuring at the methylene position between C2-C3 and C3-C4 (1.487(5) Å and 1.411(5) Å respectively) with an angle of 105.8(3)° between C4-C3-C2. The C1-C6 bond length (1.485(4) Å) is slightly shorter than found for the *ipso*-carbons of flanking mesityl

groups (C7-C12 1.497(4) Å and C11-C18 1.494(4) Å) which may be indicative of partial conjugation between the central aromatic and cyclopentadiene rings.

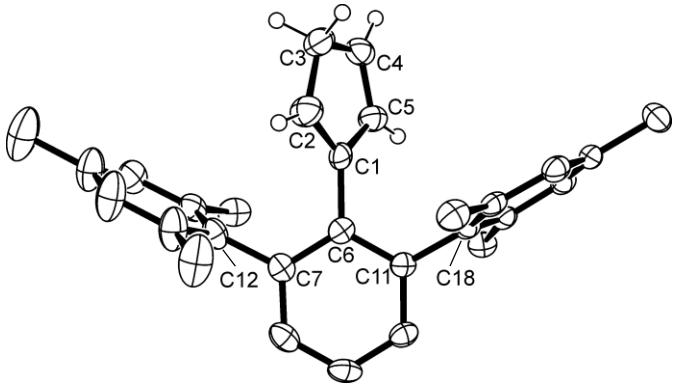

Figure 2.14. Molecular structure of **9a**. Ellipsoids are shown at the 50% probability level. Hydrogen atoms (except for those on the cyclopentadiene ring) have been omitted for clarity. Selected bond lengths (Å) and angles (°): C1-C2 1.383(4), C2-C3 1.487(5), C3-C4 1.411(5), C4-C5 1.394(4), C1-C6 1.485(4), C7-C12 1.497(4), C11-C18 1.494(4), C1-C2-C3 108.1(3), C4-C3-C2 105.8(3), C5-C4-C3 109.2(3), C4-C5-C1 109.1(3), C2-C1-C5 107.8(3), C2-C1-C6 127.8(3), C5-C1-C6 124.3(2), C6-C7-C12 121.2(3), C6-C11-C18 121.5(2).

From reactions carried out in THF, several small orange coloured crystals were obtained during crystallisation attempts. Not enough material was isolated for a complete characterisation, however single crystal X-ray diffraction studies revealed this product to be a dimeric form of **9**, which will be referred to as **9'** (Figure 2.16). The origins of this homocoupled by-product **9'** are still unknown and no relevant examples could be found in the literature for comparison. It may be catalysed by an excess amount of $FeCl_3$ from the oxidation of **8**, however this has not been tested as it was beyond the scope of this project. Provided such a dimer could be produced reliably, it would be particularly interesting to

see whether bimetallic or even tetrametallic systems could be obtained with this molecule following multiple deprotonations. The molecule **9'** crystallises in the monoclinic space group *P*2/*c* with only one half of the molecule in the asymmetric unit. At an initial glance the structure of **9'** appears to be a substituted fulvalene derivative, and admittedly hydrogen atoms can be quite difficult to identify using X-ray crystallography due to their weak X-ray scattering capabilities. However the C4-C5 bond length (1.515(3) Å) is much longer than a double bond, which would be expected for a fulvalene derivative (Figure 2.15), and is clearly in support of the proposed assignment as a dimeric form of **9**.

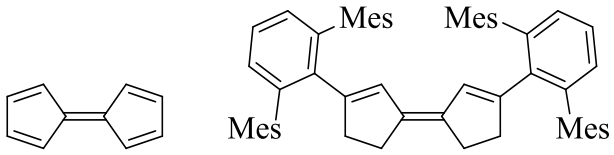

Figure 2.15. Distinction between fulvalene (left) and the dimer **9'** for clarity.

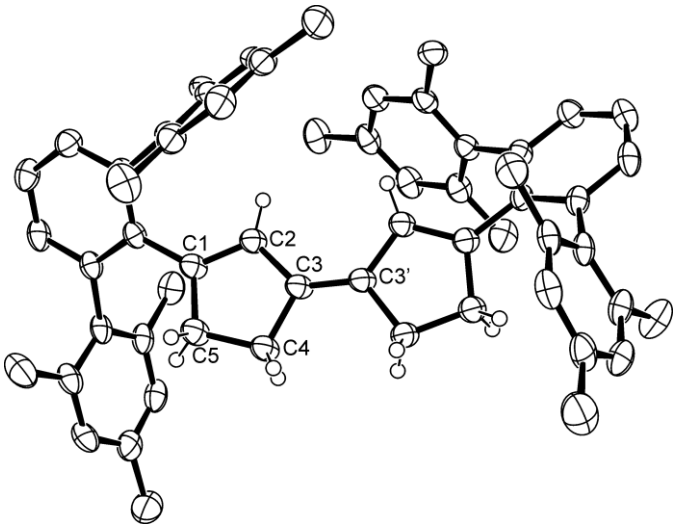

Figure 2.16. Molecular structure of **9'** obtained from the oxidation of **8** in THF. Ellipsoids are shown at the 50% probability level. Hydrogen atoms (except for those on the cyclopentadiene rings) have been omitted for clarity. Selected bond lengths (Å) and angles

(°): C1-C2 1.387(3), C2-C3 1.458(3), C3-C4 1.500(3), C4-C5 1.515(3), C3-C3' 1.356(4), C1-C2-C3 110.31(17), C2-C3-C4 107.38(16), C3-C4-C5 105.01(16), C2-C1-C5 109.81(18), C3'-C3-C2 130.02(11), C3'-C3-C4 122.60(10).

2.3.2 Alkali Metal Complexes of the Ter^{Mes}Cp Anion

2.3.2.1 General Remarks for Practical Use

The crude mixture of **9a+b** containing Ter^{Mes}H as the sole contaminate, is able to be transformed into the corresponding alkali metal salts **10-14** when combined with the appropriate alkali metal transfer reagent. The Ter^{Mes}H and any unreacted **9a+b** is easily removed from the alkali metal salts by washing multiple times with pentane, however it was observed that **12** displayed moderate solubility in pentane, which must be considered during purification.

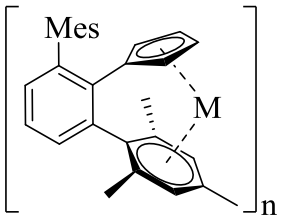

M = Li **10**
Na **11**
K **12**
Rb **13**
Cs **14**

Figure 2.17. Synthesised alkali metal complexes of the Ter^{Mes}Cp anion. For structurally characterised complexes (**10**, **12**, and **14**) oligomeric structures were found (**10**, n = 4; **12**, n = 4; and **14,** n = 6).

It was found that the reaction between the cyclopentadiene isomers **9a+b** and BuLi was unsatisfactory for the synthesis of the lithium cyclopentadienide **10**, and produced a product that was highly insoluble in most organic solvents (but slightly soluble in THF). This product could not be identified by ^{1}H NMR spectroscopy and the ^{1}H NMR spectrum bore no resemblance to what would be expected for **10** and this reagent was abandoned.

Reaction between a mixture of **9a+b** and $LiN(SiMe_3)_2$ was the most effective route to **10**, however some lithium-containing impurities were evident in the ^7Li NMR spectrum (δ = 0.30 ppm), which prevented satisfactory elemental analysis from being obtained. An additional signal was present in the ^1H NMR spectrum (δ 0.05 ppm), which is close to the starting lithium bis(trimethylsilyl) amide (δ 0.12 ppm in C_6D_6).[82] Additional support for this is based on a relatively high percentage of nitrogen (0.14 %). Similarly **11** could also be obtained from reactions of **9a+b** with $NaN(SiMe_3)_2$ and was found to be the best route, but is also accessible with NaH although the reaction is much slower and required nearly 6 equivalents of NaH to go to completion. It was found that the corresponding alkali metal bis(trimethylsilyl)amides were the best reagents for **10** and **11**, but not for the preparation of **12**. Reaction in pentane between **9a**+**b** and $KN(SiMe_3)_2$ followed by filtration and storage in a -35 °C freezer produced crystals that were later identified as $[KTer^{Mes}Cp]_2[KN(SiMe_3)_2]_2$ using X-ray crystallography. This method was not pursued further following this observation, but structural information on the salt will be discussed. Alternatively 1.2 equivalents of KH offered a much cleaner, albeit slower synthesis for **12** within three days without the use of additives such as 18-crown-6 to accelerate the reaction. No attempts at synthesising **10−12** using lithium, sodium, or potassium metal were made due to the unknown thermal stability of **9a**+**b** but should be investigated in the future. Lastly, **13** and **14** were easily accessible from the reaction between a mixture of **9a+b** and their respective alkali metals in hot THF. Unfortunately these compounds exhibited poor solubility in most organic solvents with the exception of pyridine, and required a more extensive drying step making them inconvenient for further use.

To summarise, it was determined that **12** was most suitable for further reactions partially due to its moderate to high solubility in both polar (THF, high) and non-polar (toluene, moderate; pentane, slightly to moderate) solvents making it a versatile reagent for organometallic chemistry, but mostly for its highly reliable synthesis with KH and its tendency to crystallise well from toluene. Oligomeric structures were observed for all structurally characterised (**10**, **12**, and **14**) alkali metal complexes in the solid state (described later), but in solution the degree of aggregation could not be determined quantitatively. Nonetheless **12** behaved as a reliable monomeric "KTer^{Mes}Cp" source when reacted with transition metal compounds and is recommended as the choice starting material for further coordination chemistry.

2.3.2.2 Structural and Spectroscopic Characterisation

The ^{1}H NMR spectrum of the lithium cyclopentadienide **10** in THF-d_8 reveals a symmetric set of Cp-*H* resonances between 5.30–5.15 ppm as pseudo-triplets (J_{HH} = 2.9 Hz, 2.5 Hz). This pattern is characteristic for AA'BB' spin systems in monosubstituted cyclopentadienyl complexes, and indicates that a mirror plane is present orthogonal to the plane of the Cp ring.[25,80] A total of 13 resonances were identified in the ^{13}C{^{1}H} NMR spectrum, which is also an indication of a mirror plane. The remaining Ter^{Mes} resonances are clearly visible with methyl groups appearing as singlets at 2.23 ppm and 1.97 ppm in a 1:2 ratio, a broad singlet at 6.75 ppm for the *m*-MesH environments, and the central aromatic ring appears as a doublet at 6.83 ppm ($^{3}J_{HH}$ = 7.4 Hz) and a pseudo-triplet at 7.04 ppm ($^{3}J_{HH}$ = 7.4 Hz) in a 2:1 ratio. Based on ^{1}H-^{13}C HSQC NMR spectroscopy it was determined that both mesityl rings were equivalent with the ^{1}H resonance at 6.75 ppm correlating to a single ^{13}C resonance at 128.3 ppm. Typically lithium cations prefer to adopt

a coordination number of four,[83] however recent DOSY NMR experiments have shown that the solution state structure of cyclopentadienyl lithium is CpLi·2THF.[84] Based on the spectroscopic data obtained, the likely configuration of **10** when dissolved in THF is a piano-stool type geometry with two or three THF molecules occupying the vacant coordination sites of the lithium ion (Figure 2.18).

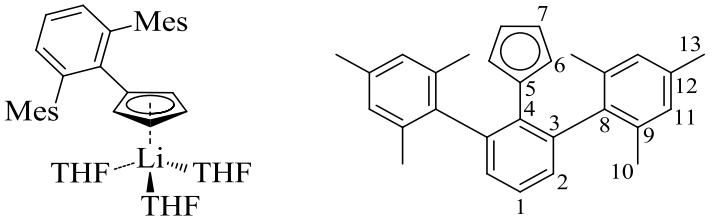

Figure 2.18. Proposed structure of **10** and unique carbon environments when dissolved in THF based on NMR spectroscopic data obtained in THF-d_8. Dashed bond indicates the THF may or may not be coordinated to the lithium ion.

The solid-state structure of **10** was confirmed by single crystal X-ray diffraction (Figure 2.20). Colourless hexagonal shaped crystals of **10** were obtained by evaporation of a C_6D_6 solution of an NMR scale reaction between $LiN(SiMe_3)_2$ and a mixture of **9a+b**. The organometallic complex **10** crystallises in the monoclinic space group *I*2/*a* as an acyclic tetramer (Figure 2.19, Figure 2.20) with two separate molecules in the asymmetric unit, each comprised of two-site lithium disorder with *ca*. 50/50 occupancy. The solid-state structure consists of a mixture of "chelated" and "non-chelated" lithium atoms, and are similar for each component of the disorder. Therefore only one component will be discussed in detail. The Cp-rings are twisted by 65.66(9)° and 52.50(7)° relative to the central aryl rings and each lithium atom adopts an η^5-coordination mode to the Cp-rings and Li1a is η^3-coordinated to the mesityl ring *via* C12, C16, and C17 with bond lengths of

2.468(7) Å, 2.552(7) Å, and 2.357(7) Å respectively. The Cp-Li1a bond lengths ranged from 1.863(8) Å to 2.454(8) Å and were within previously reported ranges for structurally characterized η^5-CpLi compounds.[85] The longest Cp-Li bond lengths described in the literature are 2.419 Å and 2.455 Å reported for the crown ether complexes CpLi·(12-crown-4) and $(RO)_2$BCpLi·(12-crown-4) respectively.[85] The distance between Li2a and C4 (2.466(9) Å) may be indicative of a bond and is statistically identical to C2-Li1a (2.454(8) Å), however this value surpasses known Cp-Li bond lengths.[85]

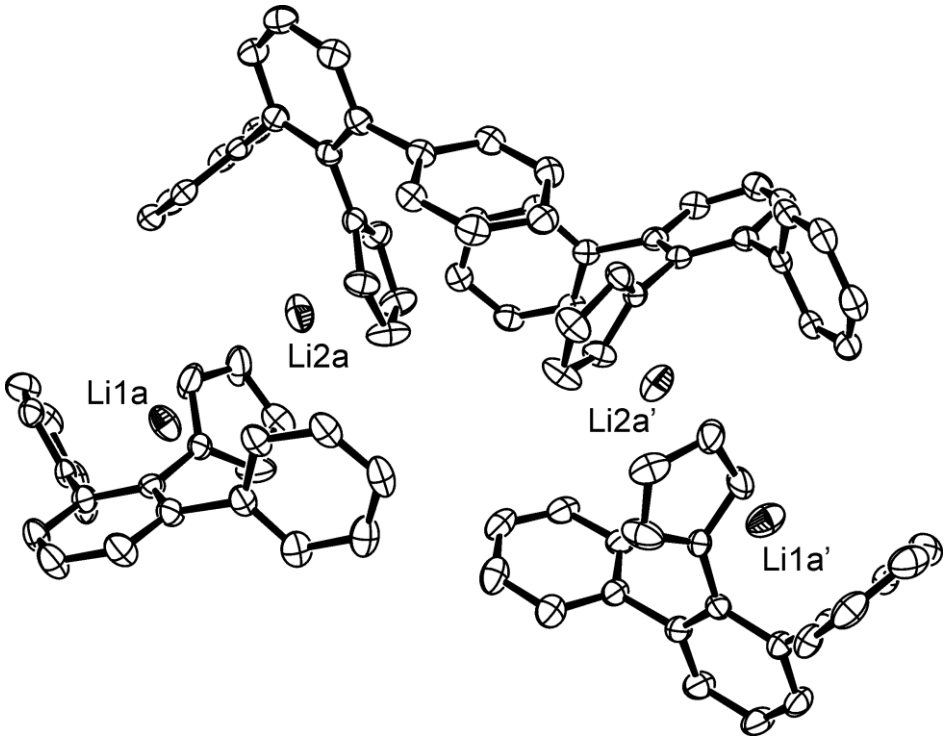

Figure 2.19. Molecular structure of **10** illustrating the tetrameric structure. Ellipsoids are shown at the 50% probability level. One component of the lithium ion disorder has been omitted for clarity. Hydrogen atoms and methyl groups have been omitted for clarity.

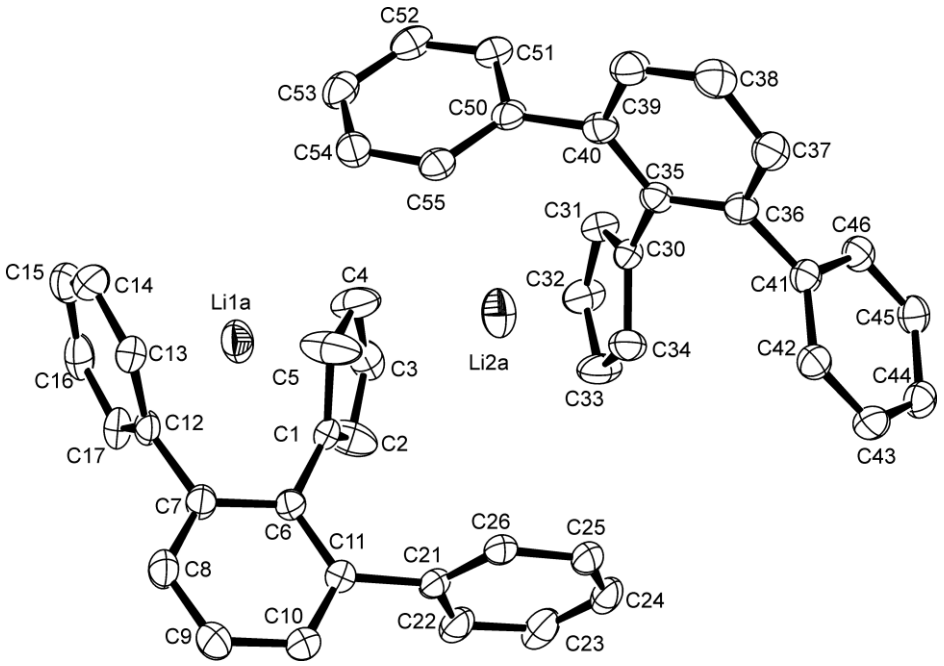

Figure 2.20. Molecular structure of the asymmetric unit of **10**. Ellipsoids are shown at the 50% probability level. One component of the lithium ion disorder has been omitted for clarity. Hydrogen atoms and methyl groups have been omitted for clarity. Selected bond lengths (Å) and angles (°): C1-Li1a 2.201(8), C2-Li1a 2.454(8), C3-Li1a 2.345(7), C4-Li1a 1.987(7), C5-Li1a 1.863(8), C12-Li1a 2.468(7), C16-Li1a 2.552(7), C17-Li1a 2.357(7), C30-Li2a 2.308(8), C31-Li2a 2.199(8), C32-Li2a 2.004(7), C33-Li2a 1.953(7), C34-Li2a 2.152(8), C5-C1-C6-C7 60.7(3), C6-C7-C12-C17 80.3(2), C10-C11-C21-C22 90.0(2), C34-C30-C35-C36 52.8(2),C37-C36-C41-C42 86.4(2), C35-C40-C50-C55 83.4(2).

The ^{1}H NMR spectrum of **11** in THF-d_8 exhibited a broad singlet Cp-*H* resonance (δ 5.27 ppm), which is different from what is observed for **10**; however broadening could be due to the coalescence of two pseudo-triplets with similar chemical shifts. Support for this proposal is evident based on correlations observed between resonances at 5.27 ppm, 103.0 ppm and 105.4 ppm in the ^{1}H-^{13}C HSQC spectrum of **11**. Another singlet resonance

was observed in this region (^{1}H δ 5.72 ppm, ^{13}C{^{1}H} δ 103.3 ppm) which was later determined to be caused by contamination with sodium cyclopentadienide,[51] when crystals of the polymer [Na(THF)Ter^{Mes}Cp·NaCp(THF)]$_{\infty}$ (**11'**) were obtained unexpectedly during crystallisation attempts from THF (Figure 2.21). Similarly to **10**, a total of 13 resonances were identified for **11** in the ^{13}C{^{1}H} NMR spectrum when coupled with 2D data and after exclusion of the peak belonging to sodium cyclopentadienide. Like **10**, this is also a clear indication of a mirror plane and suggests a similar structure as proposed for **10** in THF albeit with a higher coordination number between four and six for the sodium cation most likely.[83,84] Additional evidence of molecular symmetry is given by the remaining Ter^{Mes} resonances, which possess similar characteristics to **10** such as two unique methyl groups appearing as singlets at 2.19 ppm and 2.02 ppm in a 1:2 ratio, and a broad singlet at 6.71 ppm for both *m*-MesH environments which pairs with a single ^{13}C resonance at 127.9 ppm.

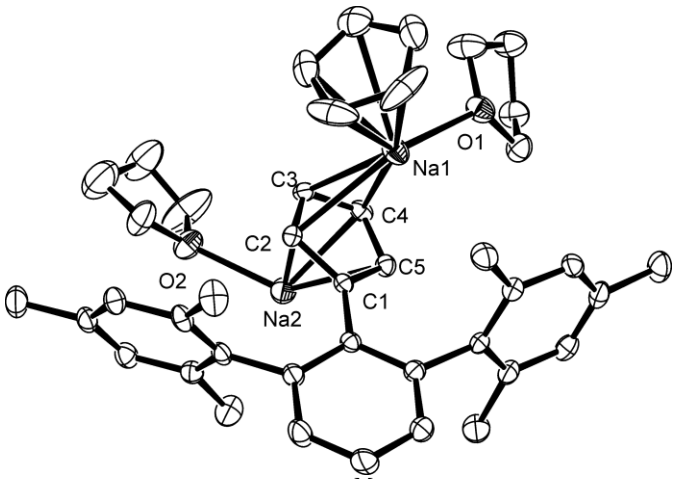

Figure 2.21. Molecular structure of Na(THF)Ter^{Mes}Cp·NaCp(THF) monomeric unit (**11'**) showing connectivity only. Ellipsoids are shown at the 50% probability level. Hydrogen atoms have been omitted for clarity. During structure refinement some disorder was present

in one of the coordinated THF molecules, and so bond lengths and angles have been excluded.

Large block-shaped, orange coloured crystals of **12** were obtained *via* pentane vapour diffusion into a saturated toluene solution. Compound **12** was found to crystallise in the monoclinic space group *I*2/*a*. The molecular structure of **12** features a cyclic tetramer with a large central square-shaped cavity (Figure 2.22). Each potassium cation occupies a corner of the cavity and are separated by 5.7652(7) Å and 5.7625(7) Å between K1-K2 and K2-K3 respectively, while the geometry of the cavity is defined by the acute K1-K2-K3 angle of 90.579(11)°. The overall cavity size as measured from opposite Cp-H atoms spans *ca*. 3.7 Å and was found to contain no solvent molecules during the structure refinement. Each potassium cation is η^3-coordinated by two Cp-rings and η^6-coordinated by two mesityl rings with an average K-Cp centroid distance of 3.0182 Å, significantly longer than what is found for typical K-Cp centroid distances (2.816 Å for CpK,[86] 2.783 Å for Cp*K·(pyridine)$_2$,[87] and 2.785 Å for Me_3SiCpK[88]).

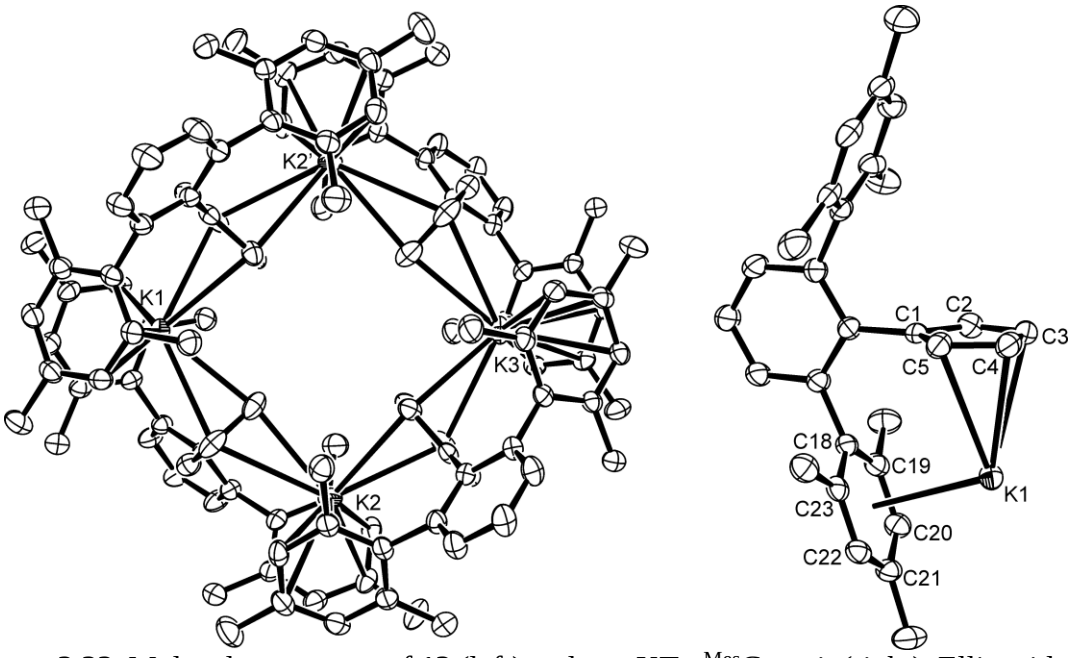

Figure 2.22. Molecular structure of **12** (left) and one KTer^{Mes}Cp unit (right). Ellipsoids are shown at the 50% probability level. Hydrogen atoms have been omitted for clarity. Selected bond lengths (Å) and angles (°): K1-C3 3.0929(19), K1-C4 2.9254(18), K1-C5 3.0993(18), K1-C18 3.369(2), K1-C19 3.492(2), K1-C20 3.445(2), K1-C21 3.3344(17), K1-C22 3.1980(17), K1-C23 3.2080(16), K1-K2-K3 90.579(11).

The NMR spectroscopic properties of **12** in THF-d_8 are similar to the lighter homologues **10** and **11**. Like **11**, a single Cp-*H* resonance is present in the ^{1}H NMR spectrum (δ 5.40 ppm) and was observed as a singlet, however it was found to correspond to only one resonance at 104.2 ppm in the ^{13}C{^{1}H} NMR spectrum. A relatively broad resonance is close to this chemical shift (δ 103.4 ppm), and is in the proper region to correspond to some of the remaining Cp carbon chemical environments. Molecular symmetry was also clearly defined by two unique methyl groups appearing as singlets at 2.20 ppm and 2.09 ppm in a 1:2 ratio, a broad singlet at 6.80 ppm for both *m*-MesH environments which pairs with a single ^{13}C NMR signal at 128.1 ppm. It is likely that **12**

also adopts a similar configuration as its lighter analogues when dissolved in THF-d_8. To further investigate its solution-state molecular structure a non-coordinating solvent was chosen to collect NMR spectroscopic data. The ^{1}H NMR spectrum of **12** in C_6D_6 was much simpler to interpret than data previously collected in THF-d_8 and is consistent with the molecular structure of **12**. Resonances for the central aromatic ring were the easiest to identify by their characteristic triplet ($^3J_{HH}$ = 7.5 Hz) and a doublet ($^3J_{HH}$ = 7.5 Hz) at 7.25 ppm and 6.92 ppm respectively in a 1:2 ratio. Three unique methyl environments are present (δ 2.36, 2.27, and 2.11 ppm) in a 1:1:1 ratio, and in addition two unique *m*-MesH environments are observed in the ^{1}H NMR spectrum as singlets (δ 7.04 ppm and 6.55 ppm) with a 1:1 ratio. Without prior knowledge of the molecular structure of **12** these observations were initially confusing to rationalise; however once the structure of **12** had been determined these resonances make complete sense when **12** is considered as a ring with both inner and outer components. Two broad Cp-*H* resonances could also be identified at 5.70 ppm and 5.63 ppm with a 3:1 ratio, consistent with the η^3-coordination mode of **12**. Based on $^{13}C\{^1H\}$ NMR data, it was determined that 18 unique carbon environments are present (Figure 2.23) which is also consistent with the tetrameric structure of **12**.

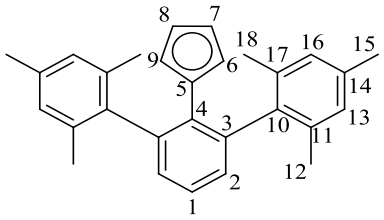

Figure 2.23. Unique carbon environments for the Ter^{Mes}Cp anion of **12** when dissolved in C_6D_6.

As mentioned previously the reaction in pentane between **9a**+**b** and $KN(SiMe_3)_2$ followed by filtration and storage in a -35 °C freezer produced crystals of $[KTer^{Mes}Cp]_2[KN(SiMe_3)_2]_2$ (**12'**). The structure of this complex is similar to **12** and features a large central, hexagonal shaped cavity. Each potassium cation is η^5-coordinated to one Cp-ring, η^6-coordinated to one mesityl ring, and lastly coordinated to a bridging $N(SiMe_3)_2$ fragment. The K-Cp centroid distances were determined to be 2.8128(12) Å and 2.7836(12) Å between K1 and K2 respectively, and are typical for cyclopentadienyl potassium complexes.[86-88] Two different K-N distances were found (K1-N1 2.7978(18) Å and K2-N1' 2.8648(16) Å), and are similar to the K-N distances reported for the dimer $[KN(SiMe_3)_2]_2$ (2.770(3) Å and 2.803(3) Å).[89] This structure is an exciting discovery as it exemplifies the potential for these molecules to form bimetallic systems (i.e. those with a 2:1 ratio of metal to Cp ligand), an avenue that should be explored in the future.

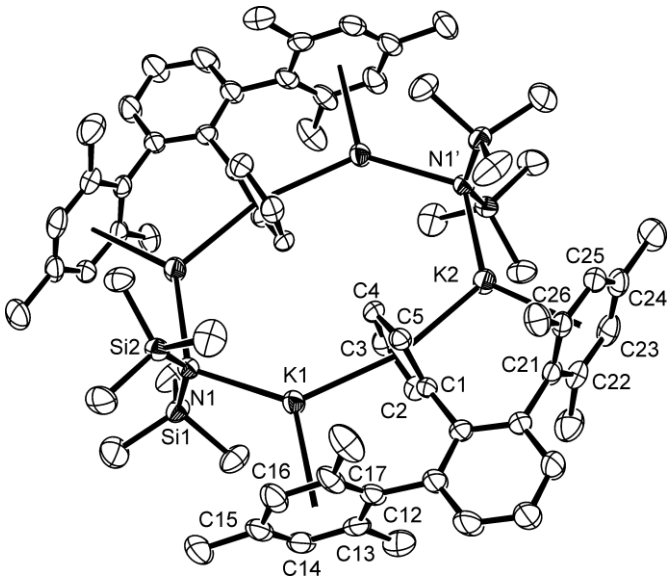

Figure 2.24. Molecular structure of **12'**. Ellipsoids are shown at the 50% probability level. Hydrogen atoms and the pentane solvate have been omitted for clarity. Selected bond lengths (Å) and angles (°): K1-C1 3.241(2), K1-C2 3.103(2), K1-C3 2.899(2), K1-C4

2.907(2), K1-C5 3.113(2), K1-N1 2.7978(18), K2-C1 3.1979(19), K2-C2 3.085(2), K2-C3 2.893(2), K2-C4 2.882(2), K2-C5 3.074(2), K2-N1' 2.8648(16), K1-N1-K2 121.05(6).

After observing a large cyclic, oligomeric structure for **12**, it seemed pertinent to synthesise the heavier rubidium and caesium analogues to investigate if this trend continues. The complexes **13** and **14** are isolated directly from the reaction mixture as faintly pink, nearly colourless powders in moderate to high yields with melting points >400 °C for **13** and between 388-391 °C for **14**. Unfortunately this failed to yield analytically pure samples of **13** or **14**, as determined by elemental analysis, due to excessive solvent incorporation into the crystal lattice. Attempts were made at removing the incorporated solvent by heating solid samples of **13** and **14** at 120 °C under vacuum for three days. This heating improved the results obtained from elemental analysis but were still unsatisfactory even with attempts at quantifying the amount of solvent present. To supplement the elemental analysis data, HRMS data was collected for **13** and **14** and both species were identified by their $[M+H]^+$ (*m/z* = 463.1451) and $[M-CH_3]^+$ (*m/z* = 495.1083) mass peaks respectively. Due to poor solubility of the complexes **13** and **14** in THF-d_8 only ^{1}H NMR data could be collected; attempts at collecting suitable $^{13}C\{^1H\}$ NMR data were unsuccessful even with 24 hour collection times and were not pursued any further. Incomplete $^{13}C\{^1H\}$ NMR spectroscopic data is provided in the Experimental section for **13** and **14** as future reference.

A single broad Cp-*H* resonance was observed in the ^{1}H NMR spectrum at 5.31 ppm for **13**. Contamination of the reaction mixture was evident based on the presence of a second sharp signal at 5.50 ppm, which was identified as rubidium cyclopentadienide,[84]

likely due to the diffusion of cyclopentadienyl vapours into the reaction mixture or from cyclopentadiene and/or dicyclopentadiene present from the starting material. Two resonances for the methyl groups were observed (δ 2.19 ppm and 2.05 ppm) in a 1:2 ratio, and in addition a single resonance was observed for the *meta*-MesH environments (δ 6.75 ppm) and overlaps with a doublet (δ 6.74 ppm, $^{3}J_{HH}$ = 7.5 Hz) attributed to the *meta*-positions of the central aromatic ring. Resonances for the *para*-position could not be found, however a shoulder peak (δ 6.77 ppm) is present with the resonances due to the *meta*-MesH environments, suggesting that a partial overlap is occurring. Further evidence for this is given by the integration value, which is slightly high. The structure of **13** is likely oligomeric in both solution and solid states. In solution, the binding energy of THF would be expected to decrease with an increase in ionic radius. This is prediction is based on the concept of soft-hard acid base theory and has been predicted for similar ligands using computational results.[90] Further evidence of an oligomeric structure is provided by the poor solubility of **13** in THF even at elevated temperatures, which suggests a large molecular structure that is stable in THF solutions. ^{1}H NMR spectroscopic data collected in pyridine-d_5, a slightly better donor solvent, indicated that a partial deaggregation of **13** had occurred. In addition to a single broad Cp-*H* resonance at 4.94 ppm, additional pseudo-triplets resembling an AA'BB' spin system had appeared between 5.93–5.83 ppm ($^{4}J_{HH}$ = 2.9 Hz, $^{4}J_{HH}$ = 2.5 Hz). The degree of aggregation was estimated using relative integration values and was found to be roughly 0.3:1 for monomer/oligomer or roughly 25% monomer, which was found to remain constant after standing for one week in the glovebox. Unfortunately no solid-state structural information for **13** could be obtained using X-ray crystallography,

however both **12** and **14** adopt large, macrocyclic oligomers (discussion on **14** is provided below) and so it seems very likely that **13** would adopt a similar structure.

Crystals of **14** were obtained from allowing a hot (*ca.* 60 °C) saturated THF solution to cool toroom temperature. Compound **14** crystallises in the triclinic space group *P-1* as large, colourless hexagonal-shaped plates. Similar to **12**, the molecular structure of **14** exhibits a large central cavity spanning *ca*. 7.8 Å across (Figure 2.25). However, the Cs1-Cs2-Cs3 angle of 119.357(7)° produces a hexagonal shape instead. The Cs-Cp bond lengths ranged considerably from 3.122(4) Å to 3.6668(5) Å, but are otherwise in the range of structurally characterized η^5-coordinated Cs-Cp compounds while each of the mesityl rings are η^6-coordinated. Multiple (>7) non-coordinating solvent molecules were visible during the structure refinement, some of which were disordered and could not be modelled properly. To remedy this, the residual electron density attributed to these molecules was removed by implementing PLATON's squeeze command,[91] removing a total electron density of 347 electrons per unit cell, which corresponded to *ca.*8.5 molecules of THF.

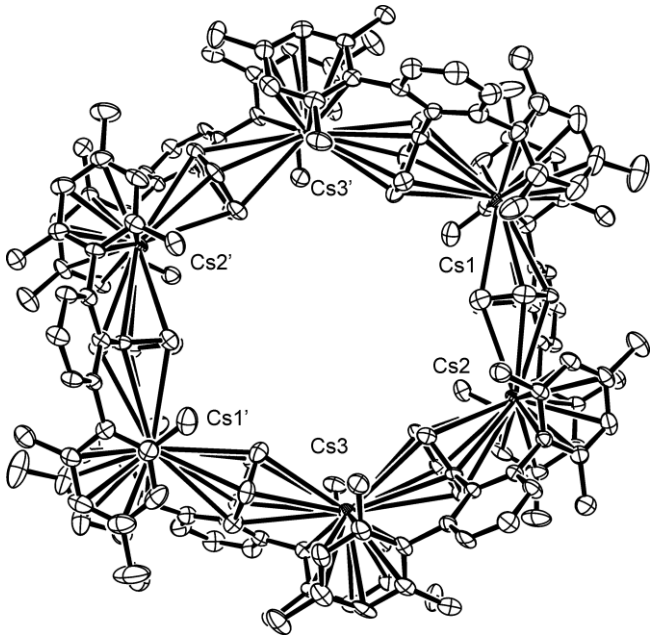

Figure 2.25. Molecular structure of **14**. Ellipsoids are shown at the 50% probability level. Hydrogen atoms and THF solvate have been removed for clarity. Selected bond lengths (Å) and angles (°) (Cp_c and Mes_c denote the ring centroids): Cs1-Cp_c (C1–C5) 3.129(2), Cs1-Mes_c (C12–C17) 3.191(3), Cs1-Cp_c (C30–C34) 3.128(3), Cs1-Mes_c (C41–C46) 3.159(2), Cs2-Cp_c (C30–C34) 3.170(2), Cs2-Mes_c (C50–C55) 3.259(3), Cs2-Cp_c (C59–C63) 3.186(3), Cs2-Mes_c (C79–C84) 3.251(2), Cs3-Cp_c (C59–C63) 3.170(3), Cs3-Mes_c (C70–C75) 3.208(2), Cs1-Cs2-Cs3 119.357(7).

The NMR spectroscopic properties for **14** were similar to **13**, with the Cp-*H* resonance appearing as a broad singlet at 5.16 ppm. The remaining Ter^{Mes} resonances were identified by the triplet-doublet pair for the central aromatic ring (δ 6.97 ppm, $^3J_{HH}$ = 7.4 Hz, and 6.76 ppm $^3J_{HH}$ = 7.4 Hz respectively) with a 1:2 integration ratio, a broad singlet at 6.71 ppm for the *m*-MesH positions, and a pair of singlets (δ 2.19 ppm and 1.99 ppm) in a 1:2 ratio for the methyl groups. Like **13**, ^{1}H NMR spectroscopic data collected in pyridine-d_5 revealed a single broad Cp-*H* resonance at 4.99 ppm and additional pseudo-

triplets for an AA'BB' spin system between 5.86–5.74 ppm ($^5J_{HH}$ = 2.9 Hz, $^5J_{HH}$ = 2.6 Hz) with a relative integration ratio of 0.7:1, corresponding to *ca*. 40% monomer.

2.3.3 Exploring the Reactivity of the K(Ter^{Mes}Cp) Tetramer

2.3.3.1 Reactions with Transition Metals

As stated earlier, **12** was determined to be the best reagent for further reactions due to its solubility properties, its highly reliable synthesis with KH, and its behavior as reliable monomeric K(Ter^{Mes}Cp) source. Once the synthesis of **12** had been optimised, the next step was to explore the coordination chemistry of this new ligand. Several different transition metals and main group elements were explored with varying degrees of success and completion. This section will summarise these results.

Metallocenes are generally described as molecules possessing a metal centre with two η^5-coordinated cyclopentadienyl ligands and were the first cyclopentadienyl complexes discovered (e.g. ferrocene). These complexes were chosen as initial targets due to their ease of synthesis and vast abundance of relevant examples for comparison. Since only one example of an *m*-terphenyl Cp complex has been synthesised in the literature, very little is known about the steric or electronic properties that these molecules impart on their respective coordination complexes. Therefore it seemed pertinent to synthesise some metallocene derivatives incorporating the Ter^{Mes}Cp ligand to establish some of these properties.

The metallocenes **15**–**17** were synthesised from a salt metathesis reaction by combining **12** with the appropriate metal halide source in a 2:1 mole ratio at room

temperature (Scheme 2.12). Attempts at isolating the monosubstitution products from this reaction using a 1:1 mole ratio were unsuccessful.

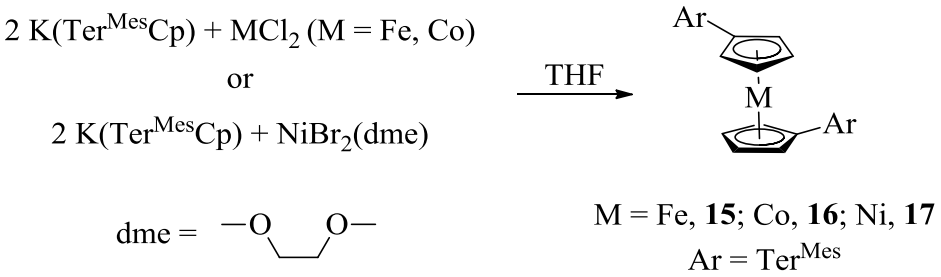

Scheme 2.12. Synthesis of metallocene complexes containing the $Ter^{Mes}Cp$ anion.

The crude yields for **15**–**17** are high (*ca.* 90%) however these were not found to be analytically pure. Attempts at purifying these molecules have been challenging as they exhibit high solubility in most organic solvents making recrystallisation difficult. After recrystallisation from pentane, the yields diminish rapidly for **15** (28%), **16** (8%), and **17** (8%). The melting points have increased significantly for **15**–**17** (252.2–253.0 °C, 250.4–251.6 °C, and 265.3–266.8 °C for **15**, **16** and **17** respectively) in comparison to the parent metallocenes,[3,92] which may prevent these compounds from subliming as well. One possibility is to purify **15–17** by column chromatography, but no attempts have been made so far at finding a suitable solvent system using thin-layer chromatography due to time restraints. Structural information for these compounds has been collected using X-ray crystallography and it was found that **15** (Figure 2.27) and **16** (Figure 2.28) display similar characteristics while **17** (Figure 2.29) is markedly different.

Most notably, the central aryl ring of the Ter^{Mes} groups are significantly twisted away by 61.44(10)° from the central Cp ring in **17**, while the largest analogous angles for **15** and **16** are only 19.35(13)° and 17.89(9)° respectively. This difference may be caused by a

combination of dispersion and/or crystal packing forces coupled. Another factor that may be responsible is the longer C-M bond lengths for **17** in comparison to **15** and **16**. The overall trend observed for C-M bond lengths was **15**<**16**<**17**, which is expected since the ferrocene analogue **15** possesses an ideal 18-electron configuration, while **16** and **17** possess additional electrons in an anti-bonding e_{1g}* molecular orbital (Figure 2.26), resulting in lower C-M bond orders for these complexes.

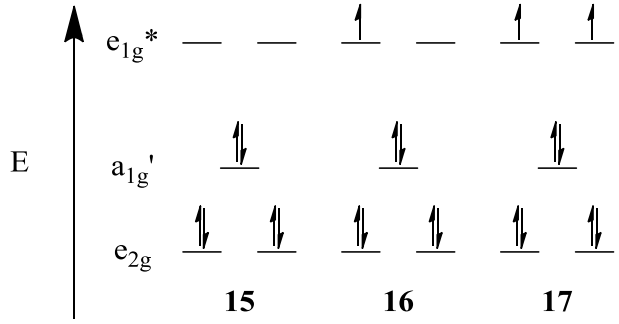

Figure 2.26. Frontier molecular orbitals with the greatest *d*-character for $(\eta^5\text{-Cp})_2$M complexes, assuming a D_{5d} (staggered) geometry. Labels on the molecular orbitals are as follows: e_{2g} (d_{xz}, d_{yz}), a_{1g}' (d_{z^2}), e_{1g}* ($d_{x^2-y^2}$, d_{xy}).

Two crystallographically independent molecules were present in the asymmetric unit of **16** with two orientations for the Ter^{Mes} groups; one molecule has been shown (Figure 2.28) while the other orientation is similar to what is found for **15** (Figure 2.27). This is most likely influenced by packing forces[93] in the crystal lattice; the rotation barrier for the parent ferrocene is quite low (*ca* 4 kJ mol^{-1})[94] in the solid state.

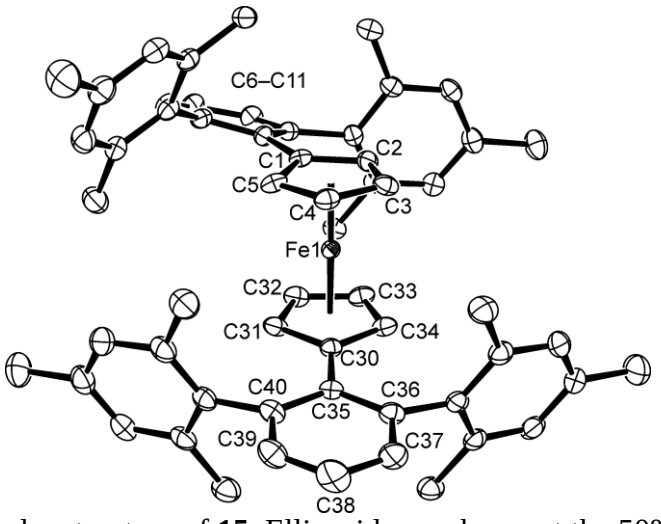

Figure 2.27. Molecular structure of **15**. Ellipsoids are shown at the 50% probability level. Only one molecule of the asymmetric unit is shown. Hydrogen atoms have been omitted for clarity. Selected bond lengths (Å) and angles (°): Fe1-C1 2.068(3), Fe1-C2 2.035(3), Fe1-C3 2.047(3), Fe1-C4 2.039(3), Fe1-C5 2.024(3), Fe1-Cp_c (C1–C5) 1.6434(17), Fe1-C30 2.098(3), Fe1-C31 2.047(3), Fe1-C32 2.030(3), Fe1-C33 2.021(3), Fe1-C34 2.043(3), Fe1-Cp_c (C30–C34) 1.6491(17), Cp (C1–C5)-Ar (C6–C11) 19.35(13), Cp (C30–C34)-Ar (C35–C40) 4.90(13).

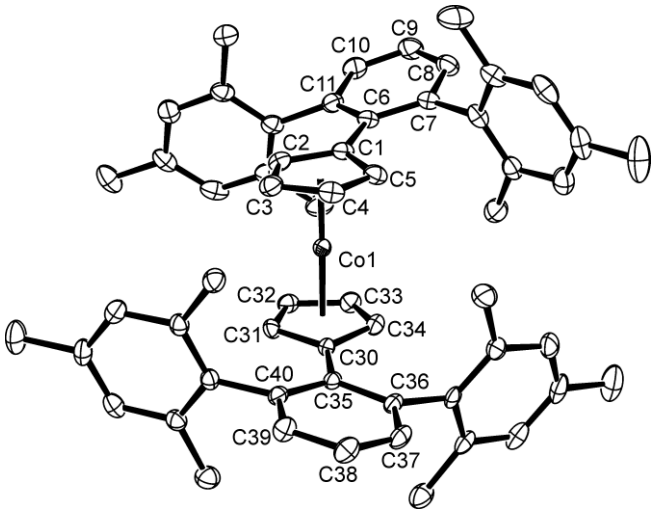

Figure 2.28. Molecular structure of **16**. Ellipsoids are shown at the 50% probability level. Only one molecule of the asymmetric unit is shown. Hydrogen atoms and pentane solvate

have been omitted for clarity. Selected bond lengths (Å) and angles (°): Co1-C1 2.210(2), Co1-C2 2.093(2), Co1-C3 2.065(2), Co1-C4 2.086(2), Co1-C5 2.078(2), Co1-Cp_c (C1–C5) 1.7237(11), Co1-C30 2.209(2), Co1-C31 2.102(2), Co1-C32 2.069(2), Co1-C33 2.089(2), Co1-C34 2.078(2), Co1-Cp_c (C30–C34) 1.7263(12), Cp (C1–C5)-Ar (C6–C11) 7.78(9), Cp (C30–C34)-Ar (C35–C40) 17.89(9).

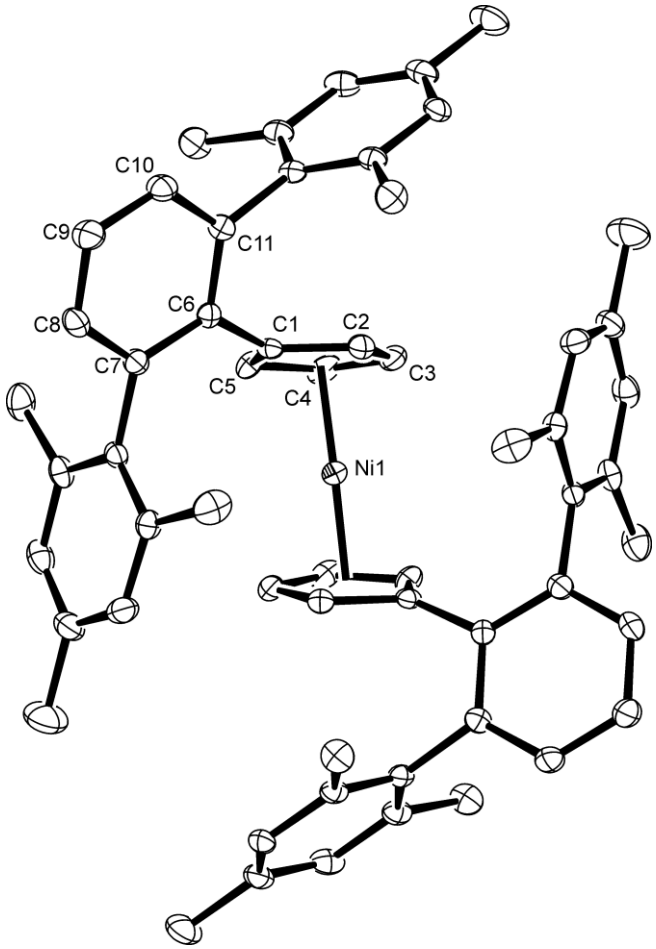

Figure 2.29. Molecular structure of **17**. Ellipsoids are shown at the 50% probability level. Hydrogen atoms have been omitted for clarity. Selected bond lengths (Å) and angles (°): Ni1-C1 2.340(3), Ni1-C2 2.197(3), Ni1-C3 2.104(2), Ni1-C4 2.138(3), Ni1-C5 2.264(3), Ni1-Cp_c (C1–C5) 1.8527(12), Cp (C1–C5)-Ar (C6–C11) 61.44(10).

The ^{1}H NMR spectrum of **15** in C_6D_6 suggests a staggered C_s orientation with a mirror plane bisecting the Cp rings, evident by two pseudo-triplet resonances at 3.90 ppm ($^{5}J_{HH}$ = 2.1 Hz) and 3.78 ppm ($^{5}J_{HH}$ = 2.1 Hz) with an AA'BB' pattern for the Cp-*H* environments. The remaining Ter^{Mes} resonances were identified by their characteristic features: a triplet-doublet pair was observed for the central aromatic ring (δ 7.02 ppm, $^{3}J_{HH}$ = 7.5 Hz, and 6.81 ppm $^{3}J_{HH}$ = 7.5 Hz respectively) with a 1:2 integration ratio, a broad singlet was clearly visible at 6.88 ppm for the *m*-MesH positions, and lastly a pair of singlets (δ 2.19 ppm and 1.99 ppm) were present in a 1:2 ratio for the methyl groups. This ratio is different from what would be expected for the molecular structure obtained for **15** but is likely due to a low rotational barrier about the Cp-Fe axis. No cyclic voltammetry has been performed for the metallocenes **15**–**17** as of yet due to difficulties in obtaining significant quantities of pure material due to solubility issues and time restraints.

Another area of fundamental interest is cyclopentadienyl complexes of Group IV metals (Ti, Zr, Hf). These complexes (e.g. Cp_2ZrCl_2) have already demonstrated practical applications in catalytic processes; most importantly they are used as precursors to catalysts that efficiently mediate the polymerisation of α-olefins,[5-10] allowing the mass production of useful materials such as polypropylene. The reaction between $ZrCl_4(THF)_2$ and one equivalent of **12** produced presumably the Zr piano-stool complex **18a** in 51% isolated yield (Scheme 2.13).

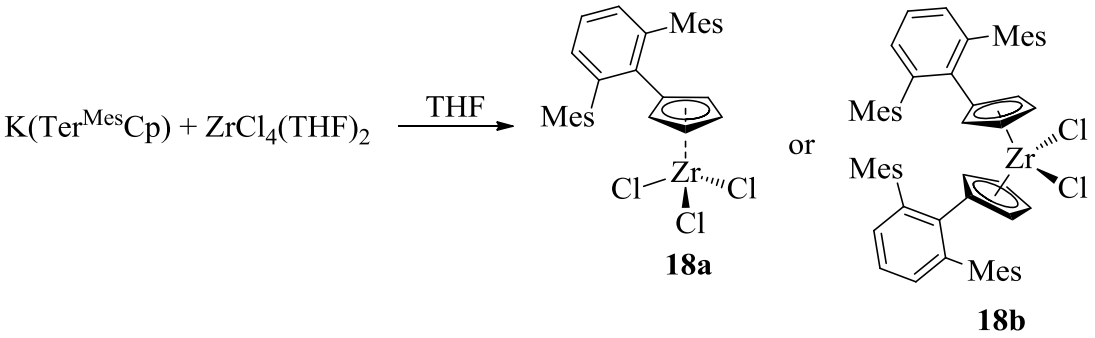

Scheme 2.13. Synthesis of a zirconium complex with the $Ter^{Mes}Cp$ anion.

In C_6D_6 characteristic pseudo-triplets with an AA'BB' pattern were observed in the ^1H NMR spectrum for the Cp-*H* at 6.12 ppm and at 5.61 ppm ($^3J_{HH}$ = 2.9 Hz). This supports a piano-stool complex similar to what is found for $Ter^{Ph}CpZr(NEt_2)_3$,[25] but admittedly the NMR spectroscopic properties for **18a** would likely be similar to the disubstituted product $(Ter^{Mes}Cp)_2ZrCl_2$ and therefore this cannot be ruled out as a possible product. Elemental analysis data certainly supports the notion that **18b** was produced inadvertently instead based on the calculated values for **18a** (C: 60.56 %, H: 5.08 %) and **18b** (C: 75.95 %, H: 6.37 %), and what was obtained experimentally (C: 74.55 %, H: 5.87 %). Unfortunately attempts at resolving the two products by their number of IR active Zr-Cl stretches (3 for **18a**, 2 for **18b**) was unsuccessful due to the position of the Zr-Cl (ν 350–150 cm^{-1})[95] vibrational bands falling outside of the lower end of the working range for KBr pellets (*ca.* 400 cm^{-1}). Currently it is anticipated that the product is the monosubstituted piano-stool complex due to the stoichiometry of the reagents used and the steric demands of the $Ter^{Mes}Cp$ ligand, however a lack of further reactivity when a second equivalent of **12** is added would suggest **18b**. Attempts at determining the product using HRMS were also unsuccessful, and so X-ray diffraction data is required to elucidate the structure. Additionally, preliminary reactivity studies demonstrated that the product of this reaction

reacts further with sodium cyclopentadienide, based on the observance of four new quartets (δ 5.88 ppm, J = 3.4 Hz, J = 2.5 Hz, 5.78 ppm, J = 3.4 Hz, J = 2.5 Hz, 5.36 ppm, J = 3.1 Hz, J = 2.7 Hz, and 5.10 ppm, J = 3.1 Hz, J = 2.7 Hz) appearing in a 1:1:1:1 ratio, but the identity of the product could not be determined. Future work will be focused on studying the reactivity of zirconium complexes incorporating the $Ter^{Mes}Cp$ ligand and determining the structure of the complex using X-ray crystallography. The analogous reaction with **12** and $TiCl_4(THF)_2$ was unsuccessful presumably due to the reducing properties of the cyclopentadienyl ligand[96], this phenomenon is quite common between alkali metal salts of Cp* and transition metal reagents in high oxidation states that are prone to reduction.

2.3.3.2 Reactions with Main Group Elements

The reactivity of **12** as well as the mixture **9a**+**b** was also explored with some typical main group element transfer reagents. Attempts at synthesising magnesium complexes from both MgI_2 and **12** *via* salt metathesis or with **9a**+**b** and $MgBu_2$ by deprotonation were unsuccessful. Gradual conversion of **12** to **9a**+**b** was observed over one hour when combined with MgI_2 while no reaction occurred at all between **9a**+**b** and $MgBu_2$ (Scheme 2.14). The reaction with MgI_2 may have been inhibited by the low solubility of MgI_2 in THF, however it still remains unclear why $MgBu_2$ failed to react with **9a**+**b**.

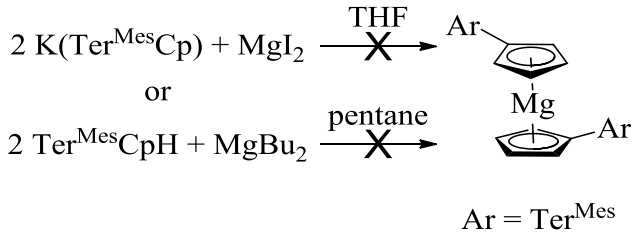

Scheme 2.14. Unsuccessful attempts at synthesising magnesium complexes.

Moving on to the *p*-block elements, the reactivity of **12** was tested with $BiCl_3$. Cyclopentadienyl complexes incorporating bismuth are quite rare and remain relatively underexplored in organometallic chemistry, so it seemed pertinent to investigate these molecules and develop this area further. The corresponding bismuth(III) compound **19** was isolated in 46% yield *via* a salt metathesis (Scheme 2.15), however only preliminary results are available for discussion.

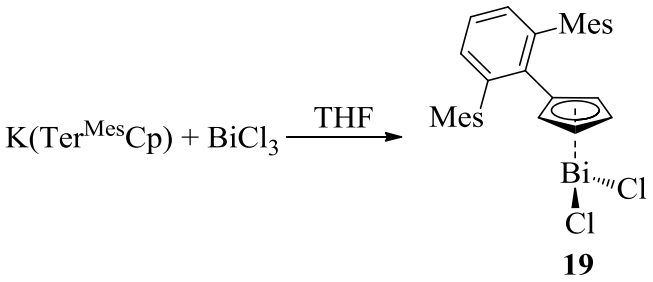

19

Scheme 2.15. Synthesis of a bismuth(III) cyclopentadienyl compound.

Compound **19** was characterised by X-ray crystallography and ^{1}H NMR spectroscopy. In C_6D_6 four unique Cp-*H* resonances are visible in the ^{1}H NMR spectrum (δ 6.55 ppm, J_{HH} = 2.5 Hz, 6.22 ppm, J_{HH} = 2.4 Hz, 5.10 ppm, J_{HH} = 2.5 Hz, and 4.23 ppm, J_{HH} = 2.4 Hz), but unfortunately most the remaining resonances could not be unambiguously assigned based on only ^{1}H NMR spectroscopic data. Perhaps the orientation of the bismuth centre results in a desymmeterisation of the molecule and causes a complex ^{1}H NMR spectrum to be observed; the integration values are consistent with the structure of **19**. The molecular structure of **19** features a trigonal pyramidal bismuth centre bound to two chlorides and an η^3-coordinated cyclopentadienyl ring (Figure 2.30). Short intermolecular contacts between Bi1-Cl2' (3.2984(13) Å) and Cl2-Cl2' (3.473(3) Å) were observed in the crystal of **19**. The Cp-Bi bond lengths were found to be 2.743(5) Å,

2.324(5) Å, 2.782(5) Å between C2, C3, and C4 respectively and are within the expected range[97] for cyclopentadienyl bismuth compounds. The Cl1-Bi1-Cl2 (92.57(5)°), C3-Bi1-Cl1 (93.99(14)°), and C3-Bi1-Cl2 (89.74(13)°) bond angles are close to 90° and indicate that minimal mixing is occurring between the p_x, p_y, and p_z orbitals. The lone pair of electrons on bismuth likely occupy a low lying 6s orbital,[98] and may not be accessible due to the inert pair effect; therefore a priority will be investigating the reactivity of this molecule with Lewis acids.

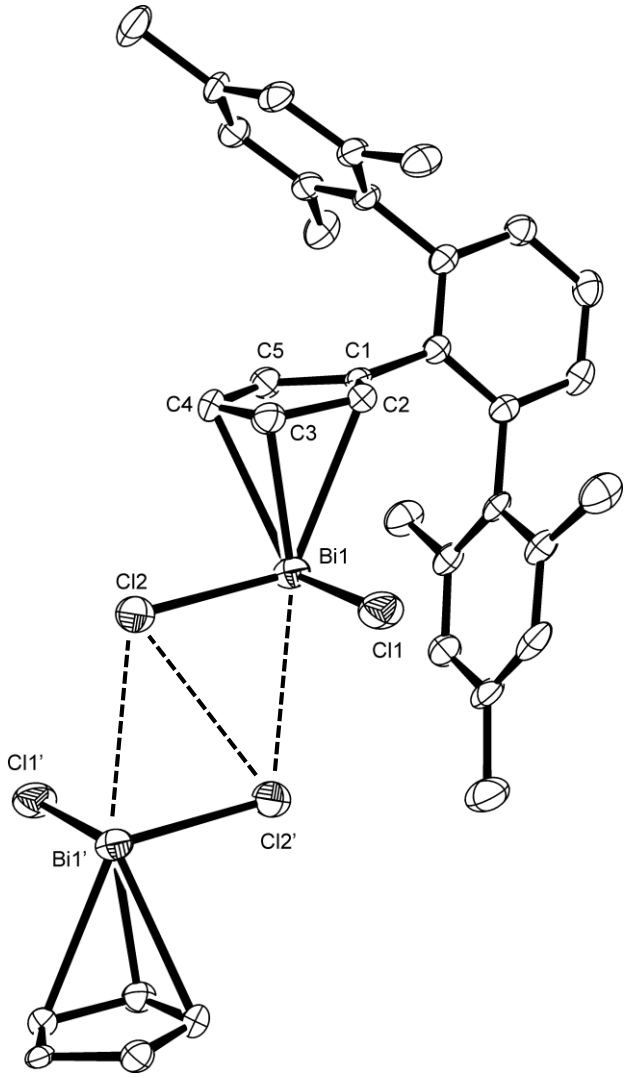

Figure 2.30. Molecular structure of **19**. Ellipsoids are shown at the 50% probability level. Hydrogen atoms have been omitted for clarity. A portion of a neighbouring molecule (related by the symmetry operator [–*x*, –*y*+1, –*z*]) is shown with the short contacts denoted by dashed lines. Selected bond lengths and short contacts (Å) and angles (°): Bi1-Cl2' 3.2984(13), Cl2-Cl2' 3.473(3), Bi1-Cl1 2.4839(15), Bi1-Cl2 2.5387(14), Bi1-C2 2.743(5), Bi1-C3 2.324(5), Bi1-C4 2.782(5), Cl1-Bi1-Cl2 92.57(5), C3-Bi1-Cl1 93.99(14), C3-Bi1-Cl2 89.74(13).

Other preliminary reactions involving main group elements included exploring the reactivity of **12** with AlI_3, PCl_3, and $SiMe_3Cl$ (Scheme 2.16). These compounds were chosen because the former two allowed for the collection of ^{27}Al and ^{31}P NMR spectroscopic data respectively, which are simpler to interpret than their corresponding ^{1}H NMR spectra and are of fundamental interest, while the latter was chosen because trimethylsilylated cyclopentadienyl ligands are important precursors to transition metal complexes; particularly for those of the Group IV metals.[96]

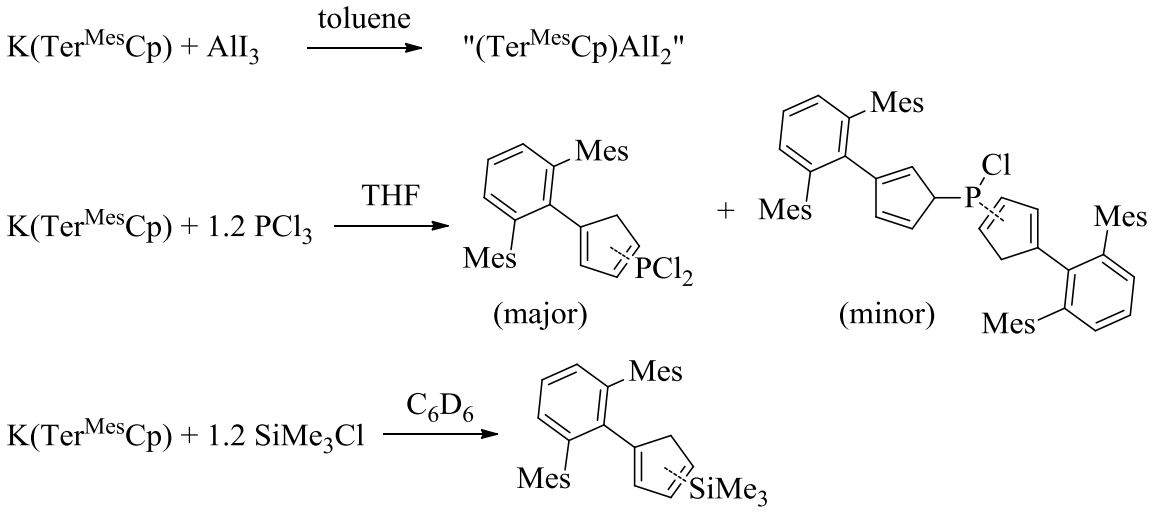

Scheme 2.16. Explored reactivity of **12** with elements of the main group. Hashed bonds indicate multiple substitutional isomers.

Reaction between **12** and one equivalent of AlI_3 produced an intensely violet coloured reaction mixture with a lavender hue. When the ^{1}H NMR spectrum was collected in C_6D_6 two new Cp-*H* resonances appeared at 5.50 ppm and 4.52 ppm as a broad singlet and doublet (J = 6.0 Hz) respectively, while the remaining signals were too complex for interpretation. Two signals were visible in the ^{27}Al NMR spectrum; one signal at 82.4 ppm corresponded to the starting material AlI_3[99] while a new signal appeared at -36.5 ppm. A

value for Cp^*AlI_2 could not be found for comparison, however this value is very close to what has been reported for the dimer $[Cp^*AlI]_2$ (δ -41.75 ppm).[100] The nature of this product has not been determined as of yet and is only given as "$(Ter^{Mes}Cp)AlI_2$". A preliminary yield on this reaction based on the $(Ter^{Mes}Cp)AlI_2$ product is 60%.

Reaction between **12** and a slight excess of PCl_3 produced a yellow coloured reaction mixture. In the ^1H NMR spectrum, complex multiplet patterns were observed at 6.29 ppm, 5.78 ppm, and 5.73 ppm, while what appeared to be a doublet was visible at 3.77 ppm (J = 8.5 Hz) all with a 2:1:1 integration ratio. Five signals with two distinct regions were visible in the ^{31}P NMR spectrum: two signals at 153.2 ppm and 150.8 ppm in a 0.13:1 ratio likely corresponded to substitutional isomers of $(Ter^{Mes}Cp)PCl_2$ (e.g. 1,2- or 1,3-substituted cyclopentadienes) while, three additional signals were present at 72.9 ppm (0.09), 72.6 ppm (0.13), and 71.2 ppm (0.16), likely substitutional isomers of the disubstituted product. A combined yield for both products based on starting material was found to be 57%.

An NMR scale test reaction between **12** and a slight excess of $SiMe_3Cl$ also produced a yellow coloured reaction mixture. In the ^1H NMR spectrum, five new broadened peaks were observed at 6.55 ppm, 6.24 ppm, 5.99 ppm, 5.91 ppm, and 5.58 ppm in a 2:3:3:3:2 relative integration ratio, while two additional singlets appeared at 0.17 ppm and -0.35 ppm in a 1:1 relative integration ratio, which do not correspond to chlorotrimethylsilane (δ *ca.* 0.5 ppm).[101] These results were promising because it demonstrated that **12** can react with $SiMe_3Cl$ and should allow a broader range of transition metal compounds to be targeted.

2.3.4 Towards Other *m*-Terphenyl Derivatives

The final question that remained was the general utility of this synthetic approach. From failed attempts at replicating the Pd-catalysed cross-coupling reported in the literature[25], it became clear that synthetic routes to *m*-terphenyl substituted cyclopentadienes are highly sensitive to steric factors when using such a bulky substitutent. Therefore the even bulkier Ter^{Dipp} analogue (Ter^{Dipp} = C_6H_2-2,6-$Dipp_2$, Dipp = C_6H_2-2, 6-iPr_2) was targeted using $Ter^{Dipp}Li$ and $[Cp_2Co][PF_6]$ (Scheme 2.17).

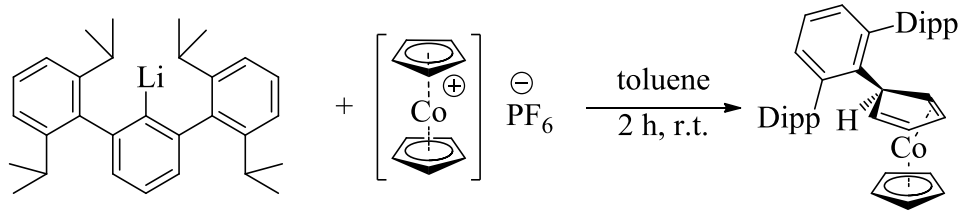

20

Scheme 2.17. Reactivity of $Ter^{Dipp}Li$ with cobaltocenium hexfafluorophosphate.

This reaction successfully produced the desired cobalt(I) complex **20** with a 49% yield following crystallisation from pentane, the crystals of which were suitible for X-ray diffraction studies. The overall yield increased by 26% after removing the solvent from the pentane filtrate resulting in a total isolated yield of 75%. The production of $Ter^{Dipp}H$ was also observed during this reaction (*ca*. 20%), which is the major factor that reduces the overall yield of this reaction. The ^{1}H NMR spectroscopic properties of **20** are similar to that of **8** in C_6D_6. A methylene resonance at 2.50 ppm was confirmed to be part of the cyclopentadiene ring by examination of correlations between resonances at 4.42 ppm and 4.61 ppm in the ^{1}H-^{1}H COSY NMR spectrum. A resonance for the η^5-cyclopentadienyl is clearly visible as a singlet at 4.36 ppm. The isopropyl resonances of the Ter^{Dipp} fragment are clearly defined by a pair of doublets at 1.36 ppm ($^3J_{HH}$ = 7.0 Hz) and 1.03 ppm

($^3J_{HH}$ = 6.8 Hz) that are present in a 1:1 ratio, and a septet at 2.70 ppm ($^3J_{HH}$ = 6.8 Hz). Most of the aromatic resonances are also well-defined, the Dipp groups are visible as a triplet-doublet pair at 7.36 ppm ($^3J_{HH}$ = 7.6 Hz) and 7.22 ppm ($^3J_{HH}$ = 7.6 Hz) respectively in a 1:2 ratio, while the remaining resonances for the central aromatic ring coalesce into a complex multiplet pattern between 7.00–6.92 ppm.

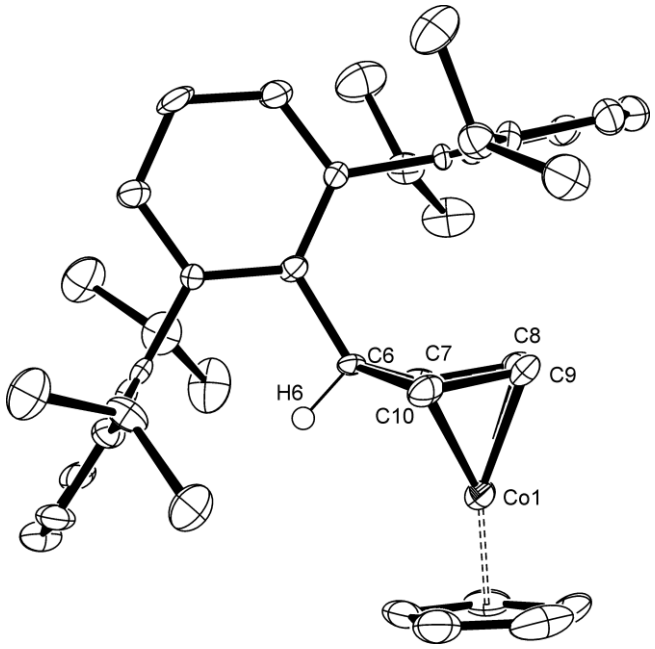

Figure 2.31. Molecular structure of **20**. Ellipsoids are shown at the 50% probability level. Hydrogen atoms and one component of disorder at the cobalt centre have been omitted for clarity. The disorder has not been completely modelled therefore bond lengths and angles are unreliable.

The molecular structure of **20** will not be discussed in great detail due to a significant amount of unresolved disorder in the molecule. The structure does show connectivity and is consistent with the NMR spectroscopic data, and it becomes immediately clear that the Ter^{Dipp} analogue exhibits significantly different steric properties. Preliminary reaction

studies have also shown that **20** can be oxidatively decomposed yielding the corresponding diene $Ter^{Dipp}CpH$ (**21**) as well, and is evident by new multiplet Cp-*H* resonances (δ 6.01, 5.92 and 2.62 ppm) in a 2:1:2 ratio, and by preliminary X-ray diffraction studies (Figure 2.32). The data is of insufficient quality to discuss bond lengths in detail; however it does provide information on connectivity and provides additional evidence that this route can be extended to bulkier *m*-terphenyls. Different solubility properties of the Ter^{Dipp} fragment complicated the column chromatography step but efforts are presently underway to optimise this reaction and obtain better structural information.

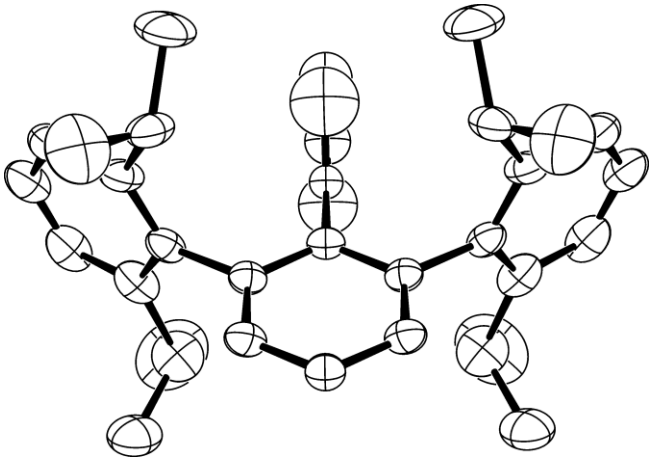

Figure 2.32. Molecular structure of **21** showing connectivity only. Ellipsoids are shown at the 50% probability level. Hydrogen atoms been omitted for clarity. The disorder has not been completely modelled therefore bond lengths and angles are unreliable.

2.3.5 Summary of Crystal Tables

Table 2.1. Summary of crystallographic data for compounds 8−12.

Compound reference	8	9	9'	10	11’	12
Chemical formula	$C_{34}H_{35}Co$	$C_{29}H_{30}$	$C_{29}H_{30}$	$C_{116}H_{116}Li_4$	$C_{21}H_{25}NaO$	$C_{116}H_{116}K_4$
Formula Mass	502.55	378.53	378.53	1537.84	316.40	1666.48
Crystal system	Monoclinic	Orthorhombic	Monoclinic	Monoclinic	Triclinic	Monoclinic
a/Å	11.3211(6)	33.276(4)	16.706(2)	17.9551(17)	9.2095(11)	22.732(2)
b/Å	13.8783(7)	8.4963(9)	9.3800(13)	13.7241(13)	9.7986(12)	17.8679(12)
c/Å	17.3882(9)	15.9855(17)	15.616(2)	36.353(4)	20.732(3)	25.5510(14)
α/°	90	90	90	90	95.129(2)	90
β/°	108.0690(10)	90	113.886(2)	94.531(4)	98.483(2)	113.133(5)
γ/°	90	90	90	90	103.703(2)	90
Unit cell volume/Å^3	2597.3(2)	4519.4(8)	2237.5(5)	8930.0(15)	1782.6(4)	9543.7(12)
Temperature/K	125(2)	125(2)	125(2)	125(2)	293(2)	125(2)
Space group	*P*21/*n*	*Pbcn*	*P*2/*c*	*I*2/*a*	$P\bar{1}$	*I*2/*a*
No. of formula units per unit cell, *Z*	4	8	4	4	4	4
No. of reflections measured	21154	32954	17958	36496	11824	39266
No. of independent reflections	6267	4888	5309	10527	6141	11560
R_{int}	0.0344	0.0550	0.0531	0.0518	0.0538	0.0430
Final R_1 values ($I > 2\sigma(I)$)	0.0382	0.0863	0.0579	0.0563	0.0753	0.0451
Final $wR(F^2)$ values ($I > 2\sigma(I)$)	0.0910	0.2006	0.1257	0.1178	0.2276	0.1001
Final R_1 values (all data)	0.0538	0.1091	0.1158	0.1135	0.0963	0.0767
Final $wR(F^2)$ values (all data)	0.0981	0.2131	0.1537	0.1432	0.2410	0.1127

Table 2.2. Summary of crystallographic data for compounds 12'−19.

Compound reference	12'	14	15	16	17	19
Chemical formula	$C_{19.08}H_{27.29}KN_{0.50}Si$	$C_{22.75}H_{23.75}Cs_{0.75}O_{0.25}$	$C_{58}H_{58}Fe$	$C_{121}H_{128}Co_2$	$C_{58}H_{58}Ni$	$C_{29}H_{29}BiCl_2$
Formula Mass	330.85	400.85	810.89	1700.09	813.75	657.40
Crystal system	Monoclinic	Triclinic	Monoclinic	Triclinic	Tetragonal	Monoclinic
a/Å	15.1601(11)	16.903(2)	23.2478(13)	13.1712(7)	13.9919(7)	8.8386(5)
b/Å	8.8159(6)	17.111(2)	10.0865(6)	19.0291(10)	13.9919(7)	12.1051(7)
c/Å	29.811(2)	19.298(3)	40.059(2)	20.3053(11)	45.126(2)	23.8287(14)
α/°	90	101.929(2)	90	73.0420(10)	90	90
β/°	93.2320(10)	111.436(2)	106.0080(10)	75.8870(10)	90	94.9870(10)
γ/°	90	100.858(2)	90	84.2750(10)	90	90
Unit cell volume/Å^3	3977.9(5)	4865.2(12)	9029.2(9)	4718.8(4)	8834.5(10)	2539.8(3)
Temperature/K	125(2)	125(2)	125(2)	125(2)	125(2)	125(2)
Space group	*P*21/*c*	$P\bar{1}$	*P*2/*c*	$P\bar{1}$	$I\bar{4}\,2d$	*P*21/*c*
No. of formula units per unit cell, *Z*	8	8	8	2	8	4
No. of reflections measured	31807	60097	72877	40494	37025	20535
No. of independent reflections	9489	23614	21914	22353	5753	6212
R_{int}	0.0451	0.0748	0.0547	0.0454	0.0669	0.0490
Final R_1 values ($I > 2\sigma(I)$)	0.0492	0.0553	0.0652	0.0545	0.0376	0.0380
Final $wR(F^2)$ values ($I > 2\sigma(I)$)	0.1095	0.1294	0.1319	0.1194	0.0881	0.0833
Final R_1 values (all data)	0.0860	0.0936	0.1066	0.0955	0.0499	0.0591
Final $wR(F^2)$ values (all data)	0.1240	0.1444	0.1458	0.1392	0.0932	0.0905

Note: Crystal data for **20** and **21** have not been included since the data was of poor quality and/or incompletely refined.

2.4 Conclusions

Nucleophilic substitution reactions to cobaltocenium salts by the organolithium reagent $Ter^{Mes}Li$ leads to the formation of the Co(I) intermediate **8**, which when reacted with $FeCl_3$ liberates the cyclopentadienyl precursors **9a+b**. The corresponding lithium (**10**), sodium (**11**), potassium (**12**), rubidium (**13**), and caesium (**14**) salts were prepared using routine synthetic approaches and were characterized using X-ray crystallography (**10**, **12**, **14**) and by multinuclear NMR and UV-Vis spectroscopies. It was also determined that **12** was the most suitible reagent for further coordination chemistry. Based on the molecular structures of **10**, **12**, **14** it was established that the $Ter^{Mes}Cp$ anion is capable of bonding through both Cp and aryl interactions.

The ferrocene (**15**), cobaltocene (**16**), and nickelocene (**17**) $Ter^{Mes}Cp$ substituted analogues were accessible by salt metathesis reactions between **12** and their corresponding metal halides and exhibit properties similar to their parent complexes. Similarly a zirconium(IV) complex was also accessible *via* salt metathesis between **12** and $ZrCl_4(THF)_2$. However, the identity of this product could not be definitively determined as both **18a** and **18b** are theoretically possible. Regardless of which product was isolated, it was found that this new Zr(IV) species exhibited reactivity with sodium cyclopentadienide. The nature of this product has yet to be determined, but may be useful as a future catalyst precursor for olefin polymerisation reactions. Reactivity was also explored with main group elements, and the bismuth(III) species **19** was prepared *via* salt metathesis with $BiCl_3$ and **12**. Structural information for this molecule revealed an η^3-cyclopendadienyl ligand bound to the Bi(III) centre with close Bi-Cl and Cl-Cl contacts between a neighbouring molecule. Additional evidence for the nature of **19** was provided by ^1H NMR spectroscopy,

but additional spectroscopic data is still required for a complete characterisation. Further reactivity studies with AlI_3, PCl_3, and $SiMe_3Cl$ show promising preliminary results but the nature of the products isolated still need to be determined.

Lastly, but arguably the most important result is that this synthetic route was successfully applied to produce the Co(I) intermediate **20**, which features an even bulkier Ter^{Dipp} substituent. This result is significant because it exemplifies the versatility of this method with respect to tolerating a variety of steric demands, and demonstrates that the steric (and in theory electronic) properties can be tailored to suit almost any situation with only a few common reagents. Further work is still required to oxidatively decompose **20** on a large scale and fully characterise the parent diene, however preliminary results show promise.

2.5 Future Work

Overall this project is very open-ended, and will likely serve as the foundation for future developments given the scant literature examples. Obviously there is a lot of potential to further develop organometallic complexes of both main group and transition metal elements that incorporate the $Ter^{Mes}Cp$ anion, and there is also the potential to develop new cyclopentadienyl ligands incorporating bulkier, or electronically different *m*-terphenyl substituents. This possibility was lightly touched upon during this work but can certainly be expanded upon. An immediate priority is to complete all of the outstanding characterisation data for **15**–**19** (covered during the Results and Discussion section) and resolve the disorder encountered during the structure refinement of **20**.

Another area that needs to be investigated immediately is the synthesis of additional cyclopentadienyl transfer agents, specifically the bromine and trimethylsilyl derivatives. These milder reagents are important because they possess a lower reduction potential than their respective alkali metal salts and may allow reactivity with electrochemically sensitive metal complexes. The trimethylsilyl derivative was investigated briefly during this project but it was not made on a synthetically useful scale, therefore this reaction will be repeated and optimised on a larger scale and its reactivity will be investigated with $TiCl_4(THF)_2$. In a similar manner the bromine derivative is a milder reagent, and should be accessible from the reaction of **9a**+**9b** with *N*-bromosuccinimide (Scheme 2.18). The reactivity of Ter^{Mes}-CpBr will then be investigated with late transition metals (e.g. Cu, Ag, Au, Pt, Pd) that favour low (0-2) oxidation states.

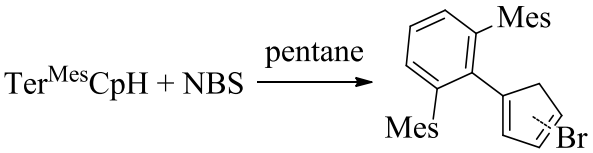

Scheme 2.18. Bromination of $Ter^{Mes}CpH$ with *N*-bromosuccinimide (NBS) to afford $Ter^{Mes}CpBr$ derivatives. Hashed bonds indicate multiple substitutional isomers.

Another aspect that needs to be considered for the future is the electrochemical properties of the Co(I) intermediates **8** and **20**. Cyclic voltammetry could be used to determine an alternative oxidising agent to the $FeCl_3$ such as aqueous hydrogen peroxide. Hydrogen peroxide is one of the cleanest oxidising agents available, and would ultimately reduce the environmental impact of this chemistry. This change may also improve the synthetic route by removing the column chromatography step; the oxidised cobalt by-products would likely be water soluble and easily separated from the desired

cyclopentadiene. Most importantly this change would eventually allow the reaction to be done on a larger scale thereby increasing the synthetic utility of this process.

2.6 References

1. Streitwieser, A.; Langworthy, W. C.; Brauman, J. I. *J. Am. Chem. Soc.* **1963**, *85*, 1761-1763.

2. Breton, G. W. *Chem. Educator* **1997**, *2*, 1-8.

3. Kealy, T. J.; Pauson, P. L. *Nature* **1951**, *168*, 1039-1040.

4. Wilkinson, G.; Rosenblum, M.; Whiting, M. C.; Woodward, R. B. *J. Am. Chem. Soc.* **1952**, *74*, 2125-2126.

5. Gomes, P. T.; Green, M. L. H.; Martins, A. M. *J. Organomet. Chem.* **1998**, *551*, 133-138.

6. Gomes, P. T.; Green, M. L. H.; Martins, A. M.; Mountford, P. *J. Organomet. Chem.* **1997**, *541*, 121-125.

7. Herrmann, W. A.; Morawietz, M. J. A. *J. Organomet. Chem.* **1994**, *482*, 169-181.

8. Shapiro, P. J.; Schaefer, W. P.; Labinger, J. A.; Bercaw, J. E.; Cotter, W. D. *J. Am. Chem. Soc.* **1994**, *116*, 4623-4640.

9. Shapiro, P. J.; Bunel, E.; Schaefer, W. P.; Bercaw, J. E. *Organometallics* **1990**, *9*, 867-869.

10. Kaminsky, W.; Arndt, M. Metallocenes for polymer catalysis. In Springer Berlin Heidelberg: 1997; Vol. 127, pp 143-187.

11. Kaminsky, W. *J. Chem. Soc., Dalton Trans.* **1998**, 1413-1418.

12. Gromada, J.; Carpentier, J.; Mortreux, A. *Coord. Chem. Rev.* **2004**, *248*, 397-410.

13. Braunschweig, H.; Breitling, F. M. *Coord. Chem. Rev.* **2006**, *250*, 2691-2720.

14. Enders, M.; Baker, R. W. *Curr. Org. Chem.* **2006**, *10*, 937-953.

15. Newton, C. G.; Kossler, D.; Cramer, N. *J. Am. Chem. Soc.* **2016**, *138*, 3935-3941.

16. Ghosh, P.; Fagan, P. J.; Marshall, W. J.; Hauptman, E.; Bullock, R. M. *Inorg. Chem.* **2009**, *48*, 6490-6500.

17. Rottink, M. K.; Angelici, R. J. *J. Am. Chem. Soc.* **1993**, *115*, 7267-7274.

18. Hull, J. F.; Balcells, D.; Blakemore, J. D.; Incarvito, C. D.; Eisenstein, O.; Brudvig, G. W.; Crabtree, R. H. *J. Am. Chem. Soc.* **2009**, *131*, 8730-8731.

19. Chakraborty, U.; Modl, M.; Mühldorf, B.; Bodensteiner, M.; Demeshko, S.; van Velzen, Niels J. C.; Scheer, M.; Harder, S.; Wolf, R. *Inorg. Chem.* **2016**, *55*, 3065-3074.

20. Jutzi, P.; Schnittger, J.; Wieland, W.; Neumann, B.; Stammler, H. *J. Organomet. Chem.* **1991**, *415*, 425-434.

21. Eichhorn, C.; Scherer, O. J.; Sögding, T.; Wolmershäuser, G. *Angew. Chem. Int. Ed.* **2001**, *40*, 2859-2861.

22. Siemeling, U.; Vorfeld, U.; Neumann, B.; Stammler, H. *Organometallics* **1998**, *17*, 483-484.

23. Jaroschik, F.; Nief, F.; Le Goff, X.; Ricard, L. *Organometallics* **2007**, *26*, 1123-1125.

24. Sitzmann, H. *Coord. Chem. Rev.* **2001**, *214*, 287-327.

25. Curnow, O. J.; Fern, G. M.; Wöll, D. *Inorg. Chem. Comm.* **2003**, *6*, 1201-1204.

26. Janiak, C.; Schumann, H. *Adv. Organomet. Chem.* **1991**, *33*, 291-393.

27. Nguyen, T.; Sutton, A. D.; Brynda, M.; Fettinger, J. C.; Long, G. J.; Power, P. P. *Science* **2005**, *310*, 844-847.

28. Duttwyler, S.; Do, Q.; Linden, A.; Baldridge, K. K.; Siegel, J. S. *Angew. Chem.* **2008**, *120*, 1743-1746.

29. Olmstead, M. M.; Simons, R. S.; Power, P. P. *J. Am. Chem. Soc.* **1997**, *119*, 11705-11706.

30. Twamley, B.; Power, P. P. *Chem. Commun.* **1998**, 1979-1980.

31. Pu, L.; Twamley, B.; Power, P. P. *J. Am. Chem. Soc.* **2000**, *122*, 3524-3525.

32. Newmann, F. H. *Justus Liebigs Ann. Chem.* **1898**, *302*, 236-244.

33. Carpenter, H. *Justus Liebigs Ann. Chem.* **1898**, *302*, 223-236.

34. Ziegler, K.; Schnell, B. *Justus Liebigs Ann. Chem.* **1925**, *445*, 266-282.

35. Sitzmann, H. *J. Organomet. Chem.* **1988**, *354*, 203-214.

36. Sitzmann, H. *Z. Naturforsch. , B* **1989**, *44*, 1293-1297.

37. Quindt, V.; Saurenz, D.; Schmitt, O.; Schär, M.; Dezember, T.; Wolmershäuser, G.; Sitzmann, H. *J. Organomet. Chem.* **1999**, *579*, 376-384.

38. Leavitt, F.; Manuel, T.; Johnson, F.; Matternas, L.; Lehman, D. *J. Am. Chem. Soc.* **1960**, *82*, 5099-5102.

39. Smith, L. I.; Hoehn, H. H. *J. Am. Chem. Soc.* **1941**, *63*, 1184-1187.

40. Mehr, L.; Becker, E. I.; Spoerri, P. E. *J. Am. Chem. Soc.* **1955**, *77*, 984-989.

41. Jutzi, P.; Sauer, R. *J. Organomet. Chem.* **1973**, *50*, C29-C30.

42. Deck, P. A.; Jackson, W. F.; Fronczek, F. R. *Organometallics* **1996**, *15*, 5287-5291.

43. Thornberry, M. P.; Slebodnick, C.; Deck, P. A.; Fronczek, F. R. *Organometallics* **2000**, *19*, 5352-5369.

44. Thornberry, M. P.; Slebodnick, C.; Deck, P. A.; Fronczek, F. R. *Organometallics* **2001**, *20*, 920-926.

45. John R. Johnson, J. R.; Grummitt, O. *Org. Synth.* **1943**, *23*, 92.

46. Janiak, C.; Schumann, H.; Stader, C.; Wrackmeyer, B.; Zuckerman, J. J. *Chem. Ber.* **1988**, *121*, 1745-1751.

47. Ogliaruso, M. A.; Romanelli, M. G.; Becker, E. I. *Chem. Rev.* **1965**, *65*, 261-367.

48. Pauson, P. *J. Am. Chem. Soc.* **1954**, *76*, 2187-2191.

49. Imamoto, T.; Takiyama, N.; Nakamura, K.; Hatajima, T.; Kamiya, Y. *J. Am. Chem. Soc.* **1989**, *111*, 4392-4398.

50. Huttenloch, M. E.; Diebold, J.; Rief, U.; Brintzinger, H. H.; Gilbert, A. M.; Katz, T. J. *Organometallics* **1992**, *11*, 3600-3607.

51. Panda, T. K.; Gamer, M. T.; Roesky, P. W. *Organometallics* **2003**, *22*, 877-878.

52. Breslow, R.; Hoffman Jr, J. M. *J. Am. Chem. Soc.* **1972**, *94*, 2110-2111.

53. Breslow, R.; Canary, J. W. *J. Am. Chem. Soc.* **1991**, *113*, 3950-3951.

54. Jack, T. R.; May, C. J.; Powell, J. *J. Am. Chem. Soc.* **1977**, *99*, 4707-4716.

55. Pedersen, S. F.; Schrock, R. R.; Churchill, M. R.; Wasserman, H. J. *J. Am. Chem. Soc.* **1982**, *104*, 6808-6809.

56. Grabowski, N. A.; Hughes, R. P.; Jaynes, B. S.; Rheingold, A. L. *J. Chem. Soc., Chem. Commun.* **1986**, 1694-1695.

57. Maron, L.; Werkema, E. L.; Perrin, L.; Eisenstein, O.; Andersen, R. A. *J. Am. Chem. Soc.* **2005**, *127*, 279-292.

58. Heeres, H. J.; Renkema, J.; Booij, M.; Meetsma, A.; Teuben, J. H. *Organometallics* **1988**, *7*, 2495-2502.

59. Becke, A. D. *J. Chem. Phys.* **1993**, *98*, 5648-5652.

60. Lee, C.; Yang, W.; Parr, R. G. *Phys. Rev. B* **1988**, *37*, 785.

61. Vosko, S. H.; Wilk, L.; Nusair, M. *Can. J. Phys.* **1980**, *58*, 1200-1211.

62. Stephens, P. J.; Devlin, F. J.; Chabalowski, C. F.; Frisch, M. J. *J. Phys. Chem.* **1994**, *98*, 11623-11627.

63. Ditchfield, R.; Hehre, W. J.; Pople, J. A. *J. Chem. Phys.* **1971**, *54*, 724-728.

64. Gaussian 09, Revision A.02, M. J. Frisch, G. W. Trucks, H. B. Schlegel, G. E. Scuseria, M. A. Robb, J. R. Cheeseman, G. Scalmani, V. Barone, G. A. Petersson, H. Nakatsuji, X. Li, M. Caricato, A. Marenich, J. Bloino, B. G. Janesko, R. Gomperts, B. Mennucci, H. P. Hratchian, J. V. Ortiz, A. F. Izmaylov, J. L. Sonnenberg, D. Williams-Young, F. Ding, F. Lipparini, F. Egidi, J. Goings, B. Peng, A. Petrone, T. Henderson, D. Ranasinghe, V. G. Zakrzewski, J. Gao, N. Rega, G. Zheng, W. Liang, M. Hada, M. Ehara, K. Toyota, R. Fukuda, J. Hasegawa, M. Ishida, T. Nakajima, Y. Honda, O. Kitao, H. Nakai, T. Vreven, K. Throssell, J. A. Montgomery, Jr., J. E. Peralta, F. Ogliaro, M. Bearpark, J. J. Heyd, E. Brothers, K. N. Kudin, V. N. Staroverov, T. Keith, R. Kobayashi,

J. Normand, K. Raghavachari, A. Rendell, J. C. Burant, S. S. Iyengar, J. Tomasi, M. Cossi, J. M. Millam, M. Klene, C. Adamo, R. Cammi, J. W. Ochterski, R. L. Martin, K. Morokuma, O. Farkas, J. B. Foresman, and D. J. Fox, Gaussian, Inc., Wallingford CT, 2009.

65. GaussView, Version 5.0.8, Dennington, Roy; Keith, T.; Millam, John. Semichem Inc., Shawnee Mission, KS, 2009.

66. Fulmer, G. R.; Miller, A. J.; Sherden, N. H.; Gottlieb, H. E.; Nudelman, A.; Stoltz, B. M.; Bercaw, J. E.; Goldberg, K. I. *Organometallics* **2010**, *29*, 2176-2179.

67. SAINT, v. 7. 6.; Bruker AXS Inc., Madison, WI, 2008.

68. SAINT, v. 8. 3.; Bruker AXS Inc, Madison, WI, 2015.

69. Sheldrick, G. M. *Acta Cryst. A* **2015**, *71*, 3-8.

70. Hübschle, C. B.; Sheldrick, G. M.; Dittrich, B. *J. App. Cryst.* **2011**, *44*, 1281-1284.

71. Sheldrick, G. M. *Acta Cryst. C* **2015**, *71*, 3-8.

72. Farrugia, L. J. *J. App. Cryst.* **2012**, *45*, 849-854.

73. Lee, P. T.; McClintick, J.; Robertson, K. N.; Clyburne, J. A. *Main Group Chem.* **2011**, *10*, 187-204.

74. Borger, J. E.; Ehlers, A. W.; Lutz, M.; Slootweg, J. C.; Lammertsma, K. *Angew. Chem. Int. Ed.* **2014**, *53*, 12836-12839.

75. Ruhlandt-Senge, K.; Ellison, J. J.; Wehmschulte, R. J.; Pauer, F.; Power, P. P. *J. Am. Chem. Soc.* **1993**, *115*, 11353-11357.

76. King, R. B.; Eisch, J. Organometallic Synthesis. In New York, NY: Academic Press: 1965; Vol. 1, pp 70-71.

77. Bockman, T. M.; Kochi, J. K. *J. Am. Chem. Soc.* **1989**, *111*, 4669-4683.

78. Vanicek, S.; Kopacka, H.; Wurst, K.; Müller, T.; Schottenberger, H.; Bildstein, B. *Organometallics* **2014**, *33*, 1152-1156.

79. Davies, S. G.; Green, M. L. H.; Mingos, D. M. P. *Tetrahedron* **1978**, *34*, 3047-3077.

80. Enders, M.; Kohl, G.; Pritzkow, H. *Organometallics* **2004**, *23*, 3832-3839.

81. Fischer, E. O.; Herberich, G. E. *Chem. Ber.* **1961**, *94*, 1517-1523.

82. Armstrong, D. R.; Herd, E.; Graham, D. V.; Hevia, E.; Kennedy, A. R.; Clegg, W.; Russo, L. *Dalton Trans.* **2008**, 1323-1330.

83. Schade, C.; Schleyer, P., von Ragué. Advances in Organometallic Chemistry. In ; Stone, F. G. A., West, R. C., Eds.; Elsevier Science: 1987; Vol. 27, pp 176.

84. Bachmann, S.; Gernert, B.; Stalke, D. *Chem. Commun.* **2016**, *52*, 12861-12864.

85. Harder, S. *Coord. Chem. Rev.* **1998**, *176*, 17-66.

86. Dinnebier, R. E.; Behrens, U.; Olbrich, F. *Organometallics* **1997**, *16*, 3855-3858.

87. Rabe, G.; Roesky, H. W.; Stalke, D.; Pauer, F.; Sheldrick, G. M. *J. Organomet. Chem.* **1991**, *403*, 11-19.

88. Jutzi, P.; Leffers, W.; Hampel, B.; Pohl, S.; Saak, W. *Angew. Chem. Int. Ed. Engl.* **1987**, *26*, 583-584.

89. Tesh, K. F.; Hanusa, T. P.; Huffman, J. C. *Inorg. Chem.* **1990**, *29*, 1584-1586.

90. Kaupp, M.; Schleyer, P. v. R. *J. Phys. Chem.* **1992**, *96*, 7316-7323.

91. Spek, A. L. *Acta Cryst. C* **2015**, *71*, 9-18.

92. Wilkinson, G.; Pauson, P.; Cotton, F. *J. Am. Chem. Soc.* **1954**, *76*, 1970-1974.

93. Campbell, A. J.; Fyfe, C. A.; Harold-smith, D.; Jeffrey, K. R. *Mol. Cryst. Liq. Cryst.* **1976**, *36*, 1-23.

94. Gardner, A.; Howard, S.; Waddington, T.; Richardson, R.; Tomkinson, J. *Chem. Phys.* **1981**, *57*, 453-460.

95. Gorsch, M.; Franken, A.; Sievertsen, S.; Homborg, H. *Z. anorg. allg. Chem.* **1995**, *621*, 607-616.

96. Llinás, G. H.; Mena, M.; Palacios, F.; Royo, P.; Serrano, R. *J. Organomet. Chem.* **1988**, *340*, 37-40.

97. Day, B. M.; Coles, M. P. *Organometallics* **2013**, *32*, 4270-4278.

98. Lyczko, K. *J. Mol. Struct.* **2017**, *1127*, 549-556.

99. Movius, W.; Matwiyoff, N. *J. Phys. Chem.* **1968**, *72*, 3063-3066.

100. Minasian, S. G.; Arnold, J. *Chem. Commun.* **2008**, 4043-4045.

101. Wang, N.; Hwu, J. R.; White, E. H. *J. Org. Chem.* **1991**, *56*, 471-475.